arXiv:1510.03669v1 [astro-ph.HE] 13 Oct 2015

# Ringed accretion disks: equilibrium configurations

D. Pugliese and Z. Stuchlík

*Institute of Physics and Research Centre of Theoretical Physics and Astrophysics, Faculty of Philosophy & Science, Silesian University in Opava, Bezručovo náměstí 13, CZ-74601 Opava, Czech Republic*

d.pugliese.physics@gmail.com;zdenek.stuchlik@physics.cz

## ABSTRACT

We investigate a model of ringed accretion disk, made up by several rings rotating around a supermassive Kerr black hole attractor. Each toroid of the ringed disk is governed by the General Relativity hydrodynamic Boyer condition of equilibrium configurations of rotating perfect fluids. Properties of the tori can be then determined by an appropriately defined effective potential reflecting the background Kerr geometry and the centrifugal effects. The ringed disks could be created in various regimes during the evolution of matter configurations around supermassive black holes. Therefore, both corotating and counterrotating rings have to be considered as being a constituent of the ringed disk. We provide constraints on the model parameters for the existence and stability of various ringed configurations and discuss occurrence of accretion onto the Kerr black hole and possible launching of jets from the ringed disk. We demonstrate that various ringed disks can be characterized by a maximum number of rings. We present also a perturbation analysis based on evolution of the oscillating components of the ringed disk. The dynamics of the unstable phases of the ringed disk evolution seems to be promising in relation to high energy phenomena demonstrated in active galactic nuclei.

*Subject headings:* Accretion disks, accretion, black hole physics, hydrodynamics

## 1. Introduction

The most energetic processes in the Universe are related to accretion disks around black holes or some alternative objects with extremely strong gravity. Such processes with extremely large radiative energy output, combined with ejection of matter associated with jet-like structures emerging from extremely small central regions, are observed in quasars and active galactic nuclei (AGN) where supermassive black holes, with mass in the interval $(10^6 - 10^{10})M_\odot$, are assumed in the center (Ziolkowski 2005). A scaled down version of these energetic processes is observed in the so called microquasars where stellar mass black holes are expected in the center (Remillard&McClintock 2006). The enormous energy emitted by the accretion disks in quasars or AGN, in the form of electromagnetic radiation and jets, can be attributed to the strong gravity of the central black hole when the gravitational binding energy of accreting matter is transformed into radiation. The efficiency of conversion of rest energy of accreting matter to radiated energy is limited by the energy of the innermost stable circular geodesic (Bardeen 1970). In the field of non-rotating black holes, the conversion efficiency $\sim 6\%$ is large enough, enabling to explain the energy output in both quasars and microquasars. In the field of the near-extreme Kerr black holes, the efficiency approaches 42% (Bardeen et al. 1972), while in the field of Kerr naked singularities the conversion efficiency can be much larger, exceeding even the 100% related to annihilation processes, and approaching 157% for the near-extreme Kerr naked singularities (Stuchlik 1980; Stuchlik et al. 2011).

There are at least three important aspects of the accretion disk structure which in turn lead to a classification of different disk models: the geometry (the vertical thickness) for which we can distinguish geometrically thin or thick disks, the matter accretion rate (defining sub- or super-Eddington luminosity), and the optical

depth (i.e., transparent or opaque disks), (Abramowicz&Fragile 2013). More specifically, geometrically thin disks are modelled as the standard Shakura-Sunayev (Keplerian) disks (Shakura 1973; Shakura&Sunyaev 1973; Novikov&Thorne 1973; Page&Thorne74 1974), the ADAF (Advection-Dominated Accretion Flow) disks (Abramowicz&Straub 2014; Narayan et al. 1998), and the slim disks (Abramowicz&Fragile 2013). Geometrically thick disks are modelled as the Polish Doughnuts (P-D) (Kozłowski et al. 1979; Abramowicz et al. 1978; Jaroszynski et al. 1980; Stuchlík et al. 2000; Rezzolla et al. 2003; Slaný&Stuchlík 2005; Stuchlik 2005; Pugliese et al. 2013a; Pugliese&Montani 2013b), or the ion tori (Rees et al. 1982). The ADAF disks and the ion tori have relatively low accretion rates (sub-Eddington), while the P-D disks have very high (super-Eddington) accretion rates. The P-D and slim disks have high optical depth being thus opaque, while the ion tori and the ADAF disks have low optical depth being thus transparent. In the geometrically thin disks, dissipative viscosity processes are relevant for accretion, being usually attributed to the magnetorotational instability of the local magnetic fields (Hawley et al. 1984; Hawley 1987, 1990, 1991; De Villiers&Hawley 2002). In the toroidal disks, pressure gradients are crucial (Abramowicz et al. 1978; Stuchlík et al. 2009). The magnetic pressures of toroidal magnetic fields could be also relevant (Komissarov 2006; Adamek&Stuchlik 2013; Hamersky&Karas 2013). Notice the influence of the global internal magnetic toroidal fields can be represented by 1D string loops (Larsen 1994; Kolo&Stuchlk 2013; Stuchlik&Kolos 2012, 2014; Cremaschini&Stuchlik 2013). While an off-equatorial "levitating" tori can be modelled by the dielectric (Kovar et al. 2011; Slany et al. 2013; Kovar et al. 2014) or kinetic (Cremaschini et al. 2013) models of toroidal charged structures if a large scale external magnetic field is present in vicinity of the central black hole. In different situation the accretion disks could be with relatively high precision modelled by using a well defined Pseudo-Newtonian potential (Paczyński 1980; Abramowicz et al. 1980; Stuchlík& Kovář 2008; Stuchlík et al. 2009), while the structure of many geometrically thin Keplerian disks and geometrically thick toroidal disks is deeply regulated by the geodesic structure of the black hole spacetime(Novikov&Thorne 1973; Abramowicz et al. 1978; Stuchlik 2005; Abramowicz&Fragile 2013). However, here we focus on the fully general relativistic approach. While we do not consider in the present paper the role of the magnetic fields, postponing this issue to future investigations.

In this article we propose a model of ringed accretion disk (or *macro-configuration*) formed by several toroidal structures, the *rings* (or *sub-configurations*), orbiting a supermassive Kerr attractor and centered in its equatorial plane–(Pugliese&Montani 2015a). The centers of all the individual tori are therefore coplanar, coinciding with the equatorial plane of the black hole. This assumption of coincidence between the orbital planes of the rings and the equatorial plane of the axisymmetric attractor, is adopted here as the simplest scenario for the first construction of such models. In fact, the majority of the current analytical and numerical models of accretion configurations assumes the axial symmetry of the extended accreting matter. There is indeed an "inheritance" of the symmetries of 1D linear test particle model in circular motion, for the toroidal 2D accreting structures orbiting extended matter under pressure gradients, characterized by a more or less significant verticalization of the accretion disk. These symmetries are also characteristic for the model of ringed disks.

A ringed disk consists thus of several tori which could be created due to various (succeeding) accretion regimes during the evolution of the matter configurations around the supermassive black hole. Construction of a ringed disk in a Kerr spacetime can be realized in two orbital stability regions, corresponding to the stable corotating and counterrotating circular orbits relative to the rotation of the black hole attractor. Of course, various accretion periods could create both corotating and counter-rotating toroidal configurations given by various initial conditions determining the succeeding accretion periods, e.g., by tidally destroyed stars corotating or counterrotating with respect to the attractor (Bardeen et al. 1972; Stuchlik 1980). The individual toroidal remnant structures can be thus both corotating or counter-rotating. In fact, in modelling evolution of supermassive black holes in AGNs both corotating and counter-rotating accretion stages are mixed (Volonteri et al. 2003a,b). On the other hand, in the galactic nuclei containing a supermassive black hole, several separated accretion regimes could be occurred in the past, leaving some remnants in the form of toroidal structures that could be reanimated, if some additional matter is supplied into the vicinity of the central black hole due to tidal distortion of a star, or some cloud of interstellar matter is captured by the

strong gravity.

The precise arrangement of ringed disks and the relations between the rings will be here completely characterized. The results of this work demonstrate significant constraints on different features of the macro-configurations, in particular on the number of rings and their specific angular momentum (differential rotation of the ringed disks). Noticeably the ringed disk model could be also seen as a unique geometrically thin accretion disk.

We trace the definition of the ringed disk model, focusing on the equilibrium configurations that ensure its physical reliability and, simultaneously, can be considered as starting points of instability phases. In fact, an essential aspect concerns the unstable phases, associated to the (super-Eddington) accretion and formation of jets.

The ringed disks have an internal structure represented by their *decomposition*, or the set of individual tori. The internal dynamics of the ringed disks is related to the dynamics of its units (individual tori). The internal dynamics of these tori may result in instabilities, associated to the accretion onto the black hole or creation of jets (Meier 2012), leading to potentially unstable phases for the entire ringed disk. In principle, an infinite number of individual tori centers with maximal pressure can exist. However the tori as actually extended objects, are not 1D strings. Consequently the extension of an individual torus is constrained by its internal dynamics (for example, by the equilibrium of the pressure gradients and gravitational and inertial forces), and by the fact that the individual tori are not isolated, but actually they exist as a part of the entire structure composing the ringed disk. In such a structure, each ring must keep its identity, avoiding the overlap of material from one ring to another. Possible collisions of rings, feeding or accretion from a ring to another one, are considered to be unstable phases of the ringed disk, which can not be immediately described by the model here considered (Boyer 1965).

The unstable states of a ringed disk system provide a classification of possible non-equilibrium configurations.The study of the equilibrium tori will be then the starting point for a future analysis of the oscillation modes in the structure of the relativistic ringed disks which can be related to various astrophysical phenomena. The results in this respects seem to be promising in view of the phenomenology associated with both the stable and unstable configurations. The radially oscillating tori of the ringed disk could be related to the high-frequency quasi periodic oscillations observed in non-thermal X-ray emission from compact objects (Torok et al. 2005; Stuchlik et al. 2013). A strong overflow of matter from a torus could be related to a jet formation. As a consequence of this analysis, we are able to locate the instability points (one or several) associated with accretion onto the Kerr accreitor, of the launching of jets inside the ringed macro-configuration, and the distribution of the specific angular momentum initially characterizing the unstable phases. Particularly interesting would be analysis of the unstable phases in which an interaction with the source is associated with consequent changes of the geometrical characteristics of the spacetime, by mutation of the mass and spin parameters of the Kerr attractor. The mutation of the geometry in turn determines a change of the dynamic properties of matter in accretion, resulting in an iterative process to be analyzed, which could be a form of runaway instability (Abramowicz et al. 1983, 1998; Font&Daigne 2002a; Rezzolla et al. 2003; Korobkin et al. 2013; Hamersky&Karas 2013; Pugliese&Quevedo 2015b).

We provide here a precise definition and a detailed description of the ringed accretion configurations in full general relativity (GR), assuming each individual torus of the ringed disk be made of perfect fluid. The tori are governed by the equipotential surfaces that can be closed, giving stable equilibrium configurations, and open, giving unstable, jet-like structures caused by the relativistic instability due to the Paczynski mechanism. More specifically, the individual toroidal (thick disk) configurations (the rings or sub-configurations) are here described by purely hydrodynamic (barotropic) models, for which the time scale of the dynamical processes (regulated by the gravitational and inertial forces) is much lower than the time scale of the thermal ones (heating and cooling processes, radiation) that is lower than the time scale of the viscous processes. Where the effects of strong gravitational fields are dominant with respect to the dissipative ones and predominant to determine the unstable phases of the systems(Font&Daigne 2002b; Abramowicz 2004; Igumenshchev 2000; Abramowicz&Fragile 2013; Pugliese&Montani 2015a; Paczyński 1980), see also (Hawley 1990; Fragile

et al. 2007; De Villiers&Hawley 2002; Hawley 1987, 1991; Hawley et al. 1984; Font 2003). The entropy is constant along the flow and, according to the von Zeipel condition, the surfaces of constant angular velocity $\Omega$ and of constant specific angular momentum $\ell$ coincide (Abramowicz 1971; Chakrabarti 1990, 1991; Zanotti&Pugliese 2014). This implies that the rotation law $\ell = \ell(\Omega)$ is independent of the equation of state (Lei et al. 2008; Abramowicz 2008). The perfect fluid equilibrium tori can be classified in a given spacetime by the specific angular momentum distribution function $\ell(r)$, and a constant $K$ determining the matter content of the tori (Abramowicz et al. 1978) [1]. These configurations have been often adopted as the initial conditions in the set up for simulations of the MHD (magnetohydrodynamic) accretion structures()(Igumenshchev 2000; Shafee et al. 2008) and (Fragile et al. 2007; De Villiers&Hawley 2002; Stuchlík et al. 2009).

The model of the tori that is used in this paper is stationary and axisymmetric, being adapted to the symmetries of the Kerr spacetime. The tori are governed by "Boyer's condition" of the analytic theory of equilibrium configurations of rotating perfect fluids (Boyer 1965). The toroidal structures of orbiting barotropic perfect fluid are determined by an effective potential reflecting the spacetime geometry and distribution of the specific angular momentum $\ell(r)$ of the orbiting fluid – such an approach is well known and widely adopted (Abramowicz et al. 1978; Pugliese&Montani 2015a; Abramowicz et al. 1996; Fishbone&Fishbone 1976; Frank et al. 2002; Pugliese et al. 2013a; Lei et al. 2008; Pugliese&Montani 2013b), and is applied in various contexts (Kucakova et al. 2011; Rezzolla et al. 2003; Stuchlik&Schee 2012; Slaný&Stuchlík 2005; Stuchlík& Slaný 2006; Stuchlík et al. 2000; Stuchlík et al. 2009; Stuchlík& Kovář 2008; Stuchlk et al 2014). Many features of the tori dynamics and morphology like their thickness, their stretching in the equatorial plane, and the location of the tori are predominantly determined by the geometric properties of spacetime via the effective potential. The gradient of the effective potential is regulating the pressure gradient of the fluid in the Euler law governing dynamics of the perfect fluid (Kozłowski et al. 1979). The boundary of any stationary, barotropic, perfect fluid body is determined by an equipotential surface, i.e., the surface of constant pressure (the Boyer surface) that is orthogonal to the gradient of the effective potential (Boyer 1965; Stuchlík et al. 2009). The equipressure surfaces that could be closed (determining equilibrium configurations), or open (determining jets). The special case of cusped equipotential surfaces allows for the accretion onto the central black hole (Kozłowski et al. 1979; Abramowicz et al. 1978; Jaroszynski et al. 1980; Paczyński 1980; Abramowicz et al. 1980) or excretion in spacetimes reflecting the cosmic repulsion (Stuchlík et al. 2000; Rezzolla et al. 2003; Slaný&Stuchlík 2005; Stuchlik 2005; Stuchlík et al. 2009). The outflow of matter through the cusp occurs due to an instability in the balance of the gravitational and inertial forces and the pressure gradients in the fluid, i.e., by the so called Paczynski mechanism of violation of mechanical equilibrium of the tori (Jaroszynski et al. 1980). The cusp governing accretion onto the black hole has to be located near the event horizon (Abramowicz et al. 1978; Paczyński& Wiita 1980; Paczyński 1980), while the cusp governing the excretion has to be located near the so called static radius where gravitational attraction of the black hole is just balanced by the cosmic repulsion (Stuchlík et al. 2000; Stuchlik 2005) independently on the rotation of the black hole (Stuchlik&Slany 2004).

The possibility of constructing the ringed disk model has been mentioned in (Pugliese&Montani 2013b). To our knowledge the present article is the first attempt to define and characterize this model of accretion disk that could, we believe, to be of some significance for the high energy astrophysics related especially to accretion onto supermassive black holes, and the extremely energetic phenomena in quasars and AGN that could be observable by the planed X-ray observatory ATHENA [2].

The new ringed disk model requires the introduction of a number of new definitions, and in this article the formalism was developed in details and extensively explained. To make more clear and simple the description and explanation of this model, the article has been structured in two parts: brief first descriptive

[1] The Polish Doughnut model (Abramowicz&Fragile 2013) represents an important example of a thick, opaque and super-Eddington, radiation pressure supported accretion disks cooled by advection with low viscosity. The morphology of a P-D model in equilibrium is a fat torus centered on the attractor. In the open configurations, critical phases are characterized by funnels of material with highly super-Eddington luminosity (Abramowicz et al. 1983).

[2] http://the-athena-x-ray-observatory.eu/

part, Secs. (2) and (3), illustrates the model, the second part, Sec. (4), presents in detail the obtained results. In order to lighten the reading, we have introduced Appendices, where various aspects of the model are detailed, and parts of the analysis, dealing with some specific topics, such as an introduction to the perturbation approach, were developed.

In details the plan of the article is the following: in Sec. (2) we briefly summarize the thick accretion disk model. The ringed disk model is introduced in Sec. (3) where the main definitions are provided. Particularly, in Sec. (3.1), we define the unstable macro-configurations in the framework of ringed disk model. The definition of the major morphological features of the ringed disks is presented in Sec. 3.2), closing first part of this work. Section (4), constituting the second part of this article, is the essential part of our analysis providing an extensive characterization of the compositions of the ringed disks. After discussing the role of the model parameters in Sec. (4.1) and (4.2), an effective potential of the ringed macro-structure is defined in Sec. (A.1). In Sec. (4.3), we deepen the role of the $\ell$-parameter introducing the definition of the differential rotation and angular momentum of the ringed macro-structures in Sec. (4.3.1). These definitions are used to find the results developed in Sec. (4.3.2). In Section (4.4) we apply this analysis to characterize two main types of the ringed macro-configurations as previously introduced: each disk can be only a combination of these two types or one of them. Finally, Sec. (4.5) closes the second part of this work with the study of some important limiting cases. Discussion and future perspectives can be found in Sec. (5). A summary with conclusions are in Sec. (6). Some Appendix sections follow: Sec. (A) presents some notes of the ringed disk morphology and the effective potential of the ringed disk. In Sec. (B) we deepen the properties of the ring angular momentum, discussing some results of general relevance for the tori governed by the Boyer model. We investigate some aspects of the macro-configuration with one or more critical points, and in particular the macro-configuration with the open (unstable) configurations associated with jets created by accreting matter in Sec. C). General considerations on the perturbations of the ringed disks and their equilibrium can be found in Sec. (D). Sec. (E) contains a collection of results we refer to along the analysis. Table. (1) provides a list of the main symbols and relevant notation used throughout this article.

## 2. Thick accretion disk model in the Kerr spacetime

In this work we consider toroidal configurations of perfect fluids orbiting a Kerr black hole **(BH)** attractor. The Kerr metric tensor can be written in the Boyer-Lindquist (BL) coordinates $\{t, r, \theta, \phi\}$ as follows

$$
\begin{aligned}
ds^2 &= -dt^2 + \frac{\rho^2}{\Delta} dr^2 + \rho^2 d\theta^2 + (r^2 + a^2)\sin^2\theta d\phi^2 + \frac{2M}{\rho^2} r (dt - a\sin^2\theta d\phi)^2 \ , \\
\rho^2 &\equiv r^2 + a^2\cos\theta^2, \quad \Delta \equiv r^2 - 2Mr + a^2,
\end{aligned}
\tag{1}
$$

here $M$ is a mass parameter and the specific angular momentum is given as $a = J/M \in ]0, 1]$, where $J$ is the total angular momentum of the gravitational source. The horizons $r_- < r_+$ and the outer static limit $r_\epsilon^+$ are respectively given by:

$$
r_\pm \equiv M \pm \sqrt{M^2 - a^2}; \quad r_\epsilon^+ \equiv M + \sqrt{M^2 - a^2\cos\theta^2}; \tag{2}
$$

there is $r_+ < r_\epsilon^+$ on $\theta \neq 0$ and $r_\epsilon^+ = 2M$ in the equatorial plane, $\theta = \pi/2$. The extreme Kerr black hole has spin-mass ratio $a/M = 1$, while the non-rotating limiting case $a = 0$ is the Schwarzschild metric. As the line element (1) is independent of $\phi$ and $t$, the covariant components $p_\phi$ and $p_t$ of a particle four–momentum are conserved along the geodesics, therefore[3] the quantities

$$
E \equiv -g_{\alpha\beta}\xi_t^\alpha p^\beta, \quad L \equiv g_{\alpha\beta}\xi_\phi^\alpha p^\beta \ , \tag{3}
$$

[3]We adopt the geometrical units $c = 1 = G$ and the $(-,+,+,+)$ signature, Greek indices run in $\{0, 1, 2, 3\}$. The four-velocity satisfy $u^a u_a = -1$. The radius $r$ has unit of mass $[M]$, and the angular momentum units of $[M]^2$, the velocities $[u^t] = [u^r] = 1$ and $[u^\varphi] = [u^\theta] = [M]^{-1}$ with $[u^\varphi/u^t] = [M]^{-1}$ and $[u_\varphi/u_t] = [M]$. For the seek of convenience, we always consider the dimensionless energy and effective potential $[V_{eff}] = 1$ and an angular momentum per unit of mass $[L]/[M] = [M]$.

| | | |
|---|---|---|
| $C$ | cross sections of the closed Boyer surfaces (equilibrium torus) | Secs. (2,3) |
| $C_x$ | cross sections of the closed cusped Boyer surfaces (accretion torus) | Secs. (2,3) |
| $O_x$ | cross sections of the open cusped Boyer surfaces | Secs. (2,3) |
| $\partial C$ | the contour of the surface $C$ in the equatorial section | Fig. (2) |
| $\mathbf{C}^n \equiv \bigcup_{i=1}^{n} C_i$ | ringed disk of order $n$ (macro-configuration) | Fig. (2) |
| $(y_3^i, y_1^i)$ | inner and outer edge of $C_i$ ring | Fig. (2) |
| $\overbrace{\mathbf{C}}^{m}$ | mixed $\ell$counterrotating sequences | Sec. (3) Fig. (4)-top. |
| $\overbrace{\mathbf{C}}^{s}$ | isolated $\ell$counterrotating sequences | Sec. (3) Fig. (4)-bottom |
| $\mathbf{C}^{\mathbf{n}}_{\odot}$ | configuration $i \in \{1, ..., n-1\}: \ \partial C_i \cap \partial C_{i+1} = \{y_1^i = y_3^{i+1}\}$ | Fig. (3) |
| $\mathfrak{r}$ | rank of $\mathbf{C}^{\mathbf{n}}_{\odot}$ | Sec. (3.1) |
| $\mathbf{C}^{\mathbf{n}}_{\mathbf{x}}$ | Ringed disk with at last one sub-configuration $C_x^i$ | Fig. (3) |
| $\mathfrak{r}_{\mathfrak{r}}$ | rank of $\mathbf{C}^{\mathbf{n}}_{\mathbf{x}}$ | Sec. (3.1) |
| $\mathbf{C}^{\mathbf{x}}_{\odot}$ | ringed disk $\mathbf{C}_{\odot}$ with a $C_x^i$ ring: $y_1^{i-1} = y_3^i = y_{cusp}$ | Sec. (3.1) |
| $\lambda_i \equiv ]y_1^i, y_3^i[ \ \lambda_i \equiv y_1^i - y_3^i$ | elongation, range and measure, of the Boyer surface | Fig. (2) |
| $\bar{\Lambda}_{i+1,i} \equiv ]y_3^{i+1}, y_1^i[ \ \bar{\lambda}_{i+1,i} \equiv y_3^{i+1} - y_1^i$ | spacing, range and measure | Fig. (2). |
| $\Lambda_{\mathbf{C}^n} \ \lambda_{\mathbf{C}^n}$ | elongation, range and measure, of $\mathbf{C}^n$ | Eq. (8) |
| $h_{\mathbf{C}^n}$ | height of $\mathbf{C}^n$ | Eq. (A1) |
| $R_{\mathbf{C}^n}$ | thickness of $\mathbf{C}^n$ | |
| $R_{\mathbf{C}^n_{\odot}}$ | thickness of $\mathbf{C}^n_{\odot}$ | Eq. (A2), Sec. (3.1) |
| $V_{eff}^{\mathbf{C}^n}\Big\vert_{K_i}$ | effective potential of the decomposed $\mathbf{C}^n$ | Sec.(A.1) Eq. (A4). |
| $V_{eff}^{\mathbf{C}^n}$ | effective potential of the configuration $\mathbf{C}^n$ | Eq. (A5). |
| $\ell_{i/i+1} \equiv \ell_i/\ell_{i+1}$ | ratio in specific angular momentum of $C_i$ and $C_{i+1}$ | Eq. (18) |
| $\bar{\ell}^n_{\mathbf{C}}$ | area angular momentum of $\mathbf{C}^n$ | Eq. (19) |
| $\bar{\bar{\ell}}^n_{\mathbf{C}}$ | volume angular momentum of $\mathbf{C}^n$ | Eq. (19) |
| $\bar{\ell}^l_{\mathbf{C}^n}$ | leading angular momentum of $\mathbf{C}^n$ | Eq. (20) |
| $\ell_h$ | apparent angular momentum of $\mathbf{C}^n$ | Eq. (20) |
| $r^{\pm}_{\mathcal{M}}$ | maximum point of derivative $\partial_r(\mp\ell^{\pm})$ for $a/M$ respectively | Sec. (4.3.2,B) |
| $a_{\aleph_1} = 0.382542M$ | $a_{\aleph_1}: \ell_{\gamma}^{-} = -\ell_{+}(r_{mso}^{-})$ | Fig. (4) |
| $a_{\aleph} \approx 0.508864526M$ | $a_{\aleph}: -\ell_{mso}^{+}(a_{\aleph}) = \ell_{\gamma}^{-}(a_{\aleph})$ | Eq. (36) Fig. (6) |
| $a_{\aleph_2} \equiv 0.172564M$ | $a_{\aleph_2}: -\ell_{mso}^{+}(a_{\aleph_2}) = \ell_{mbo}^{-}(a_{\aleph_2})$ | Sec. (4.3.2) |
| $a_{\aleph_0} \equiv 0.390781M$ | $a_{\aleph_0} \in ]a_{\aleph_1}, a_{\aleph}[: \ell_{\gamma}^{-} = -\ell_{mbo}^{+}$ | Eq. (40) |

Table 1: Lookup table with the main symbols and relevant notation used throughout the article. Links to associated sections, definitions and figures are also listed.

are constants of motion, where $\xi_t = \partial_t$ is the Killing field representing the stationarity of the Kerr geometry and $\xi_\phi = \partial_\phi$ is the rotational Killing field. The constant $E$, for timelike geodesics, may be interpreted as representing the total energy of the test particle coming from radial infinity, as measured by a static observer at infinity, and $L$ as the axial component of the angular momentum of the particle. The Kerr metric (1) is also invariant under the application of any two different transformations: $x^\alpha \to -x^\alpha$ for one of the coordinates $(t, \phi)$, or the metric parameter $a$ and the test particle dynamics is invariant under the mutual transformation of the parameters $(a, L) \to (-a, -L)$. Thus one can limit the analysis of the test particle circular motion to the case of positive values of $a$ for corotating ($L > 0$) and counterrotating ($L < 0$) orbits with respect to the black hole.

We focus here on the case of a one-species particle perfect fluid (simple fluid), described by the energy momentum tensor

$$T_{\alpha\beta} = (\varrho + p)u_\alpha u_\beta + \ pg_{\alpha\beta}, \tag{4}$$

where $\varrho$ and $p$ are the total energy density and pressure, respectively, as measured by an observer moving with the fluid whose four-velocity $u^\alpha$ is a timelike flow vector field. For the symmetries of the problem, we always assume $\partial_t \mathbf{Q} = 0$ and $\partial_\varphi \mathbf{Q} = 0$, being $\mathbf{Q}$ a generic spacetime tensor. The fluid dynamics is described by the *continuity equation* and the *Euler equation* respectively:

$$u^\alpha \nabla_\alpha \varrho + (p + \varrho)\nabla^\alpha u_\alpha = 0\,, \quad (p + \varrho)u^\alpha \nabla_\alpha u^\gamma + \ h^{\beta\gamma}\nabla_\beta p = 0\,, \tag{5}$$

where the projection tensor $h_{\alpha\beta} = g_{\alpha\beta} + u_\alpha u_\beta$ and $\nabla_\alpha g_{\beta\gamma} = 0$ (Misner et al. 1973; Pulgiese&Kroon 2012; Pugliese&Montani 2015a). We investigate the fluid toroidal configurations centered on the plane $\theta = \pi/2$, and defined by the constraint $u^r = 0$. No motion is assumed in the $\theta$ angular direction, which means $u^\theta = 0$. We assume moreover a barotropic equation of state $p = p(\varrho)$. The continuity equation in Eq. (5) is identically satisfied as consequence of the conditions. From the Euler equation (5) one can obtain

$$\frac{\partial_\mu p}{\varrho + p} = -\partial_\mu W + \frac{\Omega \partial_\mu \ell}{1 - \Omega\ell}, \quad \ell \equiv \frac{L}{E}, \quad W \equiv \ln V_{eff}(\ell), \quad V_{eff}(\ell) = u_t = \pm\sqrt{\frac{g_{\phi t}^2 - g_{tt}g_{\phi\phi}}{g_{\phi\phi} + 2\ell g_{\phi t} + \ell^2 g_{tt}}}, \tag{6}$$

the function $W$ is Paczynski-Wiita (P-W) potential, $\Omega$ is the relativistic angular frequency of the fluid relative to the distant observer, and $V_{eff}(\ell)$ provides an effective potential for the fluid, assumed here to be characterized by a conserved and constant specific angular momentum $\ell$ (see also (Lei et al. 2008; Abramowicz 2008)). The procedure adopted in the present article borrows from the Boyer theory on the equipressure surfaces applied to a P-D torus: the Boyer surfaces are given by the surfaces of constant pressure or[4] $\Sigma_i$ =constant for $i \in (p, \rho, \ell, \Omega)$, (Boyer 1965; Frank et al. 2002), where the angular frequency is indeed $\Omega = \Omega(\ell)$ and $\Sigma_i = \Sigma_j$ for $i, j \in (p, \rho, \ell, \Omega)$. The toroidal surfaces are the equipotential surfaces of the effective potential $V_{eff}(\ell)$, considered as function of $r$, solutions $\ln(V_{eff}) = \mathrm{c}$ = constant or $V_{eff} = K$ =constant.

The model is regulated by the couple of parameters $\mathbf{p} \equiv (\ell, K)$ which together uniquely identify each Boyer surface. Similarly to the case of the test particle dynamics, the function $V_{eff}(\ell)$ in Eq. (6) is invariant under the mutual transformation of the parameters $(a, \ell) \to (-a, -\ell)$, therefore we can limit the analysis to positive values of $a > 0$, for *corotating* ($\ell > 0$) and *counterrotating* ($\ell < 0$) fluids and we adopt the notation ($\pm$) for counterrotating or corotating matter respectively. The P-D, could be defined as a "geometric" model of thick accretion disks as many features of this disk model are mostly determined by the geometric properties of the spacetime background as given by some notable radii $\mathcal{R} \equiv \{r^\pm_{mso}, r^\pm_{mbo}, r^\pm_\gamma\}$, regulating the particle dynamics: the *marginally circular orbit* for timelike particles $r^\pm_\gamma$, the *marginally bounded orbit* is $r^\pm_{mbo}$, and the *marginally stable circular orbit* $r^\pm_{mso}$ (Pugliese et al. 2011; Misner et al. 1973; Chandrasekhar 1983; Pugliese et al. 2013c). Timelike circular orbits can fill the spacetime region $r > r^\pm_\gamma$, stable orbits are in $r > r^\pm_{mso}$ for counterrotating and corotating particles respectively, and $E_\pm(r^\pm_{mbo}) = 1$. Given $r_i \in \mathcal{R}$, we

[4]More generally $\Sigma_{\mathbf{Q}}$ is the surface $\mathbf{Q}$ =constant for any quantity or set of quantities $\mathbf{Q}$.

adopt the notation for any function $\mathbf{Q}(r):\ \mathbf{Q}_i \equiv \mathbf{Q}(r_i)$, therefore for example $\ell^+_{mso} \equiv \ell_+(r^+_{mso})$, and more generally given the radius $r_*$ and the function $\mathbf{Q}(r)$, there is $\mathbf{Q}_* \equiv \mathbf{Q}(r_*)$.

The closed Boyer surfaces cross the equatorial plane $\theta = \pi/2$, in $y_i = y_i(a;\mathbf{p})$, $i \in \{1,2,3\}$, where $y_2 < y_3 < y_1$, as shown in Figs. (2). We consider the orbital region $\Delta r_{crit} \equiv [r_{Max}, r_{min}]$, whose boundaries correspond to the maximum and minimum points of the effective potential respectively. The inner edge of the Boyer surface must be $y_3 \in \Delta r_{crit}$, the outer edge is $y_1 > r_{min}$. A further matter configuration (with solution $y_2$) closest to the black hole is at $r < r_{max}$. In the closed cusped configuration $C_x$, there is $y_3 = y_2$

The centers $r_{cent}$ of the closed configurations $C_\pm$ are located at the minimum points $r_{min} > r^\pm_{mso}$ of the effective potential, where the hydrostatic pressure is maximum. The toroidal surfaces are characterized by $K_\pm \in [K^\pm_{min}, K^\pm_{Max}[\subset]K^\pm_{mso}, 1[$ and momentum $\ell_+ < \ell^+_{mso} < 0$ or $\ell_- > \ell^-_{mso} > 0$ respectively. The limiting case of $K_\pm = K^\pm_{min}$ corresponds to a one-dimensional ring of matter located in $r^\pm_{min}$. The maximum points of the effective potential $r_{Max}$ are minimum points of the hydrostatic pressure or, P-W points of gravitational and hydrostatic instability. From these points an accretion overflow of matter from the closed, cusped configurations in $C^\pm_x$ (see Fig. (3)) can occur from the instability point $r^\pm_x \equiv r_{Max} \in ]r^\pm_{mbo}, r^\pm_{mso}[$ towards the attractor, if $K_{Max} \in ]K^\pm_{mso}, 1[$ with proper angular momentum $\ell \in ]\ell^+_{mbo}, \ell^+_{mso}[\cup]\ell^-_{mso}, \ell^-_{mbo}[$, respectively, for counterrotating or corotating matter. Otherwise there can be funnels of material in jets from an open configuration $O^\pm_x$ with $K^\pm_{Max} \geq 1$, launched from the point $r^\pm_J \equiv r_{Max} \in ]r^\pm_\gamma, r^\pm_{mbo}]$ with proper angular momentum $\ell \in ]\ell^+_\gamma, \ell^+_{mbo}[\cup]\ell^-_{mbo}, \ell^-_\gamma[$. Equilibrium configurations, with topology $C$, are possible for $\pm\ell_\mp > \pm\ell^\mp_{mso}$ centered in $r > r^\mp_{mso}$ respectively, but no maxima of the effective potential are for $\pm\ell_\mp > \ell^\pm_\gamma$, and therefore, for those angular momenta only equilibrium configurations are possible.

Each couple $\mathbf{p}$ identifies uniquely a Boyer surface: as discussed in (Pugliese&Montani 2015a) by a variation of the $\mathbf{p}$ parameters, we can consider a matrix $\mathfrak{B}_\mathbf{p}$ of corotating and counterrotating configurations on $\Sigma_\mathbf{p} \equiv \Sigma_K \otimes \Sigma_\ell$; keeping one parameter of the couple $\mathbf{p} \equiv (\ell, K)$ constant and changing the other one in the set of values for the formation of a Boyer surface, we could consider the "projection" $\mathfrak{B}_{\mathbf{p_j}} \equiv \mathfrak{B}_\mathbf{p}/\Sigma_{\mathbf{p_i}}$ of $\mathfrak{B}_\mathbf{p}$ on the constant surface $\Sigma_{\mathbf{p_i}}$, i.e. the sequence, array or column of elements of $\mathfrak{B}_{\mathbf{p_j}}$ on the constant $\mathbf{p_i}$ surfaces, and assigning $\mathbf{p_j}$ ($\mathbf{p_i}$ can be either $\ell$ or $K$) as a family parameter. In this work we focus on the elements of $\mathfrak{B}_\mathbf{p}$ as defined on a $\Sigma_t$ surface, and we investigate the possible multiple-configurations on the fixed $\Sigma_t$. Since the toroidal configuration can be corotating $\ell a > 0$ or counterrotating $\ell a < 0$, with respect to the black hole $a > 0$, then assuming several toroidal configurations, say the couple $(C_a, C_b)$, with proper angular momentum $(\ell_a, \ell_b)$ orbiting in the equatorial plane of a given Kerr **BH**, we need to introduce the concept of *$\ell$corotating* disks, defined by the condition $\ell_a\ell_b > 0$, and *$\ell$counterrotating* disks by the relations $\ell_a\ell_b < 0$, the two $\ell$corotating tori can be both corotating $\ell a > 0$ or counterrotating $\ell a < 0$ with respect to the central attractor.

## 3. Introduction of the ringed disk model and definitions

We first briefly introduce the ringed accretion disk model (or macro-configuration of tori), providing some fundamental definitions and explicit formalism that will be used in the following discussion. It is convenient to introduce the notation of $C$ more specifically for the cross sections of the closed Boyer surfaces and generally for boundaries $\partial C$, the contour of the surface in the equatorial section, as shown in Fig. (2). Therefore the cross section of each torus has boundary $\partial C$ (barotropic surfaces) and the fluid fills $C$. For simplicity of notation, $C_i$ will refer generally to the Boyer surfaces meaning that it could be possibly in its unstable phase, we could consider then the cusped topology $C^x_i$. In any case, when it will be relevant, we will specify this possibility. The critical phase of an $O_x$ topology, will be considered a part, as a special case.

We question the existence of "structured" toroidal accretion disks constituted by several tori orbiting and centered around a given Kerr attractor. The aim is to provide a model for the matter *structure* of the multiple thick configurations defined as the union[5] $\mathbf{C}^n \equiv \bigcup^n_{i=1} C_i$ of closed, cusped or not, torus *separated*

[5]We intend the set formed by a number $n$ of tori orbiting one Kerr **BH** attractor, the failure of rigor of this definition is hereby replaced by the intuitive immediacy, as it is shown in Figs. (1). The Latin subscript in $C_i$ usually indicates, when otherwise

*sub-configurations* $C_i \bigcap C_j = 0$ and $\partial C_i \bigcap \partial C_j = \{\emptyset, y_1, y_3\}$ of P-D thick accretion disks, whose intersection is the null set or at last the inner or outer edge of the configurations as specified below (this analysis does not take into account the lobe disk associate to the solution $y_2$), see Fig. (2) and Fig. (3). The lower-case Latin indices $i, j, ...a, b...$, either superscript or subscript, are indices of sub-configurations and indicate (uniquely in this model) each toroidal component (*ring*) of the ringed structure. For a double configuration, formed by a couple of rings, in general with (**o**) we refer here to any quantity related to the external (outer) configurations of the couple and (**i**) to the more internal, the inner one with respect to the attractor.

We define *order* of the macro-configuration $\mathbf{C}^n$ the number $n \in [1, \infty]$ of the sub-configurations of $\mathbf{C}^n$, and the set of $\{C_i\}_{i=1}^n$ as *decomposition* of the $\mathbf{C}^n$ macro-configuration of the $n$-order, the decomposition will be considered an *ordered sequence* of configurations in the sense specified below. In Fig. (1) a pictorial representation of a $\mathbf{C}^3$ ringed disk of order $n = 3$ is shown. Then, even if each sub-configuration is characterized here by a well defined and constant specific angular momentum $\ell_i$ =constant, as discussed in (Lei et al. 2008; Abramowicz 2008), this assumption can be relaxed in more general P-D models. The macro-structure inherits many of the symmetries of each toroidal sub-configuration of its decomposition, for example, the symmetry for reflection on the equatorial plane: we specify that we are considering $r^i_{min} \in \Sigma_{\theta=\pi/2}$ where $r^i_{min} = r^i_{cent}$ coincides with the center of the $C_i$ sub-configuration located in the equatorial plane of the disk, which always coincides with the symmetry plane of the attractor. All the rings are thus assumed coplanar. Therefore we limit the study to the Boyer configuration sections on the equatorial plane.

The generalization of this set up to other situations in which the rings are not coplanar or with unique plane symmetry (the symmetry plane of the disk) different from the symmetry plane of the attractor is also possible. In this article we proceed to characterize possible decompositions of a $n$-order ringed disk fixing a certain set of characteristics $\mathbf{C}^n$. The decomposition is in fact uniquely determined by the set $\mathcal{S} \equiv \{n, \mathbf{p}_{\mathbf{C}^n}\}$, where $\mathbf{p}_{\mathbf{C}^n} \equiv \{\mathbf{p}_i\}_{i=1}^n$, $n$ is the decomposition order and $i$ is as usual the index of sub-configuration, i.e. each $\mathbf{p}_i$ uniquely identifies one element, ring, of a ringed disk, its morphology as its location on the equatorial plane, as discussed in Sec. (2)[6].

Given a decomposition of $\mathbf{C}^n$, a *sequence* or also equivalently *sub-sequence* of rings, is a set $\{C_i\}$ of $n_* \leq n$ elements of its decomposition. In particular it is important to consider the $\ell$corotating sequences, formed by all the $\ell$corotating rings of the decompositions $\ell_i \ell_j > 0$, and we call $\ell$counterrotating sequences of the decomposition of $\mathbf{C}^n$ the two $\ell$corotating sequences of this, formed by the rings $\{C_{i_-}\}_{1_-}^{n_-}$ and $\{C_{i_+}\}_{1_+}^{n_+}$ with $\ell_{i_-} > 0$ and $\ell_{i_+} < 0$ respectively. Then it is $n = n_+ + n_-$.

In Fig. (3) we show different ringed disks of the order $n = 4$ made by only $\ell$corotating sequence of counterrotating rings, while Fig. (4) shows different ringed disks of the order $n = 4$ with $\ell$counterrotating sub-sequences.

We discuss the conditions for the existence of a $\mathbf{C}^n$ configuration in terms of the $\mathcal{S}$ set. We prove that the set $\mathcal{S}$ consists of mutually dependent elements, in particular we will provide constraints (specifically an upper limit) on the configuration order $n$ depending on the values of $\mathbf{p}_{\mathbf{C}^n}$. The relative rotation of the fluids belonging to different rings of the macro-structure has a decisive role in determining the ringed disk. In fact we will show that the conditions imposed on the $\ell$counterrotating sequences of the decomposition are particularly restrictive. On the other side, it is well known that the effective potential (6) for a Kerr-**BH** background does not have any double minimum or maximum. As a consequence of this fact, the set of sub-configurations $C_i \subset \mathbf{C}^n$, cannot be generated by an unique fixed constant $\mathbf{p}_i = \mathbf{p}_j$, from the same

specified the $i-$ sub-configuration of decomposition, ordered according to the scheme described in the text, see also Figs. (2 ).

[6]This is indeed, accordingly, the maximum available information as it is extractable from the model of the single ring introduced in Sec. (2), i.e., the maximum number of characteristics of each individual ring, element of the decomposition, which constitutes a ringed disk. A macro-configuration $\mathbf{C}^n$ at a fixed order $n$ *only*, in general has not a unique decomposition. In fact there can be more then one set of different rings, $\{C_i\}_{i=1}^n$ and $\{\tilde{C}_j\}_j$ with different sequences of parameters $\mathbf{p}_{\mathbf{C}^n} \equiv \{\mathbf{p}_i\}_{i=1}^n \neq \{\tilde{\mathbf{p}}_i\}_{i=1}^n \equiv \tilde{\mathbf{p}}_{\mathbf{C}^n}$. One could ask how many decompositions are possible for a disk (or in how many ways one can decompose a ring accretion disk) with a proper fixed set of characteristics. Viceversa what is, if it exists, the minimum number of morphological characteristics (such as the torus thickness, the disk elongation etc) or dynamics (the angular momentum distribution in its decomposition) to be specified, in order to uniquely determine the decomposition $\mathbf{C}^n$ (or equivalently $\mathbf{p}_{\mathbf{C}^n}$) of the disk.

effective potential $V_{eff}(\ell, a, r)$ inferred by the Euler equation. We consider in fact the disjoint union of the sub-configurations, or at last the union with a couple of double points only for each contour of one ring (i.e. the conditions $y_3^i = y_1^{i-1}$ and $y_3^{i+1} = y_1^i$–see below).

Each configuration $C_i$ is thus a solution of an Euler equation for a unique constant $\mathbf{p}_i$. The tori of the decomposition are linked by some boundary conditions, raised from the fact that they are not isolated elements but part of a macro-structure $\mathbf{C}^n$–we will discuss in details this point in the next Sections. These boundary conditions determine the macro-structure as one (structured) body along with a proper internal dynamics. In other words, although the tori are not tied by the same potential $V_{eff}(\mathbf{p})$, their presence as sub-configuration in $\mathbf{C}^n$ imposes some limits, constraining their angular momentum or thickness, their locations, number and their equilibrium. They may even lead to some instability phenomena for $\mathbf{C}^n$, or feeding of one disk from another.

More precisely, in a more *general* situation, one could generalize the definition of macro-configuration considering a toroidal configuration made up by a set of $n$ tori, obtained by the Euler equation and associated to $n$ generic parameters $\mathbf{p}_{\mathbf{C}^n} = \{\mathbf{p}_i\}_{i=1}^n$, that can then be intertwined, looped or separated at less than a double point or

***Intertwined*** tori are $C_{i+1} \cap C_i \neq \emptyset$ *and* $\partial C_{i+1} \cap \partial C_i \neq \emptyset$. We say that configurations made up by intertwined tori have an *ordered decomposition* meaning that it is possible to order the sequence of disks $C_i$ or $C_i < C_{i+1}$ if and only if $r_{cent}^i < r_{cent}^{i+1}$ for $i \in \{1, ..., n\}$.

***Looped*** tori are defined by the condition $C_i \subset C_{i+1}$ in the equatorial plane, i.e a no-crossing disk loop occurs. Turning unstable, even if formed, they could possibly turn into a single, energetically more favorable configuration, for the fluid fills the entire contour ($\partial C_i$) at equal $\ell$ to ensure the existence and stability of the orbiting matter. In other words, a loop of tori is defined as the macro-structure $\mathbf{C}^n \equiv \bigcup_{i=1}^n C_i : \; C_i \subset C_{i+1}$ and $\partial C_i \bigcap \partial C_{i+1} = \emptyset \; \forall i \in \{1, n-1\}$, where $n$ is the order of the loop. These configurations may have some relevance in models with a non-constant angular momentum distribution along each disk (Lei et al. 2008). We say that the macro-configuration $\mathbf{C}^n$ made up by looped tori admits an *ordered decomposition*, if the sequence of sub-configurations $C_i$ satisfies $C_i \subset C_{i+1}$ and $\partial C_i \subset C_{i+1}$ for $i \in \{1, ..., n\}$. A particular kind of looped tori are the ***centered*** tori defined as loops

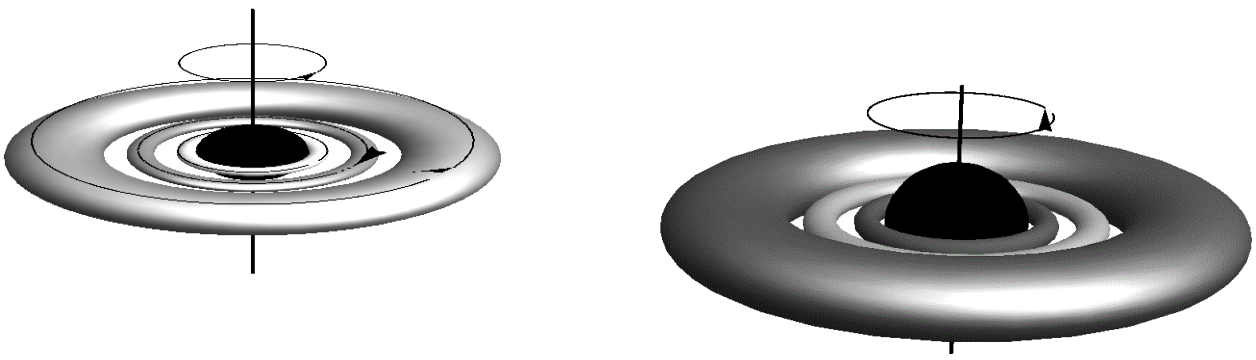


Fig. 1.— Pictorial representation of a ringed accretion disk $\mathbf{C}^3$ of order $n = 3$. The black region is $r < r_+$ where $r_+$ sets the outer horizon for a black hole attractor.

of tori where $\forall\{i, j\} \in \{1, ...n\}$ $r_{min}^i = r_{min}^j$, where $r_{min}^i$ is the disk center and also the *loop center*. We note that sub-configurations with $\ell_{(\mathbf{i})} = \ell_{(\mathbf{o})}$ are (necessarily) looped (in particular we stress it has

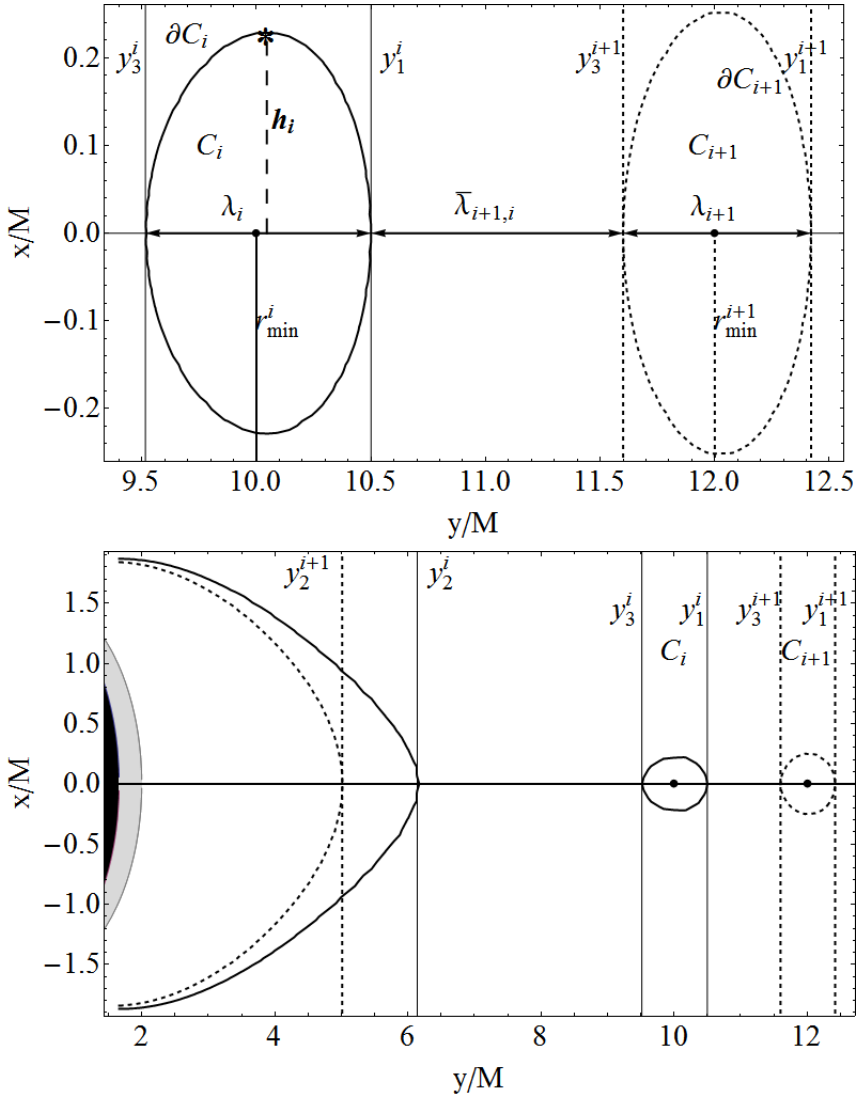



Fig. 2.— Cross sections on the equatorial plane of the consecutive Boyer surfaces of two separated rings $C_i < C_{i+1}$, with boundaries $\partial C_i$ and $\partial C_{i+1}$, the rings centers $r_{min} = r_{cent}$ are signed with points and the lines $r_{min}$ =constant. With $r/M = \sqrt{x^2+y^2}$ and $(x, y)$ are Cartesian coordinates. The inner $y_3$ and outer $y_1$ edge are also signed, $\lambda_a = y_1^a - y_3^a$ for $a \in \{i, i+1\}$ are the rings elongation and $\lambda_{i+1,i} = y_3^{i+1} - y_1^i$ is the spacing among the rings. $h_i \equiv x_{Max}^i$ is the height associated to the sub-configuration $C_i$, or the maximum point of the surface $\partial C_i$ The $\ell$corotating rings, rotate around a black hole attractor with spin $a = 0.75M$ and specific angular momentum $\ell_i = -4.2897$ and $\ell_{i+1} = -4.41883$. Black region in $r < r_+$, and gray region in $r < r_\epsilon^+$, where $r_+$ is the spacetime outer horizon while $r_\epsilon^+$ is the static limit.

to be $\partial C_i \bigcap \partial C_{i+1} = \emptyset$ that means they cannot be interwined) *and* they are (necessarily) centered (i.e. $r_{min}^{(\mathbf{i})} = r_{min}^{(\mathbf{o})}$, $r_{min}$ being the disk center).

***Separated*** tori are defined, for a $n$-order macro-structure $\mathbf{C}^n = \bigcup_1^n C_i$, according to the following condition

$$C_i \bigcap C_j = 0 \quad \text{and} \quad \partial C_i \bigcap \partial C_j = \{\emptyset, y_1^i = y_3^j\} \quad \text{where} \quad i < j. \tag{7}$$

For $n = 2$, a double configuration, $C_{(\mathbf{i})} \cap C_{(\mathbf{o})} = \emptyset$ or those with $y_1^{(\mathbf{i})} = y_3^{(\mathbf{o})}$ where the outer edge of the

inner rings coincides with the inner edge of the outer ring. In other words for macro-configurations made by separated tori, the penetration of a ring within another ring is not possible. However, as the condition $y_1^{(\mathbf{i})} = y_3^{(\mathbf{o})}$ can hold, in a limit situation the collision of matter between the two surfaces at contact point $y_1^i = y_3^j$ could be possible. Ringed disks $\mathbf{C}^n$, made by separated tori, have an *ordered decomposition*, if the sequence of rings $C_i$ satisfies $C_i < C_j$ if and only if $r^i_{cent} \equiv r^i_{min} < r^j_{min} \equiv r^j_{cent}$ for $i < j$, $C_i$ being the inner one, closest to attractor, with respect to $C_j$. Within these definitions, the rings $(C_i, C_{i+1})$ and $(C_{i-1}, C_i)$ are *consecutive* if $C_{i-1} < C_i < C_{i+1}$. Figs. (2,3). Then one can clarify condition (7) by saying that $\partial C_i \bigcap \partial C_j = \emptyset$ or it is $\partial C_i \bigcap \partial C_j = \{\emptyset, y_1^i = y_3^j\}$ if $j = i + 1$.

see also (Pugliese&Montani 2015a).

In this work we consider only macro-configurations constituted by separated tori. We introduce also the following definitions for the $\ell$counterrotating sub-sequences of a decomposition of the order $n = n_+ + n_-$, of *isolated* $\ell$counterrotating sequences if $C_{n_-} < C_{1_+}$ or $C_{n_+} < C_{1_-}$ and *mixed* $\ell$counterrotating sequences if $\exists\, i_+ \in [1_+, n_+] :\ C_{1_-} < C_{i_+} < C_{n_-}$ or viceversa $\exists\, i_- \in [1_-, n_-] :\ C_{1_+} < C_{i_-} < C_{n_+}$. Alternately,

**(i-a)** *isolated* $\ell$counterrotating sequences $\overbrace{\mathbf{C}}^{}_{s}$ : $[r^{1_-}_{min}, r^{n_-}_{min}] \cap [r^{1_+}_{min}, r^{n_+}_{min}] = 0$, then the couple of rings $C_{n_\pm}$ are consecutive and we say the $\ell$counterrotating isolated sub-sequences of order $n_\pm$ respectively are consecutive, Fig. (4)-top.

**(i-b)** *mixed* $\ell$counterrotating sequences $\overbrace{\mathbf{C}}^{}_{m}$ : $[r^{1_-}_{min}, r^{n_-}_{min}] \cap [r^{1_+}_{min}, r^{n_+}_{min}] \neq 0$ Fig. (4)-bottom.

We shall neglect the inner lobe of a ring $C_i$ in equilibrium and associated with $y_2$ as in Fig. (2). In fact, we assume that the existence of this innermost surface does not influence the outer lobe of the Boyer surface, when this is far from its critical cusped phase $C^i_x$. The basis of this assumption relies in the fact that for each closed toroidal Boyer $C$-configuration the two lobes are separated, as long as the $\mathbf{p}$ parameter of the closed $C$-ring remains far from the critical values, where the ring morphology changes for $C$ to $C_x$. The cross is then a contact point between the two surfaces, and a P-W instability cusp, in other words $y^i_2 = y^i_3$.

Therefore, at the equilibrium the two lobes of a $C_i$ ring, both regulated by Eq. (6) at equal $\mathbf{p}_i$, without considering any other further interaction due for example to possible magnetic fields of the disk environment, are geometrically separated and dynamically independent.

In Sec. (3.1) we introduce three special macro-configurations associated with the instability phases of the ringed disk. In Sec. (D) some general considerations on the perturbations of the ringed disks and their equilibrium follow. This section closes in Sec. (3.2) with a review of the major morphological features of the ringed disk $\mathbf{C}^n$, while the height and thickness of $\mathbf{C}^n$ are finally detailed in Sec. (A).

### 3.1. Unstable macro-configurations

We focus on the possible unstable ringed configurations $\mathbf{C}^n$. There are two main instabilities which lead to (global) instability for a $\mathbf{C}^n = \bigcup^n C_i$ disk and correspondingly two distinct models (with degenerate topology) of unstable configurations.

Firstly, the instability arising inside the decomposition of the macro-structure, and induced by the action of $C_i$ ring in equilibrium on the other (consecutive) $C_{i\pm1}$ ring, for overlapping of materials with consequent collisions. Secondly the P-W instability of one or more rings of the decomposition, in its unstable phase. With the consequent destabilization of the entire decomposition, resulting eventually in a different topology, where the rings are no more separated. The unstable ringed disks can be in one of the following macro-configurations

**The macro-structure $\mathbf{C}^{\mathbf{n}}_{\odot}$** In this model the disk could lead to possible unstable decompositions with feeding of matter from one ring to the other consecutive one, or collision of the orbiting material of the

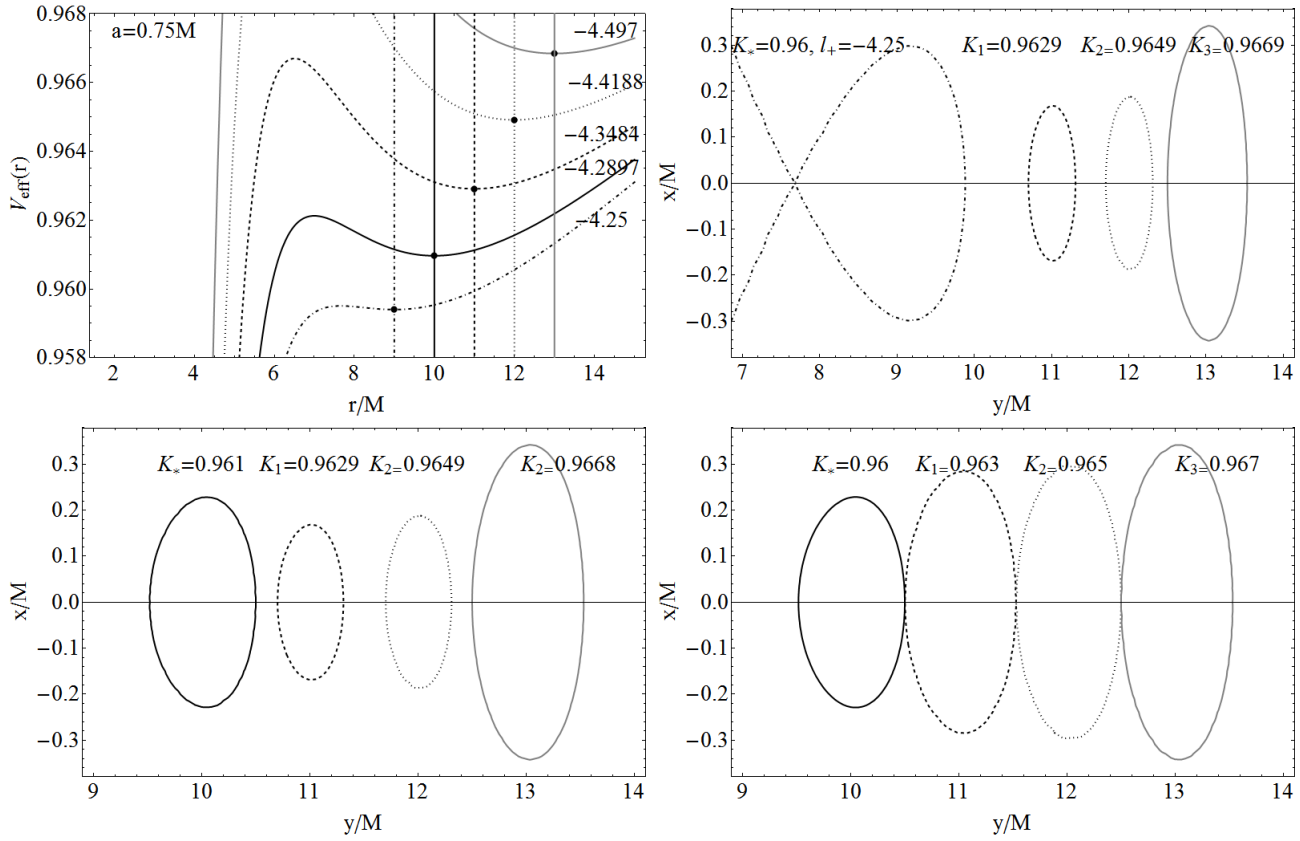



Fig. 3.— Spacetime spin $a = 0.75M$: $\ell$corotating sequences $\bar{\mathfrak{C}}_{1b}$-configurations ($\ell_i\ell_j > 0$) of counterrotating disks ($\ell_i a < 0\ \forall ij$). It follows the discussion in Sec. (4.3), Eq. (28). Upper left panel shows the effective potential as a function of $r/M$ for different values of $\ell_+$ indicated close to the curves. The minimum points of the potential are indicated by points and the lines $r_{min}$ =constant. The other panels show sections of the decompositions associated to each specific angular momentum, the values of $K_i$ for each Boyer configuration, are indicated in the figures. Upper left panel: Ringed disk $\mathbf{C}^4_x$ in accretion. Bottom left panel: separated ringed $\mathbf{C}^4_\odot$ disk. The specific angular momenta have been set so as to have a distance between the centers $\delta^{i+1,i}_{min} = M$ constant with the index configuration, then the algorithm for the choice of the sequence $\{K_i\}^n_{i=1}$ was fixed assuming $K_* = K_0 = V_{eff}(\ell_0, r^0_{min} + 1/2)$, and $K_i = V_{eff}(\ell_i, r^{i-1}_{min} + 0.7)$. Right-bottom panel: saturated ringed $\mathbf{C}^4_\odot$ disk of maximum rank $\mathfrak{r}_{Max} = 3$. In the sequences $\{K_i\}^n_{i=1}$ the difference $K^i_{min} - K_i \approx 0$ are of the order of $10^4$ c.a but the elongation $\lambda_i$ are not neglible.

two disks. For these disks there is at last $i \in \{1, ..., n-1\}$ : $C_i \cap C_{i+1} = \emptyset$ and $\partial C_i \cap \partial C_{i+1} = \{y^i_1 = y^{i+1}_3\}$, as clarified in Fig. (3); we could define $y^i_1$ as a *double* point of the decomposition. We define *rank* $\mathfrak{r}$ of a $\mathbf{C}^{\mathbf{n}}_\odot$ ringed disk the number of double points of its decomposition. The maximum possible rank for an $n$-order configuration $\mathbf{C}^{\mathbf{n}}_\odot$ is $\mathfrak{r}_{Max} = n - 1$ where $\forall i \in \{1, ..., n-1\}\ C_i \cap C_{i+1} = \{y^i_1 = y^{i+1}_3\}$. If the ringed disk $\mathbf{C}^{\mathbf{n}}_\odot$ has the maximum rank, we call it *saturated* ringed disk. Fig. (3) shows an example of saturated ringed disk of the order $n = 4$ and maximum rank $\mathfrak{r}_{Max} = 3$.

**The macro-structure $\mathbf{C}^{\mathbf{n}}_{\mathbf{x}}$** This ringed disk has at last one sub-configuration $C^i_x$ in its decomposition, that is a ringed torus with a self-cusped topology, the cross being a P-W accretion point, with $\pm\ell_\mp \in\ ]\pm\ell^\mp_{mso}, \pm\ell^\mp_\gamma[$, see Fig. (3). We define *rank* $\mathfrak{r}_\mathfrak{x}$ of the ringed disk $\mathbf{C}^{\mathbf{n}}_{\mathbf{x}}$ the number of P-W instability points

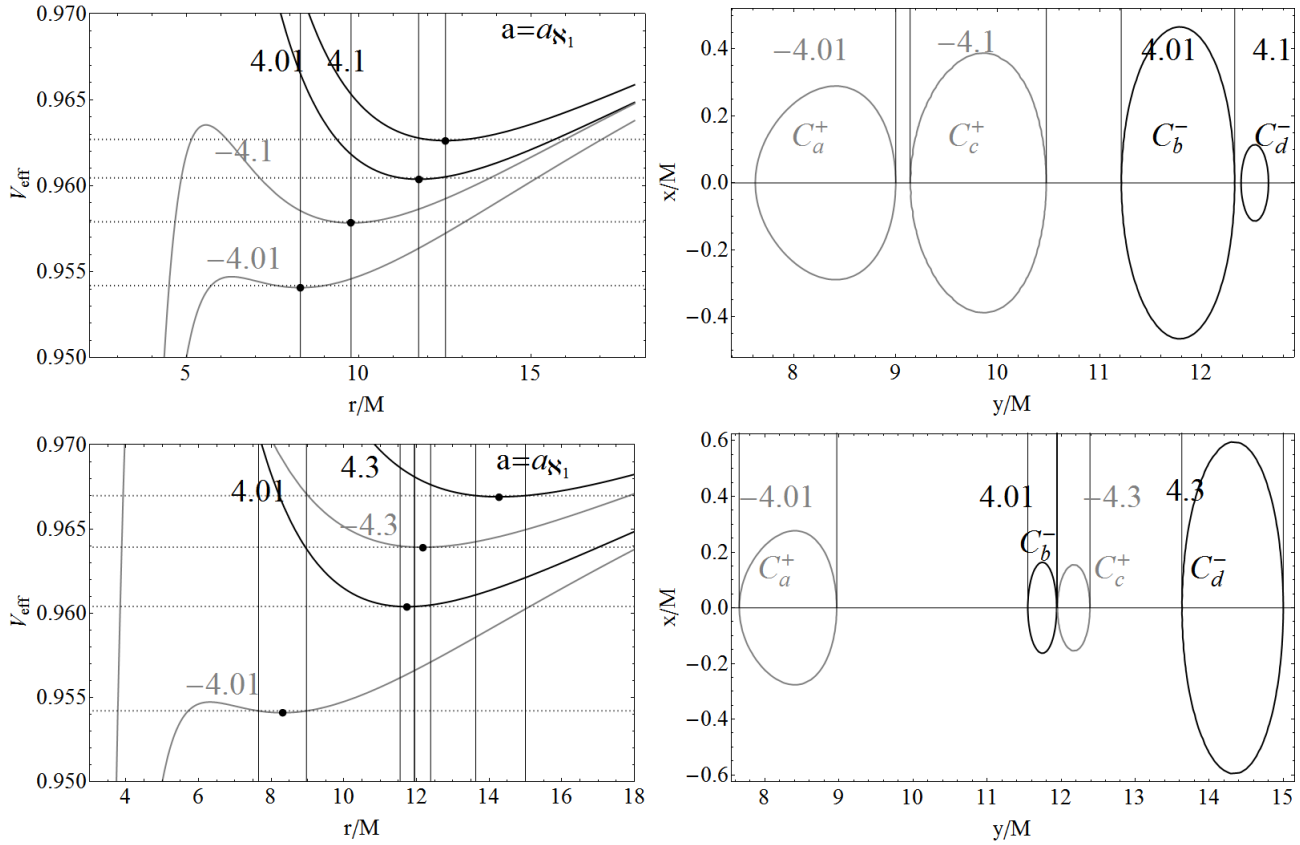



Fig. 4.— $\ell$counterrotating sequences. Spacetime $a_{\aleph_1} = 0.382542M$ The outer horizon is at $r_+ = 1.92394M$ the marginally bounded orbits are located in $r^+_{mbo} = 4.73417M$ and $r^-_{mbo} = 3.18903M$, the marginally circular orbits are in $r^+_\gamma = 3.41407M$, $r^-_\gamma = 2.51784M$. Left panels: effective potentials as functions of $r/M$. The specific angular momenta are close to the curves in gray for counterrotating matter and black for corotating fluids. Points sign the minimum of the functions. Vertical lines are the ring edges as determined by the sequences of $\{K_i\}^n_{i=1}$. Right panels: Boyer surfaces of the decomposition, the curves associated with each specific angular momentum of the effective potential are shown with curves of the same color of its potential. It follows the discussion in Sec. (4.3.2) and in particular Eq. (41). Upper panels show isolated sequences, bottom panels show mixed sequences.

in its decomposition. For a ringed disk of order $n$, the maximum rank could be in general $\mathfrak{r}_{\mathfrak{r}\,Max} = n$.We characterize these particular decompositions in details in the following Sections, especially the location of $C^i_x$ in the mixed or isolated decompositions. A $\mathbf{C}^n_x$ topology could be also a $\mathbf{C}^n_\odot$ leading to the following third macro-structure:

**The macro-structure $\mathbf{C}^{\mathbf{x}\,n}_\odot$** This $\mathbf{C}^{\mathbf{x}}_\odot$ disk is characterized at last by a $C^i_x$ ring where $y^{i-1}_1 = y^i_3 = y_{cusp}$. Clearly a $\mathbf{C}^{\mathbf{n}}_\odot$ can be also a $\mathbf{C}^{\mathbf{n}}_{\mathbf{x}}$ but not a $\mathbf{C}^{\mathbf{x}\,n}_\odot$ one. In any case ringed disk of $\mathbf{C}^{\mathbf{x}\,n}_\odot$ topology violates the condition of separation or non penetration of matter that will be discussed in more details later.

### 3.2. Definition of the major morphological features of the ringed disk $\mathbf{C}^n$

There we focus on the properties of separated ringed disks $\mathbf{C}^n$. We character the disk morphology introducing the definition of the thickness and elongation of the ringed disk. The macro-structure $\mathbf{C}^n$,

as made by an ordered set or sequence of separated rings $C_i$ of its decomposition, has a disconnected topology. The symmetry for reflection on the equatorial plane is inherited by the macro-structure $\mathbf{C}^n$, and the symmetry plane of each $C_i$ and $\mathbf{C}^n$ is also the symmetry plane of the attractor. It is useful to introduce a toroidal surface $\partial\mathbf{C}^n$ the for macro-structure $\mathbf{C}^n$, plotted as the regular toroidal surface generated by the circular cross-sections, obtained as the envelope surface $\partial\mathbf{C}$ of the (closed) $\partial C_i$, and the associated solid torus including the spacings (the vacuum regions among the sub-configurations as formally defined below), that we identify with $\mathbf{C}^n$. The introduction of this surface, could be useful in the definition of some morphological properties of the ringed accretion disk, such as the thickness, and the height defined as the respective quantities of its envelope. One may estimate the total (global) dimensions of the ringed disks, by an envelope surface. The curve $\partial\mathbf{C}$ is tangent the sub-configurations at least in the maximum points: $y^i_{Max} \in \partial\mathbf{C}$. The surface $\partial\mathbf{C}$ has yet a regular constant generatrix as generated from tori with regular generatrix, and the symmetry for reflection on the equatorial plane and the symmetry relative to the symmetry axis are inherited by the macro-configuration, but the envelope surface may have more maximum points $y^i_{Max} \in \partial C_i \cap \partial\mathbf{C}$. However, this surface can be better defined by introducing an effective potential for configuration[7] $\mathbf{C}_n$ what will be discussed in Sec. (A.1).

In the following part we give the definitions of some main features of the ringed torus on the basis of morphological characteristics of the single ring of its decomposition.

The *inner edge*, $\partial\mathbf{C}^n_-$, of any macro-configuration $\mathbf{C}^n$ of order $n$ is located in the equatorial plane and associated to the solution $y^1_3$ that is $\partial\mathbf{C}^n_- = \partial C_1$ for the inner edge of the inner ring of its decomposition and the *outer edge* $\partial\mathbf{C}^n_+$ to the solution $y^n_1$ of the outer ring of the decomposition see Fig. (2).

For any sub-configuration $C_i \subset \mathbf{C}^n$ we introduce the range $\lambda_i \equiv ]y^i_1, y^i_3[$ whose measure $\lambda_i \equiv y^i_1 - y^i_3$ is the *elongation* of the Boyer surface cross section $\partial C_i$ on the equatorial plane as shown in Fig. (2).

For any $i \in \{1, ...n-1\}$ the range $\bar{\Lambda}_{i+1,i} \equiv ]y^{i+1}_3, y^i_1[$ whose measure $\bar{\lambda}_{i+1,i} \equiv y^{i+1}_3 - y^i_1$ defines the *spacing* between two subsequent sub-configurations indicated $C_i$ and $C_{i+1}$ respectively, see Fig. (2).

It is clear that in the case of macro-configuration $\mathbf{C}^n_\odot$ of rank $\mathfrak{r}$, there are $\mathfrak{r}$ rings of its decomposition where $C_i : \ \bar{\lambda}_{i+1,i} = 0$ see Fig. (3). In the following we will use indifferently, when not necessary to specify, the term elongation and spacing for $\lambda_i$ e $\bar{\Lambda}_i$ and their measures respectively.

Thus the elongation $\Lambda_{\mathbf{C}^n}$ of $\mathbf{C}^n$ is:

$$\Lambda_{\mathbf{C}^n} \equiv [y^1_3 - y^n_1] = \left(\bigcup_{i=1}^{n} \Lambda_i\right) \bigcup \left(\bigcup_{i=1}^{n-1} \bar{\Lambda}_{i+1,i}\right) = \Lambda_n \cup \bigcup_{i=1}^{n-1} \left(\bar{\Lambda}_{i+1,i} \cup \Lambda_i\right), \tag{8}$$

whose measure is the elongation $\lambda_{\mathbf{C}^n}$ of the (separated) configuration $\mathbf{C}^n$, that is explicitly:

$$\lambda_{\mathbf{C}^n} \equiv y^n_1 - y^1_3 = \sum_i^n \lambda_i + \sum_{i=1}^{n-1} \bar{\lambda}_{i+1,i} \geq \lambda^{inf}_{\mathbf{C}^n} \equiv \sum_i^n \lambda_i \Big|_{\sum_i \lambda_i} . \tag{9}$$

Equation (9) shows that the minimum value $\lambda^{inf}_{\mathbf{C}^n}$ of the elongation $\lambda_{\mathbf{C}^n}$ is achieved, *at fixed* $\sum_i^n \lambda_i$, when $\bar{\lambda}_{i+1,i} = 0; \forall i$ that is for a $\mathbf{C}^n_\odot$ configuration of rank $\mathfrak{r} = \mathfrak{r}_{Max}$.

We should note that the total elongation of the ringed disk $\lambda_{\mathbf{C}^n}$ can be regarded, as shown by the second equality of Eq. (9), as the addition of two components: the sum $\mathcal{S}_\lambda > 0$ of the elongations of each of its sub configurations, which is a strictly positive quantity, and the sum $\mathcal{S}_{\bar{\lambda}} \geq 0$ of its spacings, where this quantity

[7] Actually the equation for the envelope could be $\mathcal{V}_{eff}(i, x, y) = V_{eff}(i, x, y) - K_i = 0$, and $\partial_i \mathcal{V}_{eff}(i, x, y) = 0$ where the envelope index $i$ is the (ordered) decomposition index attached to each sub-configuration, then as $\partial_i \equiv \partial_{r_{min}}$.

may be positive or zero. There is $\mathcal{S}_{\bar{\lambda}} = 0$ for the saturated configuration $\mathbf{C}^n_{\odot}$, realizing simultaneously **(a.)** the ringed configuration of minimum elongation $\lambda_{\mathbf{C}^n}|_{\mathcal{S}_\lambda}$ *at fixed sum* $\mathcal{S}_\lambda$ and, **(b.)** consistently the maximum elongation $\lambda_{\mathbf{C}^n}$, when the sum $\mathcal{S}_\lambda$ is, at fixed order $n$, a variable.

The property **(a.)** comes straightforwardly, once one considers the key aspect that the sum $\mathcal{S}_\lambda$ has been kept fixed, independently from $\mathcal{S}_{\bar{\lambda}}$. This is immediately obtained from Eq. (9). To be more explicit if, for example, we consider $\mathcal{S}_\lambda$ as a known data, by canceling the second contribution to the total elongation derived from the displacement, then $\lambda_{\mathbf{C}^n}$ has the sole, invariant, $\mathcal{S}_\lambda$ component. This immediately implies that all the ringed disks with equal $\mathcal{S}_\lambda$ have the same minimum elongation when they are saturated, i.e., the part on the equatorial plane occupied by matter is the same *independently* of the distribution of angular momentum, or the order $n$, which can be $n = 1$ or also arbitrarily large.

The property **(b.)** stands as $\mathcal{S}_\lambda$ is considered no longer as a fixed quantity. We should note in fact that, if we evaluate the infimum $\inf \lambda_{\mathbf{C}^n}$ of the total elongation, by minimizing $\sum_i^n \lambda^i_{min}$, (no longer regarded as fixed) i.e. rearranging the decomposition to minimize each term $\lambda_i$ (or rather to minimize the total sum $\mathcal{S}_\lambda$), one would disregard the fact that the spacings $\bar{\lambda}_{i+1,i}$ are indeed related to the functions $\lambda_i$. As a consequence of this fact the minimization of $\lambda_i$ could lead to $\bar{\lambda}_{i+1,i} \neq 0$. Viceversa, the sub-configurations satisfying $\bar{\lambda}_{i+1,i} \neq 0$ could lead to a greater $\sum_i^n \lambda_i$. While, at fixed $\sum_i^n \lambda_i$, the inequality in (9) is certainly verified as it is $\bar{\lambda}_{i+1,i} \geq 0$, and thus the definition $\lambda^{inf}_{\mathbf{C}^n}$ is not inconsistent. It can be shown that the $n$-order decomposition of the (fixed) macro-structure realizing the condition $\bar{\lambda}_{i+1,i} = 0\ \forall i$ maximizes the total sum $S_\lambda = \sum_i^n \lambda_i$ of the elongations. Thus this decomposition provides the maximum elongation for the ringed accretion disk. In other words in the former case **(a.)** the elongation $\lambda_{\mathbf{C}^n}$ is minimized as function of $\mathcal{S}_{\bar{\lambda}}$ with $\mathcal{S}_\lambda$ being a fixed parameter. Therefore, by minimizing $\mathcal{S}_{\bar{\lambda}}$ at fixed $\mathcal{S}_\lambda$, in the **(b.)** case we maximize $\lambda_{\mathbf{C}^n}$ considering $\mathcal{S}_\lambda$ as a function of $\mathcal{S}_{\bar{\lambda}}$, showing that the first is maximized when the second is minimized[8].

It is convenient to show the dependence of the elongation $\lambda_{\mathbf{C}^n}$ from the spacing $\bar{\lambda}_{\mathbf{C}^n}$ defined below, by explicit the sum in (9):

$$\lambda_{\mathbf{C}^n} = y^n_1 - y^1_3 = \sum_{i=1}^{n}(y^i_1 - y^i_3) + \sum_{i=1}^{n-1}(y^{i+1}_3 - y^i_1) = \sum_{i=1}^{n-1}(y^{i+1}_3 - y^i_3) + \lambda_n \tag{10}$$

$$\bar{\Lambda}_{\mathbf{C}^n} \equiv \bigcup_{i=1}^{n-1} \bar{\Lambda}_{i+1,i}, \quad \bar{\lambda}_{\mathbf{C}^n} \equiv \sum_{i=1}^{n-1} \bar{\lambda}_{i+1,i} = +(y^n_3 - y^1_1) - \sum_{i=2}^{n-1}\Big|_{n>2} \lambda_i \geq 0. \tag{11}$$

Equation (10) relates the elongation $\lambda_{\mathbf{C}^n}$ of the $n$-order configuration $\mathbf{C}^n$ to the elongation $\lambda_n$ of the $n$th-sub-configuration $C_n$ and to the relative position of the inner edges of the remaining sub-configurations of the decomposition, so that one need to know only $\lambda_n$ and the location of the inner edges on the interior rings $y^i_3$, to establish the elongation $\lambda_{\mathbf{C}^n}$. Because the sum in Eq. (10) does not include any term related to the $n$th-configuration, the minimization of the two distances at the right side of Eq. (10), is independent of each other.

Equation (11) is the sum of the spacings $\bar{\lambda}_i$ (we note that this is precisely $S_{\bar{\lambda}}$), it indicates how large portion of the macro-structure $\mathbf{C}^n$ is not filled with the fluid.

Moreover, it explicits the dependence of $\bar{\lambda}_{\mathbf{C}^n}$, from the elongations $\lambda_i$ of the rings $C_i \in \{2, n-1\}$.For a configuration of the order $n = 2$, there is $\bar{\lambda}_{\mathbf{C}^2} \equiv \bar{\lambda}_{2,1} = +(y^2_3 - y^1_1)$. However, since the ring elongations contribute negatively to the total spacing, we infer from the inequality in (11) that $y^n_3 - y^1_1$ (the distance between the inner edge of the external configuration $\partial C^-_n$ and the outer one $\partial C^+_1$ of the inner one) is greater that the sum of the elongations of the $2, ..., n-1$ rings. The sum does not include any term related to the $C_1$ and $C_n$ sub-configurations, as such minimization of the two terms in (11) can be considered a priori independently.

[8] The issue if any ringed disk, at fixed $\{\ell_i\}^n_{i=1}$, could be set in a saturated configuration (i.e. $\mathcal{S}_{\bar{\lambda}} = 0$) is faced in Sec. (4.3.2) where we will discuss more thoroughly this problem, also considering the constraints that the corresponding sequence of parameters $\{K_i\}^n_{i=1}$ has to satisfy in order to be realized as saturated configuration.

Then the smaller is the elongation of the interior configurations the larger is the spacing $\bar{\lambda}_{\mathbf{C}^n}$, where the minimum $\bar{\lambda}_{\mathbf{C}^n} = \bar{\lambda}^{inf}_{\mathbf{C}^n} = 0$ is realized in Eq. (11) when $\sum_{i=2}^{n-1}\Big|_{n>2} \lambda_i = (y_3^n - y_1^1)$, which corresponds to a saturated $\mathbf{C}^n_\odot$ configuration. A definition of *height* and *thickness* of the ringed disk is discussed in Sec. (A), this allows to characterize morphologically the disk as a single body.

## 4. Decompositions and analysis of the model parameters

Any sub-configuration $C_i$ in equilibrium[9] satisfies the following property:

$$\Delta r^i_{crit} \cap \lambda_i = \{y^i_3\}, \quad \forall i. \tag{12}$$

or, we can write the condition (13) explicitly as

$$r^i_{mbo} < r^i_{Max} < y^i_3 < r^i_{min} < y^i_1 \quad \text{and} \quad r^i_{min} > r^i_{mso}. \tag{13}$$

For a $n$-order configuration $\mathbf{C}^n$ the separation condition:

$$\mathbf{C}^n : \ \lambda_i \cap \Lambda_j = \emptyset \ \forall i,j \in \{1,...,n\} \quad \text{and} \quad \mathbf{C}^n_\odot : \ \lambda_i \cap \Lambda_j = \{y^i_1 = y^j_3\} \ \forall i < j \in \{1,...,n\} \tag{14}$$

must be satisfied, where $\lambda_i$ are the elongation ranges as introduced in Sec. (3.2). Conditions (14) are in fact equivalent to the condition of separation or no penetration of the material in Eq. (7). To fix the ideas we can consider the case of the macro-structures $\mathbf{C}^2$, then we use explicitly the condition (14) for the case of $n = 2$. Considering the role of the maximum and minimum points, we obtain the following conditions:

$$\begin{aligned} &r^{(\mathbf{i})}_{Max} \le y^{(\mathbf{i})}_3 < r^{(\mathbf{i})}_{min} < y^{(\mathbf{i})}_1 \le y^{(\mathbf{o})}_3 < r^{(\mathbf{o})}_{min} < y^{(\mathbf{o})}_1, \\ &r^{(\mathbf{i})}_{mso} < r^{(\mathbf{i})}_{min} < r^{(\mathbf{o})}_{min} \quad \text{and} \quad r^{(\mathbf{o})}_{mso} < r^{(\mathbf{o})}_{min}. \end{aligned} \tag{15}$$

On the other hand, the generalization of Eqs. (15,15) to an $n$-order configuration is straightforward.

Relation Eq. (15) is a very general condition for existence of the separated configurations. This relation is necessary for the existence of disjoint configurations for that it can be considered as a criterion to establish the *inner* (**i**) and *outer* (**o**) configurations, Fig. (2). However Eq. (15) do not indicate the relative position of the marginally stable orbits, which obviously determines the order of the corotating and counterrotating rings, neither the relative location of the maximum points which, as shown in the next Sections, could be able by itself to constraint in some cases the order $n$ of the decomposition. It is thus necessary to fix the couple $\Delta^{(\mathbf{i},\mathbf{o})}_{mso} \equiv (r^{(\mathbf{i})}_{mso}, r^{(\mathbf{o})}_{mso})$ and $\Delta^{(\mathbf{i},\mathbf{o})}_{Max} \equiv (r^{(\mathbf{i})}_{Max}, r^{(\mathbf{o})}_{Max})$ as related to each other. If the measure $\delta^{(\mathbf{i},\mathbf{o})}_{mso} = r^{(\mathbf{o})}_{mso} - r^{(\mathbf{i})}_{mso} = 0$, the configurations are $\ell$corotating, while for $\delta^{(\mathbf{i},\mathbf{o})}_{mso} > 0$, the outer ring is counterotating while the inner one is corotating, and viceversa for $\delta^{(\mathbf{i},\mathbf{o})}_{mso} < 0$.

Within the condition in Eq. (15) for a couple of rings, two cases can occur, according to the location of the maximum points $\Delta^{(\mathbf{i},\mathbf{o})}_{Max}$ and to the permutation in the ordered couple $(r^{(\mathbf{i})}_{min}, r^{(\mathbf{o})}_{Max})$; the case $r^{(\mathbf{i})}_{min} \equiv r^{(\mathbf{o})}_{Max}$ will be discussed in Sec. (4.5.4)). More generally for a $\mathbf{C}^n$ configuration, there are the possibilities

$\bar{\mathfrak{C}}_0$**:** corresponding to $\Delta^i_{cri} \cap \Delta^{i+1}_{cri} = \emptyset$, or explicitly $r^i_{Max} < r^i_{min} < r^{i+1}_{Max} < r^{i+1}_{min}$;

Then there can be $r^{i+1}_{Max} < r^i_{min}$.

Considering the role of $r^i_{Max}$, it can be either:

[9]For the considerations of this section and in the most of this work we will assume the existence of $\Delta r^i_{crit}$, in particular the existence of a maximum point of the effective potential. But we should specify here, as already mentioned earlier, that the minimum, center of the configuration, always exists for $\pm\ell^{\mp} > \pm\ell^{\mp}_{mso}$, while the minimum point, corresponding to instability exists only if $\pm\ell^{\mp} \in ]\pm\ell^{\mp}_{mso}, \pm\ell^{\mp}_{\gamma}[$ with the consequence that if $\pm\ell^{\mp} \ge \pm\ell^{\mp}_{\gamma}$, only equilibrium configurations may exist. For $\pm\ell^{\mp} > \ell^{\mp}_{\gamma}$, it is possible generalize these definitions as done in (Pugliese&Stuchlik 2015)

$\bar{\mathfrak{C}}_{1a}$**:** that is $r^{i+1}_{Max} \in \Delta^i_{crit}$, explicitly $r^i_{Max} < r^{i+1}_{Max} < r^i_{min} < r^{i+1}_{min}$ or
$\bar{\mathfrak{C}}_{1b}$**:** that is $\Delta^i_{crit} \subset \Delta^{i+1}_{crit}$ or explicitly $r^{i+1}_{Max} < r^i_{Max} < r^i_{min} < r^{i+1}_{min}$ Fig. (3).

These cases, detailed in Sec. (4.4), and their generic combination in the decomposition of the order $n$ exhaust all the possibilities: the ringed disk can be $\bar{\mathfrak{C}}_0$, $\bar{\mathfrak{C}}_{1a}$ and $\bar{\mathfrak{C}}_{1b}$, or could have also a decomposition with consecutive rings belonging to one or the other cases. In the remainder of this section we characterize the role of the parameter $\mathbf{p} = (\ell, K)$ in Sec. (4.1), by focusing on the $K$-parameter in the ringed disks, in Sec. (4.2), and $\ell$-parameter and the relation between these in Sec. (4.3). Existence and structure of the ringed configurations is a topic of Sec. (4.4) which will continue in Sec. (4.5), with the analysis of the limiting cases on the $K$ parameters for a $n$-order decomposition. Some appendix sections complete the discussion of this section and particularly Sec. (B), (A.1) and (D).

### 4.1. The role of the parameter $\mathbf{p} = (\ell, K)$

The parameter $\mathbf{p}_{\mathbf{C}^n}$ associated to the macro-configuration of order $n$ is a sequence of ordered $n$-tuplet of couples $\{\mathbf{p}_i\}_{i=1}^n$ where $\mathbf{p}_i \equiv (\ell_i, K_i)$. Setting the ordered multi-parameter $\mathbf{p}_{\mathbf{C}^n}$ of the configuration means fixing univocally the macro-configuration $\mathbf{C}^n$ and its decomposition. According to the condition of separation (15), not all the choices of $\mathbf{p}_{\mathbf{C}^n}$ are possible, then a double (closed) configuration ($n = 2$) may exist if there is a couple of parameters

$$(\mathbf{p}_{(\mathbf{i})}, \mathbf{p}_{(\mathbf{o})}) : \quad \mathbf{p}_{(\mathbf{i})} \neq \mathbf{p}_{(\mathbf{o})} \quad \text{and} \quad y_1^{(\mathbf{i})} \leq y_3^{(\mathbf{o})}. \tag{16}$$

Then, in analogy with the case of the single torus (ring), we can define, at fixed order $n$, the matrix $\mathcal{B}^n_{\mathbf{p}}$ generated by all the possible variation of the couple $\mathbf{p}$, and the projections $(\mathcal{B}^n_\ell, \mathcal{B}^n_K)$ are generalized straightforwardly. For an $n$-order disk with $\mathbf{p}_i \neq \mathbf{p}_j$, three cases can occur:

**1.** $K_i = K_j$ This case give rise of $\mathcal{B}_\ell$ sequence. The stability conditions are discussed in Sec. (4.2) and Sec. (4.5).

**2.** $\ell_i = \ell_j$ The second case with sequences $\mathcal{B}_K$ of equal specific angular momentum is immediately ruled out, as these are evidently centered configurations (see also Fig. (6)). At constant $\ell$ the effective potential is uniquely defined as function of $r/M$, and there is only one minimum, if $\pm\ell^\mp > \pm\ell^\mp_{mso}$, and maximum, if $\pm\ell^\mp \in ]\pm\ell^\mp_{mso}, \pm\ell^\mp_\gamma[$ . The separated sub-configurations must have different specific angular momentum $\ell_i \neq \ell_j$, no separated rings with equal specific angular momentum can rotate one **BH** attractor. However, in the case of a $\ell$corotating couple $(C, O_x)$ with launching of jets from the P-W instability point $O_x$, the situation $\ell_i/\ell_j = 1$ would be possible, under a relaxation of the condition in (15) and $K = K_{Max} > 1$ for the open configuration governing the jets, and $K \in ]K_{min}, 1[$ for the concentric configuration $C$ in equilibrium.

**3.** $K_i \neq K_j$ **and** $\ell_i \neq \ell_j \quad \forall(i, j)$ . This is the most general case the couple parameters are both different.

### 4.2. On the individual role of the $K$-parameter in the ringed disks

The choice of the $K$ parameter for the decomposition of a ringed disk is very strict as each $K_i$ fixes the elongation $\lambda_i$ of the sub-configuration $C_i$. At fixed specific angular momentum $\ell_i$ one and only one $K_i$ can be set, although typically in an infinite but bounded range of values, constrained only by the condition of separations between the rings in equilibrium or in accretion. Conversely, for a fixed $K_i$, we can set in general a number $n$ of different specific angular momenta defining the ordered decomposition. We will use this last property to set in Sec. (A.1), definition of effective potential for the ringed configuration. The case **1.** of Sec. (4.1) $K_i = K_j$, with sequences $\mathcal{B}_\ell$, is solved for any couple of fluid specific angular momenta $\ell_i \neq \ell_j$ : $\exists! K = K_j = K_i$ where $K_i$ is a value of the effective potential function associated to the $C_i \subset \mathbf{C}_n$. If $K_i = K_j = K \; \forall K$ then $K$ plays the role of the *$K$-parameter or $K^n_{\mathbf{C}}$-for the macro-configuration* $\mathbf{C}^n$ entirely

decomposed by a sequence $\mathcal{B}_\ell$ . This condition has to be completed then by condition given in Eq. (15), but in general the condition for existence of a common $K$ can be stated as follows

$$\Delta_{\mathbf{K}} \equiv \bigcap_{i=1}^{n} \mathbf{K}^i_{crit} \neq \emptyset \quad \delta_{\mathbf{K}} \equiv \inf_{i=1}^{n} K^i_{Max} - \sup_{j=1}^{n} K^j_{min} > 0 \quad \text{where} \quad \mathbf{K}^i_{crit} \equiv [K^i_{min}, K^i_{Max}] \quad \text{and} \quad \beth(\Delta_{\mathbf{K}}) \geq 1, \tag{17}$$

where $\beth(\Delta_{\mathbf{K}})$ is the number of elements of the intersection set $\Delta_{\mathbf{K}}$ or, equivalently, the number of possible values of the $K$ parameter as they came from the cross set. Therefore the crossing set has at least one element[10] $i$, $\delta_{\mathbf{K}}$, is then the measure of $\Delta_{\mathbf{K}}$ and the inf and sup will refer to one or more sub-configurations. Then $K^i_{Max} = K^j_{Max}$, and/or $K^i_{min} = K^j_{min}$; these particular cases will be discussed extensively in Sec. (4.5.2).

In general, any $n$-order decomposition at fixed $\{K_i\}_{i=1}^n$ (thus also $K_i \neq K_j$) can be realized by the sequences $\{\ell_i\}_{i=1}^n$ with $K_i \in \Delta^i_{\mathbf{K}}$. It is clear that the condition $\delta_{\mathbf{K}} = 0$ could mean $K^i_{Max} = K^j_{min}\ \forall\{i,j\}$ *or* $\exists(i,j) : K^i_{Max} = K^j_{min}$, but in this last case the order of the configuration *must* be $n_{Max} = 2$, see also Fig. (5). Further details on the rings $K^i_{Max} = K^j_{min}$ are provided in Sec. (4.5.1). As $K^-_{mso} < K^+_{mso}$, in

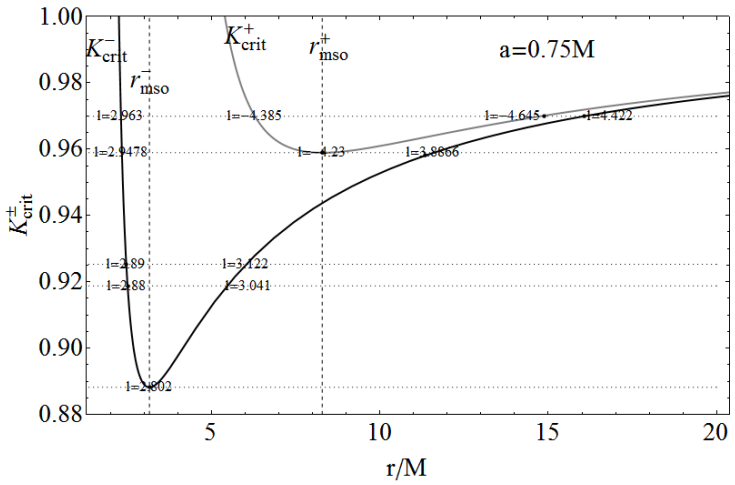



Fig. 5.— Fluids orbiting in a **BH**-spacetime with $a = 0.75M$. The $K^{\pm}_{crit} = V_{eff}(\ell_\pm)$ curves as functions of $r/M$, for corotating $K^-_{crit}$ (black curve) and counterrotating $K^+_{crit}$ matter (gray curve). Marginally stable circular orbits $r^{\pm}_{mso}$ are signed with dashed vertical lines. Points on the curves set the critical points and the corresponding values of the specific angular momentum. The values $\ell$ =constant are signed with dotted (horizontal) lines.

general $\delta_{\mathbf{K}} \in ]0, 1 - K^{\pm}_{mso}[$, where $^{(+)}$ holds at last one ring is counterrotating, and $^{(-)}$ holds if all the rings are corotating[11]. In Fig. (3) an example of procedure adopted for the selection of the sequence $\{K_i\}_{i=1}^n$ at $\{\ell_i\}_{i=1}^n$ fixed, is demonstrated. In Sec. (A.1) we introduce the important notion of effective potential of the ringed disk, which also enables to clarify further the role of the sequence of the parameters $\{K_i\}_{i=1}^n$.

[10] We assume that the couple $(K^i_{min}, K^i_{Max})$ is well defined for any $i$. In this case, it is clear, in fact, that the necessary condition for the existence of any two rings of a common $K = K_i = K_j$ is $K \in \Delta_{\mathbf{K}}$ (as it has to be, for each $i$, $K_i \in [K^i_{min}, K^i_{Max}]$). On the other hand, there could be many more common possible values of $K$ belonging to the set $\Delta_{\mathbf{K}}$, actually an entire range of values $K \in \Delta_{\mathbf{K}}$ as it is clear, for example, from the effective potential of $C_2$ ($\ell_2 = -4.4188$) and $C_1$ ($\ell_1 = -4.3484$) in Fig. (3)-upper.

[11] It is a wide margin: we imposed a cut at $K = 1$ as supremum of the range, being in any case $K < 1$, or a configuration of order $n$ could have $n$ jets. The infimum of the $K$ for each ring is clearly $K^{\pm}_{mso}$ respectively for counterrotating and corotating rings, therefore the supremum of the range of a common $K$ is $\sup K_{crit} - \inf K_{crit} = 1 - K^{\pm}_{mso}$.

### 4.3. On the role of the $\ell$-parameter: differential rotation and angular momentum of the macro-structure

The specific angular momentum of the sub-configuration $C_i$ determines the center $r^i_{cent} = r^i_{min}$, and the instability point $r^i_{cusp} = r^i_{Max}$, determining also if, in its unstable phase, the ring $C_i$ can generate jets of matter *or* it will be accreting onto the black hole. So far we have taken into account particularly the reciprocal sign of the specific angular momentum for the two consecutive rings, but not their magnitude. An important feature of the ringed disk structure is the ratio in specific angular momentum between two consecutive rings $C_i$ and $C_{i+1}$,

$$\ell_{i/i+1} \equiv \ell_i/\ell_{i+1} \neq 1, \tag{18}$$

whose sign defines the $\ell$corotating or $\ell$counterrotatings rings. Definition (18) can be extended for any pair of rings $C_i < C_j$ of the $\mathbf{C}^n$ decomposition and also to values $\ell_{i/i+1} = -1$, see also discussion in (Pugliese&Montani 2015a). Configurations $\ell_{i/i+1} = 1$ could perhaps be permissible for a couple $(C, O_x)$, but providing to a weakening of the separation condition (15) when the decomposition includes open critical surfaces. We can characterize the decompositions of a ringed disk establishing a relationship between the specific angular momenta of the sub-configurations in terms of the ratios $\ell_{i/j}$. An analogue analysis will be similarly done in terms of the parameter $K$, in Sec. (4.2) and in Sec. (4.5). In Sec. (4.3.1) we introduce the concept of differential rotation of the macro-structure, providing also a definition for the ringed disk angular momentum. The analysis of the role of the ring specific angular momentum $\ell_i$ in the formation of the ringed disk continues in Sec. (4.3.2) where, considering the $\ell$corotating and $\ell$counterrotating sequences separately, we shall explore the mutual influence of the set of parameters $\{\ell_i\}^n_{i=1}$ and $\{K_i\}^n_{i=1}$, showing also this relation in the special case of a saturated disk.

#### *4.3.1. Differential rotation and the disk angular momentum*

The macro-structure $\mathbf{C}^n$ is not characterized by an univocal specific angular momentum equal for any rings, and one can say it has a *differential rotation*: meaning the ordered sequence of parameters $\{\ell_i\}^n_{i=1}$ : $\ell_i \neq \ell_j$ and, as discussed in Sec. (A.1), unequivocally defining the potential in Eq. (A5) of the macro-structure, the order of the decomposition, but not its decomposition. Further details on the differential rotation will be provided also in Sec. (B) and Sec. (D) where the perturbation of the $\mathbf{C}^n$ disk will be addressed. In this Section we introduce a definition of (specific) angular momentum associated to the ringed disk $\mathbf{C}^n$, taking into account its differential rotation.

**The area angular momentum $\bar{\ell}^n_{\mathbf{C}}$ and the volume angular momentum $\bar{\bar{\ell}}^n_{\mathbf{C}}$** of the macro-configuration of the order $n$ are defined respectively as the algebraic sums:

$$\bar{\ell}^n_{\mathbf{C}} \equiv \frac{\sum_{i=1}^n \ell_i \mathcal{A}_i}{\sum_{i=1}^n \mathcal{A}_i}, \quad \bar{\bar{\ell}}^n_{\mathbf{C}} \equiv \frac{\sum_{i=1}^n \ell_i \mathrm{V}_i}{\sum_{i=1}^n \mathrm{V}_i} \quad \text{and} \quad \bar{\bar{\ell}}^n_{\mathbf{C}} \approx \frac{\sum_{i=1}^n \ell_i \mathcal{A}_i r^i_{min}}{\sum_{i=1}^n \mathcal{A}_i r^i_{min}} \tag{19}$$

where $\mathcal{A}_i$ is the surface area of the $C_i$ cross section in the equatorial plane[12], and $\mathrm{V}_i$ is proportional to the total mass of the system is the interior volume of the $C_i$-ring, which is approximately evaluated in the equality in (19) considering the Guldinus theorem (or Pappus'centroid theorem-see for example (Kern&Bland 1948)) as the system has a constant[13] centroid, taking the centroid function and its geometric centroid corresponding to the disk center and maximum pressure $r_{min}$. The first definition $\bar{\ell}^n_{\mathbf{C}}$ in Eq. (19) relates the total angular momentum to the section of the Boyer surface in the equatorial plane, the second $\bar{\bar{\ell}}^n_{\mathbf{C}}$, consider the total volume of each ring.

[12] That is $\mathcal{A}_i = 2\int_{y^i_3}^{y^i_1} \partial C^i_+ dy$ where $d\lambda \equiv dy$ (the boundary $\partial C_+$ is a properly oriented curve in $y > 0$)

[13] Standard approaches of rotating bodies considers rigid ($\Omega(r)$ =const) and differential ($\Omega(r)$ $\neq$const) rotation. There we shift the meaning of differential rotation of ringed disk to those ringed tori having $\ell_i(r)$ =const, but $\ell_i(r) = \text{const} \neq \ell_j(r) = \text{const}$.

**The leading $\bar{\ell}^l_{\mathbf{C}^n}$ and the apparent $\ell_h$ angular momentum** The specific angular momentum $\ell_1$, associated to the inner ring $C_1$, and the momentum $\ell_n$ of the outer ring $C_n$, play a major role in the equilibrium of the decomposition and also in determining the morphological characteristics of the ringed structure. However, one might consider, in analogy to the definition of the thickness and height of the ringed disk provided respectively in Eq. (A1) and Eq. (A2). by defining the *leading* specific angular momenta

$$\bar{\ell}^l_{\mathbf{C}^n} \equiv \sup |\ell_i| \mathcal{A}_i, \quad \text{or} \quad \bar{\bar{\ell}}^l_{\mathbf{C}^n} \equiv \sup |\ell_i| \mathrm{V}^i. \tag{20}$$

Henceforth we indicate equally these two and the *apparent* $\ell_h$ specific angular momentum of the sub-configurations with maximum heights $h$.

In the following Sections, characterizing decompositions with sequences $\ell$counterrotating, we face the problem if the existence of (stable) ringed configurations with $\bar{\ell}^n_{\mathbf{C}} = 0$ (or $\bar{\bar{\ell}}^n_{\mathbf{C}} = 0$) for a $\mathbf{C}^2$ disk is possible; for example to be zero $\bar{\ell}^2_{\mathbf{C}} = 0$ implies $\ell_{1/2} = -\mathcal{A}_2/\mathcal{A}_1$ and $\bar{\bar{\ell}}^2_{\mathbf{C}} = 0$ implies $\ell_{1/2} = -(\mathcal{A}_2/\mathcal{A}_1)(r^2_{min}/r^1_{min})$.

The analysis considers then particular ratios $\ell_{i/j}$ between the specific angular momenta of the rings, but one can consider the relation:

$$|\ell_i| = |\ell_j| + \epsilon_{ji} \quad \text{with} \quad \epsilon_{ij} \approx 0 : \ \ell_i \neq \ell_k \quad \text{and more generally} \qquad r^i_{min} \neq r^k_{min} \ \forall i \neq k, \tag{21}$$

where the (trace null) totally antisymmetric matrix of *displacements* $\epsilon$ : $\epsilon_{ij} = -\epsilon_{ji} \approx 0$ would have a leading role in the perturbation of the decomposition and therefore of the $V^{\mathbf{C}^n}_{eff}$ potential in (A5), see also Sec. (D). As $\epsilon_{ij} \approx 0$, we can use the relation (21) as a procedure to build up a model of a (geometrically thin) disk consisting of a very large number $n$ of possibly $\ell$corotating rings, to avoid collisions in this peculiar disk model, or with $\ell$counterrotating isolated $\overbrace{\mathbf{C}_s}$ bends (i-a)) with a given differential rotation. As proved in Secs. (4.3.2,B), the procedure (21) is particularly suitable for isolated decompositions, or decomposition constituted by an $\ell$corotating sequence only as in this case there is $\partial_i|\ell| > 0$, where $\partial_i$ stands for a variation with respect to the configuration index as detailed below. It would be a discrete one-dimensional model of geometrically thin disks, where the only relevant dimension is the radial one. The hydrostatic pressure shall have $n$ maximum points in the equatorial plane, and would be constant on each ring surface, being approximately coincident with a portion of the envelope surface of the macro-structure. However, it remains to define the stability of the ringed disk in this model that could be also unstable- see also Sec. (D) on the perturbations of the decomposition. The difference with a dust disk (bundles of one-dimensional geodesics) is clearly that each ring in this model is a thick disk with a pronounced verticalization ($R_i \approx 1$) but obedient to a similar dynamic equation: one could write $V^i_{eff} = V^j_{eff} + f(\epsilon_{ij})$, considering that if the two rings are $\ell$counterrotating, $f(\epsilon_{ij})$ is not in general a small correction term for $V^j_{eff}$.

As we have already mentioned, the potential (A5) is uniquely determined by the differential rotation, but it is undetermined by the choice of the sequence $\{K_i\}^n_{i=1}$. Nevertheless, one can always choose an appropriate $K_i$ for a $\ell_i$ such that the spacing $\lambda_{i\pm1}$ is small enough, see also Secs.4.2 and 4.5. In Sec. (4.3.2) we propose a procedure to set the suitable sequences $\{K_i\}^n_{i=1}$, and we analyze also some limiting cases where $\epsilon_{ij} = 0$.

Concerning the gradient of the differential rotation or the derivative $\partial_i \ell$, with respect to the configuration index, we note that, if $\epsilon_{ij}$ is the distance between the two specific angular momenta, the distance between $(r^i_{min}, r^j_{min})$ is fixed and it will be a function of $\epsilon_{ij}$. As any specific angular momentum is attached to a ring center, we could characterize the differential rotation in a more general sense as a discrete function of the sub-configuration index ($i$) and then evaluate the derivative $\partial_i$ as $\partial_r \ell_{crit}$ for $r$ being a discrete variable with values in $\{r^i_{min}\}^n_{i=1}$, see also Secs. (B) and (D). We will show in Sec. (4.3.2) and Sec. (B) that the differential rotation for any $\ell$corotating sub-sequence is always increasing in magnitude with the configuration index (that is with the distance from the source) but not monotonically with the index (for equidistant centers).

We note finally that, if we start from two generating $\ell$counterrotating rings, the *seeds* $C^{\pm}_1$, as the inner rings of the two $\ell$counterrotating sub-sequences, then, the displacement matrices in Eq. (21) might automatically generate an isolated decomposition with a shift between the two subsequences function of $\epsilon_{1_+1_-}$, according

to the initial data on the generating couple (a similar situation would be obtained by perturbing a suitable preexisting decomposition). In other words, a separation in the decomposition by the action of a displacement matrix between the two $\ell$counterrotating sub-sequences of the disk could be obtained, depending on the initial configuration. Assuming for simplicity to divide the process of the translational displacements generated by the two matrices $\epsilon^{\pm}_{ij}$, on the $\ell$counterrotating sequences with $n = n_+ + n_-$ with a general initial (seed) couple $C_\pm$, the spacing between the two $\ell$counterrotaing bends will be

$$\bar{\lambda}_\mp = y_3^{1_-} - y_1^{n_+} \quad \text{if} \quad C_- > C_+, \quad \bar{\lambda}_\pm = y_3^{1_+} - y_1^{n_-} \quad \text{if} \quad C_+ > C_-, \quad \ell^{\pm}_{n_\pm} = \ell_{1_\pm} + \sum_{i=1_\pm}^{n_\pm - 1} \epsilon^{\pm}_{i,i+1}, \tag{22}$$

with the elements $\epsilon^{\pm}_{ij}$ small enough to lead to a $\overbrace{\mathbf{C}}^{s}$ sequence. However, for each $\ell$corotating sub-sequence the sum in Eq. (22) increases in magnitude with the sub-sequence order ($n_\pm$ respectively). As we have already noted, the ringed disk has specific angular momenta increasing in magnitude outwardly but one can properly set the initial rings such that $|\ell_-| - |\ell_+| \approx 0$, and if we can choice $K_\pm$ such that $\mathcal{A}_- \approx \mathcal{A}_+$, then the angular momentum of the disk $\bar{\ell}^n_{\mathbf{C}} \approx |\ell_\pm||n_+ - n_-|$.

*4.3.2. Some notes on the ring specific angular momentum and the differential rotation of the disk*

The curves $\ell_\pm$ plotted in Fig. (6,7), locate, for $\ell_i$ =constant, the critical points $r^i_{crit} = \{r^i_{Max}, r^i_{min}\}$ of the $C_i$ ring, that is the center on $C_i$ and the inner edge of its unstable phase. The investigation of the decomposition of a $n$-order disk with the unstable rings is simplified by noting that the curves $K^i_{crit}$ =constant, plotted in Fig. (5), locate exactly the inner edge and the *outer* edge of the $C^i_x$ rings but not, directly, the ring center $r^i_{min}$ and therefore the value $K^i_{min}$. Moreover, as the curves $K^i_{crit}$ =constant provide $K^i_{Max}$ for the unstable phases (but not $K^i_{min}$), the information on the ring topology in its unstable phase is provided, when it can accrete on the source or create jet. On the other hand, the location of $r^i_{min}$ is easily identifiable, from the plot of the specific angular momenta, knowing $r^i_{Max}$ from the curve $K_{crit}$=constant:

$$\partial_{r^i_{Max}} r^i_{min} < 0 \quad \text{and} \quad \partial_{|\ell_i|} r^i_{min} > 0, \quad \partial_{|\ell_i|} \lambda^i_x > 0, \tag{23}$$

where $\lambda^i_x$ is the elongation of $C_i$ ring in its accretion phase (if this exists). Here and in the following $\partial_{\mathbf{B}}\mathbf{Q} > 0$ we mean the quantity $\mathbf{Q}$ increases as the quantity $\mathbf{B}$ increases and viceversa–see also Note III. Furthermore, the elongation $\lambda$ of the equilibrium disk is smaller than the elongation of its accretion configuration $\lambda_x$:

$$\lambda_i < \lambda^i_x, \quad \Lambda_i \subset \Lambda^i_x, \quad K \in ]K^i_{min}, K^i_{Max}[\subset]K_{mso}, K^i_{Max}[, \tag{24}$$

$\Lambda^i_x \equiv [y^i_3, y^i_1]_x$ is the elongation range of the accreting ring. However the inner edge of the disk in accretion must be $y^i_3\big|_x = r^i_{Max} \in ]r_b, r_{mso}[$, therefore $r_{mso} \in C^x_i$, but for a disk in equilibrium $y^i_3 \in ]r^i_{Max}, r_{mso}[$, therefore $r_{mso} \in C_i$ or $y^i_3 \in ]r_{mso}, r_{min}[$, where $r_{mso} \notin C_i$ does not belong to the $C_i$ disk. The elongation of the disk in the first configuration is larger then the elongation of the second and therefore it requires a $K_i \in ]K_{mso}, K^i_{Max}[$ greater then in the second configuration. In Fig. (3) an example of how stringent can be the choice of the $K$ parameter in the decomposition with a ring in accretion is shown.

**$\ell$corotating rings**

We focus first on the case of the $\ell$corotating rings as shown in Fig. (3) and Fig. (6,7) where there are the curves $\mp\ell_\pm$ for different attractors in $r > r^\pm_\gamma$ respectively. The inner rings of each $\ell$corotating sequence of not necessarily consecutive rings, have their specific angular momentum magnitude lower than the outer ones, $|\ell_a| < |\ell_b| \ \forall \ C_a < C_b$. To ensure the separation between the outer lobes of the $\ell$corotating disks in accretion as in Eq. (15), only the inner ring of each $\ell$corotating sub-sequences of not necessarily consecutive rings can be in accretion, i.e. in $C_x$ topology, implying that no "feeding" is possible by a P-W instability mechanism among the $\ell$corotating rings of a ringed $\mathbf{C}^n_x$ configuration. The configurations $C^i_x$ must be the inner one of the $\ell$corotating (non necessarily consecutive) sequences. We can thus deduce the following

result: given a ringed disk of order $n$ and any its decomposition with specific angular momenta $\{\ell_i\}_{i=1}^n$, the subset of not *necessarily consecutive* $\ell$corotating rings with specific angular momenta $\{\ell_j\}_{j=1}^k$, $k \leq n$, allows *only* one configuration $C_x$–only the inner ring of the disk can accrete onto the attractor and the inner one has the lowest specific angular momentum magnitude. Thus the outer configuration must be in $C$ topology, see Fig. (3). The highest possible rank of a $\mathbf{C}_x^n$ configuration is then $\mathfrak{r}_{\mathfrak{r}Max} = 1$, and accretion onto the black hole can occur only in the inner corotating or the inner counterrotating ring, see Fig. (3). An unstable $\ell$corotating couple of rings $(C, O_x)$ could be characterized by $\ell_{i/j} = 1$, the couple having an unique center of maximum pressure provided that $\ell_i \in ]\ell_\gamma, \ell_{mbo}[$, that is an $r_{Max} \in ]r_\gamma, r_{mbo}[$: $K_{Max} > 1$. One could have two centered configurations at equal (algebraically) specific angular momentum, a closed one in equilibrium, and the other being open and governing a jet with launching point placed in $r_{Max}$. In any case also the couple $(C, O_x)$ would violate the condition in Eq. (15), this case will be considered in more details in Sec. (C).

It follows then that the rings of the $\ell$corotating sub-sequences of an $n$-order decomposition satisfy the property $\bar{\mathfrak{C}}_{1b}$ as in $(\bar{\mathfrak{C}}_{1b})$. A specific characterization of the decompositions $\bar{\mathfrak{C}}_{1b}$ is in Sec. (4.4). It is therefore necessary to briefly discuss the condition on maximum in $\bar{\mathfrak{C}}_1$ in Eq. (15) for the $\ell$corotating sequences: with reference to Fig. (6,7), we consider a couple of constant specific angular momenta $\ell = \ell_i,\ i \in \{a, b\}$ with $\ell_a < \ell_b$. Then $\Delta^a_{crit} \subset \Delta^b_{crit}$, in other words the ringed 2nd order configuration $\mathbf{C}^2 = C_a \cup C_b$ is a $\bar{\mathfrak{C}}_{1b}$ one. Clearly, this property generalizes straightforwardly to any order $n$. However, it is immediate to prove the condition in Eq. (15). Increasing the spacing between the rings centers, or by adding a ring to a $\ell$corotating ringed configuration, it is necessary to supply additional angular momentum to the outer ring.[14] Considering the definition (18), there is always $|\ell_{i/i+1}| \in ]0, 1[$, the rings do not need to be consecutive and then one can generalize this relation as

$$0 < |\ell_{i/j}| < 1,\ \forall i < j \quad C_i < C_j \quad \ell_i \ell_j > 0. \tag{25}$$

Another way to express this result is the following: the distance between the two minima $(r^a_{min}, r^b_{min})$ is increasing with increasing the difference between the two specific angular momenta magnitude. This can be seen from the slope of the curve $\ell(r)$ at $r > r_{mso}$, or from the radial first derivative of the specific angular momentum in $r > r_{mso}$ which is always positive. The ring elongation and thickness is determined, as in Eqs. (23,24), by the gap in the specific angular momentum in condition (15). However, it is important to note that the derivative $\partial_r(\mp\ell^\pm)$ does not grow monotonically[15] but it has a maximum point $r^\pm_{\mathcal{M}}$ respectively, different for each attractor, as we detailed in Sec. (B). Increasing of the specific angular momentum magnitude with the radial distance from the attractor is not constant but it rises up to a limiting radius, different for the $\ell$counterrotating sequences. Radii $r^\pm_{\mathcal{M}}$ are functions of the attractor spin-mass ratio, Figs. (8,9). As proved in Sec. (B), this is a relativistic effects that disappears in the Newtonian limit when the orbital distance is large enough with respect to $r^\pm_{\mathcal{M}}$, and $r^+_{\mathcal{M}} = r^-_{\mathcal{M}}$ disappears in the case of static spacetimes; clearly these effects occur due to the presence of the intrinsic spin of the attractor. This behavior of the specific angular momentum distinguishes the two $\ell$corotating sub-sequences of corotating and counterrotating rings of a generic decomposition: the **BH** spin has a stabilizing effect for the corotating matter and destabilizing for the counterrotating one, as $\partial_{|a|} r^\mp_{\mathcal{M}} \lessgtr 0$. We prove these results in Sec. (B).

We consider first the case of a $\ell$corotating $\mathbf{C}^3_\odot$ configuration of rank $\mathfrak{r} \leq 2$. There must be at least a couple $y^a_1 = y^b_3$:

$$r^a_{Max} < r^b_{Max} < r^c_{Max} < r_{mso} < y^a_3 < r^c_{min} < y^a_1 = y^b_3 < r^b_{min} < y^b_1 < y^a_3 < r^a_{min} < y^a_1, \quad \text{where} \quad |\ell_a| > |\ell_b| > |\ell_c|. \tag{26}$$

[14] We note that the critical $\ell$corotating-rings and the correspondent effective potentials are centered in $r_{mso}$.

[15] The distance between two the centers of the two $\ell$corotating configurations $|\ell_i| < |\ell_j|$ is $\delta^{i,j}_{min} \approx \left(\nabla\ell^\pm\right)^{-1}(\ell_j - \ell_i)$ where $\nabla\ell^\pm$ is the incremental ratio of the specific angular momentum function, but if the configuration indices are $j = i + \epsilon$ with $\epsilon \gtrapprox 0$, that is, the two rings have very close values of the specicic angular momentum (and therefore very close effective potentials) the spacing among them is very small. The elongation is determined trivially from the radial derivative of the specific angular momentum.

We note that the specific angular momentum of the fluid and the associated effective potential grow in magnitude simultaneously. This property holds in particular in the critical points $K_{crit}$, as it is clear from Figs. (6,7) Note I and Note III). Then, increasing the magnitude of the fluid momentum, at fixed $r$ and therefore at fixed $y_1^a = y_3^b$, there are increasing values of $V_{eff}$ and viceversa, it is:

$$V_{eff}(\ell_a, y_1^a) = K_a > K_b = V_{eff}(\ell_b, y_3^b) \quad \text{for} \quad y_3^b = y_1^a, \quad \ell_a \ell_b > 0, \quad |\ell_{ab}| > 1, \tag{27}$$

see Note I, Note II and Note III. On the other hand, the maximum in $r_{Max} \in ]r_\gamma, r_{mso}[$ decreases with the magnitude of the angular momentum at fixed $K$, that is increasing $K_{min}$, potentially the disk elongation tends to increase because the distance between the point of maximum and minimum increases; as for fixed $\ell_a : \ K^a_{Max} > K^b_{min}$–see Fig. (6,7). This relation can be iterated for any order $n$, see also (a.)) and (b.).

We consider now the parameters $K$ associated with two separated sub-configurations. For $|\ell_a| < |\ell_b|$, it has to be $K_{mso} < K^a_{min} < K^b_{min} < K^b$ as shown in Fig. (6,7), but we can have $K_a = K_b$ or $K_a \neq K_b$. Therefore, the relation $(K_a, K_b)$ and the elongation of the rings is not yet settled. It is worth noting that there may be two different specific angular momenta such that $K^a_{Max} = K^b_{min}$; this is the case illustrated in (Pugliese&Montani 2015a) and considered in Sec. (4.5.1).

For a $\mathbf{C}^n_\odot$ ringed disk we deduce from Fig. (5,6,7), that fixing, say, the inner margin $y_3^1$ of the the inner sub-configuration $C_1$ (or equivalently $K_1$ or $y_1^1$ fixing one of the three parameters $(y_3^i, y_1^i, K_i)$ automatically identifies the other two quantities), then the entire ringed $\mathbf{C}^n_\odot$ structure is fixed. In fact, considering the potential $V^{\mathbf{C}^n}_{eff}$ in Eq. (A5), if it exists, then there is *one and only one* $\ell$corotating sub-sequence of the ringed decomposition of $\mathbf{C}^n_\odot$ with $y_1^{i+1} = y_3^i$. Then we say $y_3^1$ to be a "starting point" *uniquely* fixing the decomposition of the $\ell$corotating sub-sequence of $\mathbf{C}^n_\odot$.

If the ringed $\mathbf{C}^n_\odot$ with $n > 2$ is made by $\ell$counterrotating rings, we can say $y_3^{1\mp}$ to be a "starting point" to fix the *two* sequences of $\ell$corotating disks of the decomposition of $\mathbf{C}^n_\odot$ of corotating $(y_3^{1-})$ and counterrotating $(y_3^{1+})$ disks separately, maintaining then the constraints imposed by separation of the rings. So the couple $y_3^{1\mp}$ constraints the decomposition uniquely but not entirely. As we are not considering here the $\ell$counterrotating tori together: given $y_3^{1\mp}$, we fix the two sequences separately to be combined to form of a $\mathbf{C}^n_\odot$ disk. Then it could be in need to make a reduction of the order $n = n_+ + n_-$. The number of rings in fact depends on the differential rotation, but mostly by the choice of the "starting point": the greater the elongation in the equatorial plane of the first ring, then smaller in general is the second $\ell$corotating disk. So one could say that the elongation of two consecutive $\ell$corotating disks is inversely proportional–$\partial_{\lambda_i} \lambda_{i+1} < 0$ exact law could be found that depends on the specific angular momentum, irrespectively of the number of consecutive[16] $\ell$corotating disks. Some general notes on the perturbations of $\mathbf{C}^n$ and the relation with the elongation and spacings have been addressed in Sec. (D) and Sec. (B). More generally, regarding the relation between the order of the decomposition and the distances $\delta^{i,j}_{min}$ between two minima of an $\ell$corotating sequence, one can deduce from Fig. (3) that the elongation of the ordered $\ell$corotating disks, although of not consecutive rings, depends on $\ell$ and the starting point of the iteration. We can further clarify these statements as follows, assuming for convenience the iterative parameter $K$ for a generic $\mathbf{C}^{n+1}$ configuration, and fixing the inner edge with $K_0$. As discussed in Sec. (4.2) then $K$ should obey a necessary condition verified for each

[16]The hypothesis of consecutiveness between the rings is adopted here only to explicit the exclusion of a possible $\ell$counterrotating configurations $C^+_{i+1}$ between two $\ell$corotating rings $C^-_i < C^+_{i+1} < C^-_{i+2}$ that would clearly impose further restrictions on the starting point. This case is discussed later for the $\ell$counterrottaing rings.

$\ell$corotating sub-sequence. Considering the property $\partial_{|\ell|} r_{min} > 0$, it has to be

$$\begin{aligned}
&K_0 \in ]K^0_{min}, V_{eff}(\ell_0, r^1_{min})], \\
&K_1 \in ]K^1_{min}, \inf\{V_{eff}(\ell_1, r^2_{min}), V_{eff}(\ell_1, y^0_1)\}], \\
&\qquad ... \\
&K_i \in ]K^i_{min}, \inf\{V_{eff}(\ell_i, r^{i+1}_{min}), V_{eff}(\ell_i, y^{i-1}_1)\}], \quad \forall i \in [1, n-1] \\
&\qquad ... \\
&K_n \in ]K^n_{min}, V_{eff}(\ell_n, y^{n-1}_1)].
\end{aligned} \tag{28}$$

This is a necessary but not sufficient condition for the existence of a $\ell$corotating ringed disk $\mathbf{C}^{n+1}$. If it is a $\mathbf{C}^{n+1}_{\odot}$ configuration with rank $\mathfrak{r} = \mathfrak{r}_{Max} = n$, then $K_i = V_{eff}(\ell_i, y^{i-1}_1)$, and it is univocally determined by the appropriate choice of $K_0$ with the constraint $K_0 \in ]K^0_{min}, V_{eff}(\ell_0, r^1_{min})]$. The condition could be written as $y^o_3 : \ y^0_1 \in ]r^0_{min}, r^1_{min}[ \cup ... y^i_1 \in ]r^i_{min}, r^{i+1}_{min}[$. The construction of this ringed disk is carried out in an iterative process where the starting point is not necessarily $K_0$. In the case of $\mathbf{C}^{n+1}_{\odot}$ topology, the choice of $K_0$ uniquely fixes the sequence $\{K_i\}^n_{i=0}$.

For the case of $\mathbf{C}^n$ ringed disk, considering the distance $\delta^{j,i}_{min} = r^j_{min} - r^i_{min}$ between the minima of the $C_i < C_j$, the maximum elongation $\lambda^{Max}_i$ as the upper bound realized at zero spacings between consecutive rings of the configurations $\mathbf{C}_{\odot}$ and finally the maximum possible spacing $\bar{\lambda}^{Max}_{i+1,i}$ between the $C_i$ and $C_{i+1}$ rings, the following relations hold:

$$\frac{\partial \delta^{j,i}_{min}}{\partial \ell_{j/i}} > 0, \quad \frac{\partial \lambda^{Max}_i}{\partial \ell_{i/(i-1)}} > 0, \quad \frac{\partial \bar{\lambda}^{Max}_{i+1,i}}{\partial \ell_{(i+1)/i}} > 0, \quad \frac{\partial \lambda^{Max}_i}{\partial \lambda_{i-(2k+1)}} < 0, \quad \frac{\partial \lambda^{Max}_i}{\partial \lambda_{i-2k}} > 0, \quad \forall i < j \quad k \in \mathbb{N}. \tag{29}$$

see also Note III, Note IV, these variations could indeed be evaluated exactly, for example in the treatment of the perturbations as discussed in Sec. (D). However, for a fixed $\ell$corotating sequence $\{\ell_i\}^n_1$, for the $\ell$corotating couple $C_a > C_b$ within the Note III and ((b.)), we can have $K_a = K_b$ or $K_a \neq K_b \in ]K^b_{min}, K^b_{Max}[ \subset ]K^a_{min}, K^a_{Max}[$. In the latter case, however, any inequality can be satisfied because none of the two ring edges is a critical point. There are no crossing points of the two functions $V^a_{eff} > V^b_{eff}$ (see Fig. (3) in the stability region, or for any $a \neq b \nexists r$: $V_{eff}(\ell_a)|_r = V_{eff}(\ell_b)|_r$, with $\ell_a \ell_b > 0$ (with the exclusion of $\ell_a = \ell_a$, in that case clearly it is only one effective potential), and for a $\mathbf{C}^n_{\odot}$ configuration Eq. (27) holds.

A overview of the results for the $\ell$corotating sequences is in Table (2)

**$\ell$counterrotating rings**

We now study the $\ell$counterrotating sequences of a $n$-decomposition, considering simultaneously the couple of curves $\ell_{\pm}$ shown in Figs. (6,7). As discussed in (Pugliese&Montani 2015a), many morphological characteristics of a toroidal accretion disks show a symmetry under the transformation $\ell \to -\ell$, then we expect a similar symmetry to be conserved in the macro-structure $\mathbf{C}^n$, and so find analogies between the $\ell$corotating and $\ell$counterrotating sub-sequences. A property that we will often use is the following:

$$\forall\, \bar{r} > r_+, \ \ \ell > 0 \qquad V_{eff}(-\ell, \bar{r}) < V_{eff}(\ell, \bar{r}), \tag{30}$$

$$K_{crit}(\bar{r}, \ell_+) > K_{crit}(\ell_-) \quad \text{and} \quad -\ell_+(\bar{r}) > \ell_-(\bar{r}), \tag{31}$$

and an equality in Eqs. (30) occurs only for $a = 0$. It is convenient to start our consideration with the analysis of the limiting case $\ell^- = -\ell^+$, that is $\ell_{i/j} = -1$ for some $C_i$ and $C_j$. It is simple to prove that if $C_i < C_j$, then it follows that $C_i$ is counterrotating and $C_j$ is corotating with respect to the black hole, therefore

$$r^-_{Max} < r^+_{Max} < r^+_{mso} < r^+_{min} < r^-_{min}, \quad K^-_{mso} < K^+_{mso} < K^+_{min} < K^-_{min}, \quad K^+_{Max} < K^-_{Max}, \qquad \text{for} \quad \ell_{i/j} = -1, \tag{32}$$

see Fig. (6,7). The rings with $\ell_{i/j} = -1$ are possible only in $r > r^+_{mso}$ and $\ell > -\ell^+_{mso}$, we note that Eq. (32) does not fully constraint the couple $K_\pm$, while the relation between the critical points follows from the following considerations:

$$\mathbf{K^+_{min}} < \mathbf{K^-_{min}}: \quad V_{eff}(-\ell, r^+_{min}) = K^+_{min} < V_{eff}(-\ell, r^-_{min}) < V_{eff}(\ell, r^-_{min}) = K^-_{min} < V_{eff}(\ell, r^+_{min}). \quad (33)$$

The first inequality in Eq. (33) is given as definition of minimum of $V_{eff}(-\ell)$; using the first of (32), the second of Eq. (33) is an application of Eq. (30), the third follows from the definition of minimum point of the function $V_{eff}(\ell)$. Finally, in the fourth inequality closing Eq. (33), the property (30) has been applied again. Similarly for the maxima $K_{Max}$ one has

$$\mathbf{K^+_{Max}} < \mathbf{K^-_{Max}}: \quad K^+_{mso} < V_{eff}(-\ell, r^+_{Max}) = K^+_{Max} < V_{eff}(-\ell, r^-_{Max}) < V_{eff}(\ell, r^-_{Max}) = K^-_{Max}, \quad (34)$$

where we used the definition of maximum point assuming that each function is well defined, i.e., in this case it means to consider the location of $r^\pm_\gamma$, see Fig. (5). On the other hand, the limiting case $V_{eff}(-\ell^+) = V_{eff}(\ell^-)$ is verified only in the static geometry with $a = 0$. Each (consecutive) couple $\ell_{i/i+1} = -1$ is $\bar{\mathfrak{C}}_{1b}: \ \Delta^+_{crit} \in \Delta^-_{crit}$ as defined in $\bar{\mathfrak{C}}_{1b}$ of Sec. (4). More generally, for any couple of rings, even not consecutive at $\ell_{a/b} = -1$, the condition $\bar{\mathfrak{C}}_{1b}$ holds, but the relationship between the critical points associated with elements of different couples, i.e., for a general ratio $\ell_{a/b} < 0$, can be different. The maximum order of a macro-configuration $\mathbf{C}^n$ where all rings have $\ell_{i/j} = -1$ is $n_{Max} = 2$: in other words, there cannot be more then two rings with $\ell_{i/j} = -1$. However there can be possibly an infinite number of couples $\ell_{a/b} = -1$ and $\ell_{c/d} = -1$, and we consider the case of two couples closing this section. This analysis, being clearly important in investigation of the unstable configurations, considers the maximum points of the effective potential $V^i_{eff}$ associated with each ring (i.e. $|\ell_\pm| \in ]|\ell^\pm_{mso}|, |\ell^\pm_\gamma|[$). The inner counterrotating configuration can be then in accretion or even opened for jets.

As we have already discussed, the presence of an outer ring in its unstable phase would imply a violation of the condition (7) on the separation of material of different rings. However, especially in the case of couples with open external configurations in jets, this condition could be relaxed and a thorough study of this case could be done. From the analysis of the instability of corotating ring of the couple $C^+_i < C^-_j$ with $\ell_{i/j} = -1$, we can draw useful general conditions of instability in the ringed disks. It is not necessary to consider the maximum for the corotating ring, but if it exists then, for any couple of $\ell$counterrotating rings with $\ell^- = -\ell^+$, one of the two conditions has to be satisfied:

$$\breve{\mathrm{C}}_I: \ r^+_{Max} \in ]r^-_{Max}, r^-_{mso}[ \quad \text{or} \quad \breve{\mathrm{C}}_{II}: \ r^-_{mso} \in ]r^-_{Max}, r^+_{Max}[, \quad (35)$$

see Figs. (6,7). In general, the two cases ($\breve{\mathrm{C}}_I$, $\breve{\mathrm{C}}_{II}$) are regulated primarily by the parameter $K_{crit}$ and the properties of the **BH** attractor through its spin-mass ratio $a/M$. Indeed, for $a/M$ sufficiently low and specific angular momentum sufficiently large [17], there is always a specific angular momentum $\ell = \mp\ell_\pm$ with $r^-_{Max}$; these conditions are discussed in the following points.

**Existence of $r^-_{Max}$** The first necessary condition for the existence of $r^-_{Max}$ with $\ell_{i/j} = -1$ is $\ell^-_\gamma \geq -\ell^+_{mso}$, this is the case only of ringed disks orbiting a sufficiently low spin of the attractor

$$a < a_\aleph \approx 0.508864526M : -\ell^+_{mso}(a_\aleph) = \ell^-_\gamma(a_\aleph) \quad (36)$$

see Figs. (6,7,8,9)). There are no circular geodesic orbits at $r < r^-_\gamma$, thus if $\ell = \mp\ell_\pm$ such that $\ell > -\ell^+_{mso} > \ell^-_\gamma$, there is no maximum point for the effective potential of the corotating matter, formally then there is no P-W instability point. For $a = a_\aleph$, there is $\mp\ell_\pm = -\ell^+_{mso}$, and the limiting

[17] With reference to Fig. (6) for $C^-_x$ ring, requiring $K_- = K^-_{Max} < 1$, and $r^-_{Max} \in ]r^-_{mbo}, r^-_{mso}[$, it has to be $\ell_- \in ]\ell^-_{mso}, \ell^-_{mbo}[$, for the $O^-_x$ rings, requiring $K_- = K^-_{Max} > 1$, and $r^-_{Max} \in ]r^-_\gamma, r^-_{mbo}[$, it has to be $\ell_- \in ]\ell^-_{mbo}, \ell^-_\gamma[$, and similar relations can be found for the counterrotating case.

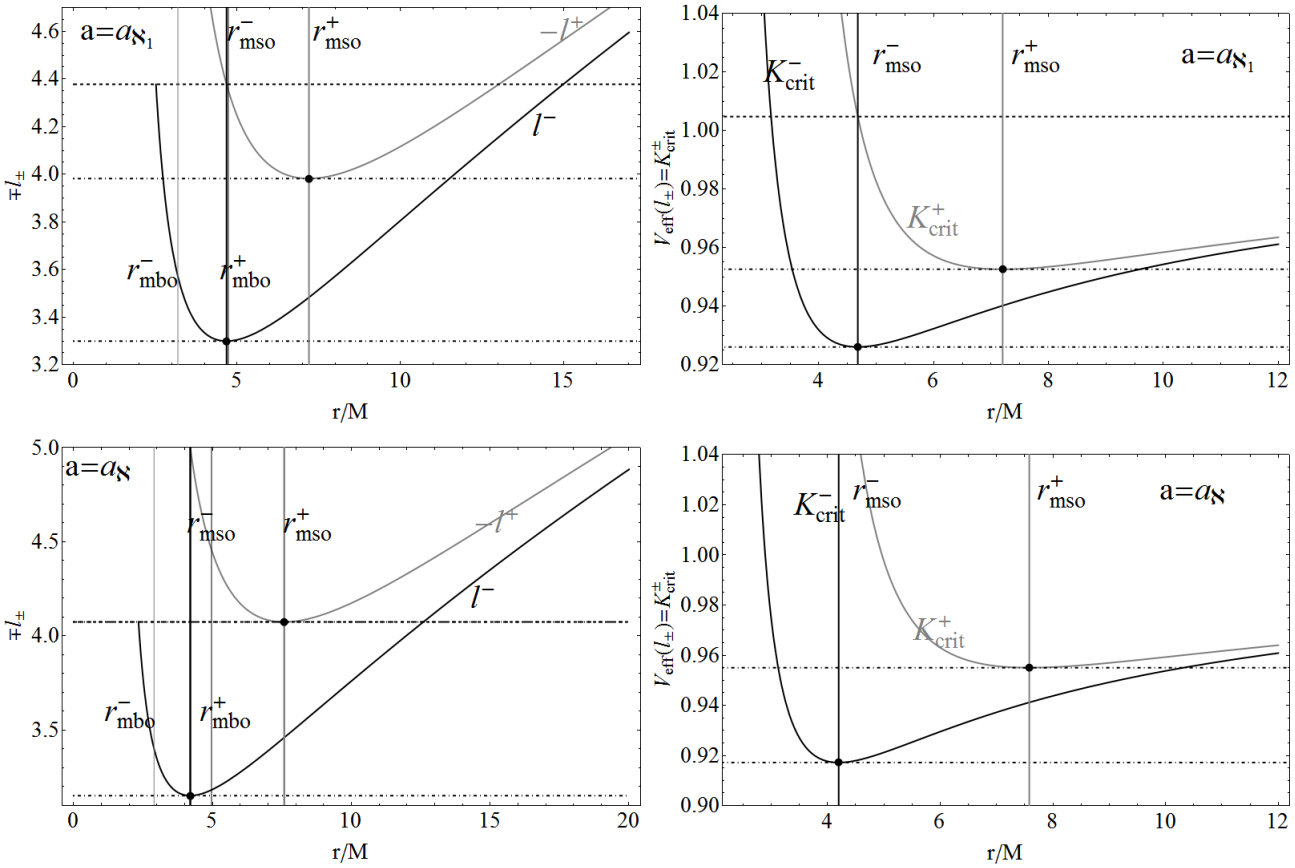



Fig. 6.— Left panels show the fluid specific angular momentum for corotating $\ell_-$ (black curves) and counterrotating $\ell_+$ (gray curves) as functions of the $r/M$. Right panels are the $K^\pm_{crit} = V_{eff}(\ell_\pm)$ as functions of $r/M$. Marginally stable circular orbits $r^\pm_{mso}$ are signed with points on the curves and black/gray lines $r^\pm_{mso}$ =constant respectively, see also Fig. (7). On $a_{\aleph_1} = 0.382542M$ : $\ell^-_\gamma = -\ell_+(r^-_{mso})$ and $a_{\aleph} = 0.508865M$ : $\ell^-_\gamma = -\ell^+_{mso}$, see also Fig. (7). For the spacetime $a = a_{\aleph_1}$ it is $r_+ = 1.92394$, $r^+_{mbo} = 4.73417M$, $r^-_{mbo} = 3.18903M$, $r^+_\gamma = 3.41407M$, $r^-_\gamma = 2.51784M$. Spacetime $a = a_{\aleph} = 0.508865M$ it is $r_+ = 1.86085M$, $r^+_{mbo} = 4.96558M$, $r^-_{mbo} = 2.89276M$, $r^+_\gamma = 3.54085M$, $r^-_\gamma = 2.33381M$. Where $r_+$ is the outer horizon, $r^\pm_{mbo}$ are the marginally bounded orbits, $r^\pm_\gamma$ the marginally circular orbits.

case $\ell^- = -\ell^+_{mso}$ gives rise to a limiting unstable line configuration of counterrotating dust material with the unstable point at $r^+_{mso}$. The constraint $a < a_{\aleph}$ is necessary for the corotating ring of the couple to be unstable. In general this condition applies as well for a general ratio $\ell_{a/b} < 0$ where the inner, corotating ring is unstable and the distance among the centers, $\delta^{ba}_{min} < \delta^\pm_{mso}$. However, this condition is only necessary for the existence of configurations with equal magnitude of specific angular momentum and unstable points. To distinguish the two cases in Eq. (35), we require a further constraint on the spacetime spin. These conditions only consider the role of the specific angular momentum of the couple, once assumed that the maximum should be located in $r > r^-_\gamma$, but they do not set the topology of the unstable configuration. Following the same reasoning, and as $\ell^-_{mso} < \ell^-_{mbo} < \ell^-_\gamma$ for a $C^-_x$ inner ring, it has to be $-\ell^+_{mso} < \ell_- \in ]\ell^-_{mso}, \ell^-_{mbo}[\subset]\ell^-_{mso}, \ell^-_\gamma[$; in particular, $\ell^-_{mbo} > -\ell^+_{mso}$, see Fig. (7). This situation occurs only for $\ell$counterrotating couple orbiting attractors with dimensionless

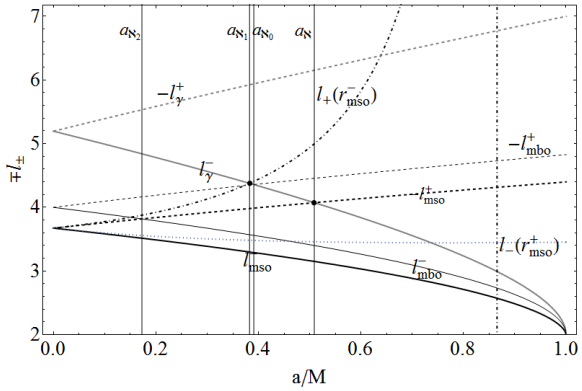



Fig. 7.— Angular momenta for corotating $\ell_- > 0$ and counterrotating $\ell_+ < 0$ fluids, on the last stable circular orbits $r^\pm_{mso}$ as functions of the spin-mass ratio of the attractor $a/M$. $r^\pm_\gamma$ are the marginally circular orbits, marginally bounded orbits are $r^\pm_{mbo}$ .

spin $a < a_{\aleph_2} \equiv 0.172564M$ where there $-\ell^+_{mso}(a_{\aleph_2}) = \ell^-_{mbo}(a_{\aleph_2})$. For higher spacetime spin $a > a_{\aleph_2}$, there is $\ell^-_{mbo} \in ]\ell^-_{mso}, -\ell^+_{mso}[$ and $C_-$ cannot be in accretion phase. Similarly for open configuration $O^-_x$, it has to be $-\ell^-_{mso} < \ell_- \in ]\ell^-_{mbo}, \ell^-_\gamma[$, but for this to happen, the condition $-\ell^+_{mso} < \ell^-_\gamma$ has to be satisfied, i.e. for $a < a_{\aleph}$. The location of the points of instability can be inferred from Fig. (8). This discussion will be summarized and explained later.

**Conditions $\breve{\mathrm{C}}_I$ and $\breve{\mathrm{C}}_{II}$**

For $\breve{\mathrm{C}}_I$ with the condition $r^+_{Max} < r^-_{mso}$ it should be [18] $\mp\ell^\pm \in ] - \ell^+_{mso}, \ell^-_\gamma[$. Then $\ell^-_\gamma > -\ell^+_{mso}$ but also $\ell^-_\gamma > -\ell^+(r^-_{mso})$, see Figs. (6,7,8,9). This can be satisfied only for **BH** attractors with $a < a_{\aleph_1} \equiv 0.38254M$, where for $a = a_{\aleph_1}$ there is $\ell^-_\gamma = -\ell^+(r^-_{mso})$. On the other side, double configurations with $\breve{\mathrm{C}}_{II}$ are possible[19] in the spacetimes $a \in ]a_{\aleph_1}, a_{\aleph}[$.

**Instability of the inner counterrotating ring $C_+$**

The role of the radius $r^+_{mbo}$ is to distinguish the two cases– accretion with $r^+_{mbo} < y^+_3 = r^+_{Max} < r^+_{mso}$, and launching of jets with $r^+_\gamma < y^+_3 = r^+_{Max} \leq r^+_{mbo} < r^+_{mso}$ respectively. Then it is clear that if $K^+_{Max} \geq 1$, for configurations with open jet from the point $r_J = r^+_{Max}$, the corresponding corotating inner ring with $\ell = -\ell^+$ can not exist, because it would violate the condition of no matter penetration. In reality this condition could be relaxed and, although in this work we neglect the analysis of open sub-configurations, we can trace some conclusions here, discussing this case in Sec. (C). In some cases, double configurations with $\ell_{i/j} = -1$ can not give rise to any instability with accretion or launching of jets (by P-W mechanism). Accretion starts from the point:

$$C_+ < C_- \quad r^+_{Max} \in ]r^+_{mbo}, r^+_{mso}[, \quad \text{with} \quad K^+_{Max} < 1, \quad |\ell| \equiv \ell_- = -\ell_+ > -\ell^+_{mbo} > \ell^-_\gamma, \tag{37}$$

[18] We remind that in terms of the fluid specific angular momentum only $C_x$ configurations are at $K < 1$ and $\ell \in ]\ell^+_{mbo}, \ell^+_{mso}[\cup]\ell^-_{mso}, \ell^-_{mbo}[$, $C$ rings are for $K \in ]K^\pm_{mso}, 1[$, $\ell < \ell^+_{mso} < 0 \cup \ell > \ell^-_{mso} > 0$ and $r > r^\pm_{mso}$, $O_x$ open configurations at $K > 1$ $\ell \in ]\ell^+_\gamma, \ell^+_{mbo}[\cup]\ell^-_{mbo}, \ell^-_\gamma[$.

[19] In terms of the fluid specific angular momentum only $C_x$ configurations have $\ell \in ]\ell^+_{mbo}, \ell^+_{mso}[\cup]\ell^-_{mso}, \ell^-_{mbo}[$. For equilibrium rings $C$, it has to be $\ell < \ell^+_{mso} \cup \ell > \ell^-_{mso}$. As pointed out in (Pugliese&Montani 2015a), one can write these results in terms of a rationalized angular momentum $\bar{\ell} \equiv \ell/a$.

the last equality is to ensure the potential associated to the corotating ring of the pair has a maximum point. However, for the accretion, where $r^+_{Max} > r^+_{mbo} > r^-_{mbo}$, it can be either

$$\breve{\mathrm{C}}_\alpha : \; r^-_{Max} < r^-_{mbo} < r^+_{mbo} < r^+_{Max} \quad \text{with} \quad K^+_{Max} < K^-_{Max} < 1 \quad \text{or} \tag{38}$$

$$\breve{\mathrm{C}}_\beta : \; r^-_{mbo} < r^-_{Max} < r^+_{mbo} < r^+_{Max} \quad \text{with} \quad K^+_{Max} < 1 \leq K^-_{Max}, \tag{39}$$

where we used Eq. (34). The conditions above distinguish only inner accreting configurations. Note that, if the outer ring $C_-$ cannot generate jets, for $K^-_{Max} < 1$ (that is the case $\breve{\mathrm{C}}_\alpha$), then also the inner ring $C_+$ does not fulfil the necessary condition for the generation of the jets. On the other hand, if $K^-_{Max} > 1$, then it could be that $K^+_{Max} > 1$, implying possibly a double jet from the inner point $r^-_J = r^-_{Max}$ (with matter corotating with the attractor) and the outer point of launch $r^+_J = r^+_{Max}$ (with matter counterrotating with respect to the central object). For the case $\breve{\mathrm{C}}_\beta$, we can obtain a combined instability with the *inner* (corotating) funnel of matter and the *outer* (counterrotating) accretion point, see for further details discussion in Sec. (C).

The two cases in Eq. (38) are discriminated by the spin requiring a value of:

$$a_{\aleph_0} \equiv 0.390781M \in ]a_{\aleph_1}, a_{\aleph}[ : \ell^-_\gamma = -\ell^+_{mbo}. \tag{40}$$

For $a > a_{\aleph_0}$ there is $\ell^-_\gamma < -\ell^+_{mbo}$, when $K^+_{Max} < 1$, and we obtain the cases $\breve{\mathrm{C}}_\alpha$ or $\breve{\mathrm{C}}_\beta$. Clearly, to satisfy $\ell^-_{mbo} > -\ell^+_{mso}$, with open corotating ring, it has to be $a < a_{\aleph_2} \equiv 0.172564M : -\ell^+_{mso} = \ell^-_{mbo}$. For higher spacetime spin $a > a_{\aleph_2}$, it is $\ell^-_{mbo} < -\ell^+_{mso}$, and there cannot be open corotating configurations in jets (within the condition $\ell_{i/j} = -1$). To have an open configuration in the spacetimes with $a > a_{\aleph_2}$, one has to ensure a ratio $|\ell_{i/j}|$ sufficiently high and, therefore, the necessary separation between the points of maximum pressure (the minimum $r^\pm_{min}$ of the effective potential function see also Note III). This distance can be easily evaluated and it increases with the attractor spin, as can be seen in Figs. (6,7), evaluating $\partial_{a_*}(\ell^-_{mbo} + \ell^+_{mso}) < 0$ and correspondingly $\partial_{a_*}(r^+_{mso} - r^-_{mbo}) > 0$.

We focus now on the constraints of the parameter $K$ for the existence of the $\ell$counterrotating sequences of separated rings (or with double points as in $\mathbf{C}_\odot$) with couples $\ell_{a/b} = -1$. Then similarly to condition (28) for the $\ell$corotating sub-sequences, we can set the necessary condition

$$K_+ \in ]K^+_{min}, V_{eff}(-\ell, r^-_{min})], \quad K_- \in ]K^-_{min}, \inf\{V_{eff}(\ell, r^2_{min}), V_{eff}(\ell, y^+_1)\}], \tag{41}$$

where we considered the existence of a third ring centered in $r^2_{min}$.

If there is only a couple, then

$$K_+ \in ]K^+_{min}, V_{eff}(-\ell, r^-_{min})] \quad \text{and} \quad K_- \in ]K^-_{min}, V_{eff}(\ell, y^+_1)]. \tag{42}$$

We note that consistency of the constraint Eq. (41) on the $K_+$ and Eq. (42) is ensured by Eq. (33). The constraint on $K_-$ in both Eqs. (41,42) is guaranteed by the constraint on $K_+$ and the definition of minimum point. It deserves to say that the range $]K^+_{mso}, V_{eff}(-\ell, r^-_{min})[$, is not null since it is $K^+_{mso} = V_{eff}(-\ell, r^+_{mso}) < V_{eff}(-\ell, r^-_{min})$, however the range for $K$ increases as the difference $(r^-_{min} - r^+_{mso})$ increases and this clearly increases with the magnitude of the specific angular momentum. In any case, the distance $\delta^{-,+}_{min} = (r^-_{min} - r^+_{min})$, and possibly also the distance between the maxima $\delta^{+-}_{Max} = (r^+_{Max} - r^-_{Max})$, decreases with increasing of the specific angular momentum magnitude, see also Note III and Note IV. In analogy with Eq. (29), we arrive to the relations

$$\frac{\partial \delta^{-,+}_{min}}{\partial|\ell|} < 0 \quad \frac{\delta^{+-}_{min}}{\partial|\ell|} < 0 \quad \left.\frac{\partial \bar{\lambda}^{-,+}_{Max}}{\partial|\ell|}\right|_{\lambda_+} < 0 \quad \left.\frac{\partial \lambda^{Max}_{+}}{\partial|\ell|}\right|_{\bar{\lambda}_{-,+}} < 0, \tag{43}$$

where $\bar{\lambda}_{-,+}^{Max}$ is the maximum spacing at fixed elongation $\lambda_+$, and $\lambda_+^{Max}$ is the maximum elongation, see also [20] Figs (6,7,4). Finally, we note that relations (43) show the existence of possible constraints in the number of rings with respect to a range of specific angular momenta–see Note IV for the elongation $\lambda_\pm \neq 0$.

**Decomposition of order $n$: $\ell$counterrotating rings $\ell_a \ell_b < 0$**

We can trace some considerations on the $\ell$contourrotating couples at $|\ell_{(i+1)/i}| > 1$ from the analysis of the multiple configuration with couples $|\ell_{(i+1)/i}| = 1$.

We start our discussion considering the $\ell$counterrotating sequence in *accretion* i.e.

$$\exists\, i:\ \ell_i \ell_{i+1} < 0 \quad \text{with} \quad C_x^{i+1}. \tag{44}$$

Then the outer configuration has to be counterrotating as $C_x^{i+1}$ clearly marks the infimum of the counterrotating sequence whose centers can only be placed at $r_{min}^j > r_{min}^{i+1}$. This does not imply that its sequences are isolated in the disk, see definition (i-a). Indeed we can easily prove this by noting that for two configurations $C_i < C_x^o$, it is

$$r_{Max}^i \leq y_3^i < r_{mso}^i < r_{min}^i < y_1^i \leq y_3^o = r_{Max}^o < r_{mso}^o < r_{min}^o < y_1^o \quad \text{with} \quad r_{Max}^o > r_{mbo}^o. \tag{45}$$

In particular, $r_{mso}^i < r_{mso}^o$ that proves $C_i = C_i^-$ and $C_x^o = C_x^{o+}$. Moreover, the necessary condition for the closed configuration is :

$$r_{Max}^+ > r_{mbo}^+ > r_{mbo}^-, \quad K_{min}^- < K_{min}^+ < K_+ = K_{Max}^+ < 1, \quad \ell_- < -\ell_+, \tag{46}$$

see III. for the relation between $K_{min}$ and Figs (6,7,5). If $r_{Max}^+ \in ]r_\gamma^+, r_{mbo}^+]$ then there can be open rings, allowing for funnels of counterrotating material from a point $r_{Max}^+$ of the disk–see Fig. (10). Further considerations are in Sec. (C). It is worth noting that the point of launching of jets $r_J^+ \equiv r_{Max}^+$ is located at $r_J^+ > r_{min}^-$, considering conditions in Eq. (24).

However, we are mostly interested in the situation where the inner ring of the decomposition has to be unstable, therefore

$$\exists i\ :\ \ell_i \ell_{i+1} < 0 \quad \text{with} \quad C_x^i. \tag{47}$$

This condition alone is not sufficient to establish the distribution of the specific angular momentum. We can set some conclusions by considering together the curves of $K_{crit}$ as in Fig. (5), the curves $\ell_\pm$ as in Figs. (6,7) and Figs. (8,9) for the radii of the set $\mathcal{R}$:

**From Fig. (8,9):** As $r_{mso}^- < r_{mso}^+$, the inner unstable configuration, in accretion or jets, is $C_i^x = C_-^x$. The accretion point or jet launching of corotating matter approaches the source as its spin-mass ratio increases, viceversa for the counterrotating matter. The measure $\delta_J$ of orbital region $\Delta_J$ where the launch of jets, or the accretion $(\delta_x, \Delta_x)$, occurs reduces for the corotating matter. This fact emphasizes a preference for the equilibrium configurations of corotating matter for too large spin-mass ratio of the black hole, while the situation is just the opposite for the counterrotating matter. We can summarize the situation for corotating and counterrotating fluids as follows:

$$\Delta_J^\pm < \Delta_x^\pm. \quad \delta_J^\pm < \delta_x^\pm, \quad \partial_{a_*}\delta_J^\pm \gtrless 0, \quad \partial_{a_*}\delta_x^\pm \gtrless 0, \quad a_* \equiv a/M. \tag{48}$$

The **BH** spin-mass ratio distinguishes the morphology and topology of the $\ell$counterrotating rings as in general the orbital instability regions for corotating matter are smaller then the counterrotating ones, or $\delta_c^- < \delta_c^+$ for $c \in \{J, x\}$, for any spin except $a = 0$, where there is no point to distinguish the two $\ell$counterrotating subsequences. We note that a similar relation between the orbital range as for their measures $\Delta_c^- < \Delta_c^+$ for $c \in \{J, x\}$, is only possible for the rings in rotation around attractors

[20] This could be exactly evaluated, considering that $(\ell^- + \ell^+) = 0$ for large $r$, as $(-6a/r)$. Close to the static case (for very slow attractors) there is $\ell^- + \ell^+ \approx 2(4M - 3r)a/(r - 2M)^2$, for $r > 6M$.

with spin-mass ratios sufficiently high. As explained below, this behavior occurs also for the range of the specific angular momentum of the unstable configurations, further discussion can be found also in Sec. (C) where we deepen the case of a $\ell$counterrotating critical couple of sub-configurations. For the couple $C_x^- < C^+$, it is in general:

$$\partial_{\ell_-} K^-_{Max} > 0, \quad \partial_{K_-} \lambda_- > 0, \quad \ell_- \in [\ell^-_{mso}, \ell^-_{mbo}]. \tag{49}$$

For a $C_-$ configuration, we can have also $\ell_- > \ell^-_{mbo}$, for $K_- < 1$ (analogously for a counterrotating ring). Therefore, with increasing attractor spin one can say on the basis of the orbital regions allowed for the points of instability that the unstable corotating configurations are significantly disadvantaged with respect to the counterrotating ones. In other words, according also to the considerations in (Pugliese&Montani 2015a), the rotation of the black hole favors the stability of the corotating configurations, and has a destabilizing effect on the counterrotating ones, separating therefore the $\ell$counterotating rings of the decomposition[21]. Furthermore, at high values of attractor spin, the specific angular momentum required for the corotating ring to be in accretion is closest to the minimum $\ell^-_{mso}$. Then $\ell^-_\gamma$ close to $\ell^-_{mbo}$ is required for a jet–this analysis should be completed with the study of the momentum ranges and the range of the $K$ parameters.

**From Fig. (6) and Fig. (7)** Consider, in analogy to Eq. (48), the ranges for the specific angular momentum:

$$\delta\ell^\pm_J > \delta\ell^\pm_x, \quad \partial_{a_*}\delta\ell^\pm_J \gtrless 0, \quad \partial_{a_*}\delta\ell^\pm_x \gtrless 0, \quad \delta\ell^-_s < \delta\ell^+_s \qquad s \in \{J, x\}, \quad a_* \equiv a/M. \tag{50}$$

For the unstable corotating configurations, $\Delta\ell^-_s$ and their measures $\delta\ell^-_s$ decrease with increasing spin, as the ratio $\ell/a$ increases. The opposite happens for the counterrotating rings of the decomposition. In other words, we need more specific angular momentum for the accretion of a counterrotating ring (or to launch a counterrotating-jet of matter) thus for the corotating ones. This situation, is less and less pronounced as the spin of the attractor decreases or even inverted for spin-mass ratios small enough, namely $a < a_{\aleph_1}$ for the open sub-configuration and $a < a_{\aleph_2}$ for those in accretion. Indeed, we note that similarly to what observed for the range of orbital instability and their measurements, the condition $\Delta\ell^-_s < \Delta\ell^+_s$ $s \in \{J, x\}$ only applies to rings around attractors fast enough, that is with high spin-mass ratio with respect to the limits in $\{a_{\aleph_0}, a_\aleph, a_{\aleph_2}\}$. However, although this analysis would suggest that the unstable modes for the counterrotating rings are disadvantaged at large spin, we note from Eq. (50) that the gap between the $\ell$counterrotating momentum of the accretion phases increases with the spin, distinguishing clearly and unequivocally the two configurations, but at small spin this gap tends to zero or changes sign. Moreover, the ratio $\ell/a$ for corotating rings decreases with the spin while for the counterrotating increases in magnitude with the **BH** spin. The range of possible specific angular momenta for corotating rings in accretion or jets decreases with the spin-mass ratio to a smaller, bounded set of possible values, while it increases for the counterrotating ones. For corotating rings it would be therefore increasingly difficult to select the specific angular momentum for the emergence of the unstable mode, particularly for the jets. Large specific angular momentum corotating jets would then be favorite although $\delta^-_J$ (and $\Delta^-_J$) decreases with the spin, confirming the preference for the stable corotating rings for fast attractors. Then it is also more easy to move from one critical topological class to the other at very high spin. In the region very close to the source, the possibility, for a small change in the specific angular momentum, of a transition from the accretion to jet launch becomes more significant then for the lower spin. The opposite is the situation for the counterrotating matter.

[21] This situation could be described using the analogy with the electromagnetic interactions in the dynamics of electric charges in the Kerr-Newman spacetimes, suggesting the spin-orbital momentum couple in $\ell a \gtrless 0$, as coupling between spin charges, as the electromagnetic couple $Qq \gtrless 0$ for the attractor and particle respectively in the electrical charges case, see for example (Pugliese&Quevedo 2015b)

**From Fig. (5)** The specific angular momentum and the $K$ parameter required for the accretion and the opening up in jet in the corotating sub-configurations orbiting slow attractor is greater than for faster sources, instead the inverse holds for the counterrotating ones, for which at high-spin greater specific angular momentum in magnitude and greater parameter $K$ are required. This situation is clearly less evident for small spin-mass ratios where the distinction between $\ell$counterrotating rings becomes less dominant. As the Eq. (24) holds, we can draw some qualitative considerations on the spacing and elongations of the rings. Being:

$$\partial_{a_*}(1 - K^{\pm}_{mso}) \lessgtr 0, \quad \partial_{a_*}|\Delta K^{\pm}_{mso}| > 0, \quad a_* \equiv a/M, \tag{51}$$

for the two kinds of rings the values of $K_{\pm} \in ]K^{\pm}_{mso}, 1[$, and therefore the range of supremum elongations $\lambda_x$ at the accretion in the two kinds of rings are smaller for the counterrotating rings at higher spin with similar elongations, $K_+ > K^+_{mso}$. The rings (in equilibrium or in accretion) are morphologically similar around faster attractors if they are counterrotating, the inverse is for corotating rings. As just noted, the stability of corotating rings for high attractor spins is favoured and the elongation of the corotating rings can be very diversified.

If $C^+_x < C_-$, then the couple is located at $r > r^+_{mbo}$, see also Note III. This arrangement does not allow the instability in the outer disk confined to distant regions. If $C^-_x < C_+$ and therefore the couple is whole confined at $r > r^-_{mbo}$, the outer ring can be in accretion and in some spacetimes it could open up for jets, see end of Sec. (C). Then one can refer to the relations (48) and (50). We conclude this part by noting that if the outer configurations allows jets, the point of launch will be outer then the accretion point if orbiting sufficiently fast attractors. For slow attractors it can happen that the inner accreting disk overlapS the couterrotating jets and even be $r^-_{Max} \lessapprox r^+_{Max} : \; K^{\mp}_{Max} \lessgtr 1$; further details can be found in Sec. (C).

In conclusion, an increase of the attractor spin-mass ratio acts we could say "centrifugally", separating spatially and morphologically the $\ell$counterrotating rings of the ringed disk decomposition. If the ringed disk is unstable, it is interacting with the source. Such an interaction can result in a slow change in the spin and mass of the attractor with a consequent backreaction on the disk itself. This effect might have relevant consequences as a runway instability of relativistic thick disks (Abramowicz et al. 1983, 1998; Font&Daigne 2002a; Korobkin et al. 2013; Hamersky&Karas 2013; Pugliese&Quevedo 2015b). Then there could occur a the spin up or down of the attractor and a consequent change of the ring disk stability and equilibrium, finally leading to a positive or negative feedback process with alternate phases, periodic or quasi periodic, up to a asymptotic adjustment towards equilibrium or conversely a further evolutionary phase of instability. This clearly depends on several factors including the initial decomposition of the ringed disk, and in particular its differential rotation and topology in accretion. Indeed, the attractor-ringed disk interaction takes place from the inner ring $C_1$, but a perturbation induced by this interaction has consequences on the entire stability of the ringed disk, mainly as consequence of the change of the spin-mass ratio and a change of the parameters of the first ring, see also Sec. (D).

We close this Section considering two couples of rings in equilibrium at equal magnitude of momenta, suppose

$$|\ell^+_{mso}| < |\ell_a| = |\ell_b| < |\ell_c| = |\ell_d| \quad \text{and} \quad C_a < C_b \quad \text{and} \quad C_c < C_d. \tag{52}$$

Then $-\ell^+_{mso} < -\ell^+_a = \ell^-_b < -\ell^+_c = \ell^-_d$, and considering the couples $\ell_{a/b} = -1$, the particular Eq. (32), and using the properties of the $\ell$corotaing sequences summarized in (a.) and (b.), for the couples $(C^+_a, C^+_c)$ and $(C^-_b, C^-_d)$, we finally obtain the following relations:

$$\begin{array}{ccccccccc}
C^+_a < C^-_b & & r^{b_-}_{Max} < r^{a_+}_{Max} < r^{a_+}_{min} < r^{b_-}_{min} & & K^{a_+}_{min} < K^{b_-}_{min} & & K^{a_+}_{Max} < K^{b_-}_{Max} \\
\wedge \quad \wedge & & \vee \quad \vee \quad \wedge \quad \wedge & & \wedge \quad \wedge & & \wedge \quad \wedge \\
C^+_c < C^-_d & & r^{d_-}_{Max} < r^{c_+}_{Max} < r^{c_+}_{min} < r^{d_-}_{min} & & K^{c_+}_{min} < K^{d_-}_{min} & & K^{c_+}_{Max} < K^{d_-}_{Max}.
\end{array} \tag{53}$$

By using the conditions on $K_{min}$ and $K_{Max}$, one cannot obtain any upper boundary on $K_{Max}$ and so a constraint on the existence of the open configurations for jets or closed for accretion. However, the couple $(C_a^+, C_d^-)$, inner and outer rings of the macro-structure, plays an essential role in the determination of the precise decomposition and instability of this $\mathbf{C}^4$ macro-structure. From the relations (53), it is clear that if $C_d^-$ does not satisfy the necessary condition for the jet formation, then no jets can be launched at any point of the entire configuration. On the other hand, to have the inner $C_a^+$ related to jets it the necessary condition for all the rings of the decomposition has to be guaranteed. On the basis of these considerations only, one could say that the outer corotating ring $C_-^d$ of the decomposition is the most favoured for a jet, consistently the launch takes place in the point $r_J^{d-}$ closest to the attractor, as seen from the second square of (53). The same argument can be applied to the couple $(C_b^-, C_c^+)$ when the launch of jet would happen in the middle of the decomposition. The determination of the location for the couple $(C_b^-, C_c^+)$ requires further discussions on the specific angular momentum of the pair. This case has to be further restricted when considered together with the properties (41) derived essentially from the analysis of the specific angular momenta.

This ringed disk of the order $n = 4$ represents an interesting case for investigation of the equilibrium and the instability with accretion or launching of jets. Here, as in the following, we are considering limiting configurations as $|\ell_{a/b}| = 1$. The physical meaning, and therefore the interest in these peculiar cases, lies in the fact that, as it follows from the continuity of the functions, the results apply, or the most part can be straightforwardly extended, to the non exact case (as $|\ell_{a/b}| \neq 1$ or to be more precisely, one could say $|1 - |\ell_{a/b}||/(|\ell_{c/a}| - 1) \in ]0, 1[$).

However, not all of the **BH** attractors allow indifferently one or the settings for the jet launching. Indeed, one has to consider the strict constraints provided by the specific angular momentum where $r_{Max}^{\pm} \in ]r_\gamma^{\pm}, r_{mbo}^{\pm}[$ and [18] $\ell \in ]\pm\ell_{mbo}^{\mp}, \pm\ell_\gamma^{\mp}[$, Figs (6,7). In the cross of these regions, multiple jets are possible only for sufficiently slow **BH** attractors. Considering the results from Eqs. (37)traced for the instability when $\ell_{a/b} = -1$, we infer that there could be four points of jets launching if $a < a_{\aleph_1}$, or four accretion points say for $a \lessapprox a_{\aleph_2}$. We point out that the accretion phase for the corotating couple $(C_b^-, C_d^-)$ is prevented in this scheme by the condition (7), assumed to avoid the penetration of matter with the inner second couple.

Relations (53) are not sufficient to set uniquely the decomposition. One can say in some way that the first square (53) has two vertices in $(C_d^-, C_a^+)$, providing respectively the inner and outer edge of $\mathbf{C}^4$ crucially constraining the stability of the entire system. Starting from a vertex of the square and considering the segment $]C_a^+, C_d^-[$ with extremes on the two vertices, one has to establish the relative position of $C_b^-$ and $C_c^+$. According to the commutation in the couple $(C_b^-, C_c^+)$, one can obtain two different sequences depending on the specific angular momentum of the inner counterrotating configuration. Precisely, it can be either isolated or mixed $\ell$counterrotating sub-sequence:

$$\overbrace{\mathbf{C}}^{}_{s} : \; -\ell_c^+ \in ]-\ell_a^+, -\ell^+(r_{min}^{b-})[, \quad C_a^+ < C_c^+ < C_b^- < C_d^-, \tag{54}$$

$$\overbrace{\mathbf{C}}^{}_{m} : \; -\ell_c^+ > -\ell^+(r_{min}^{b-}), \quad C_a^+ < C_b^- < C_c^+ < C_d^-; \tag{55}$$

see (i-a) and (i-b), the two sequences are in Fig. (4). Notice that the same consideration can be done for a generic relation $\ell_{a/b} < -1$, the main difference here is the further simplification as we assumed to consider any specific angular momenta with $|\ell| > |\ell_{mso}^+|$. Let us focus first on the isolated case $\overbrace{\mathbf{C}}^{}_{s}$, where the center of the counterrotating ring $C_b^+ \in ]C_a^+, C_c^-[ \subset ]C_a^+, C_d^-[$. Its distance is easily assessable from the solutions of the equation for the specific angular momentum and, as shown in Fig. (4), it decreases with increasing distance from the source, but not with the spin of the attractor. Thus one can say that, at great distances, it is less favoured for separate decompositions with couples of equal (or close) specific angular momentum magnitude, which should therefore be a wild feature of the accretion disks very close to the source or associated with very large spins, that is for $R = r/a > r_{mso}^+/a$ small enough. In general, by increasing the spin of the attractor, the distance between the curves $\mp\ell^{\pm}$ increases, consistently the distinction between corotating and counterrotating matter becomes more relevant. In other words, at fixed $r$ the difference $(-\ell^+ - \ell_-)$

increases, but also $\mp\ell^{\pm}_{mso}$ increases, and it is evident from the limit $a < a_{\aleph}$ imposed to get the maximum points for the corotating ring that

$$\partial_{a_*}(-\ell^+ - \ell_-)\big|_r > 0 \quad \text{and} \quad \partial_{a_*}(\delta^{-+}_{min})\big|_{\mp\ell^{\pm}} > 0, \quad a_* \equiv a/M. \tag{56}$$

In terms of the dimensionless radius $R \equiv r/a$, one can say that for $R$ sufficiently large, the distance between the curves is very small and the $\overbrace{\mathbf{C}}^{}_{s}$ decomposition is possible for very close specific angular momenta magnitudes, i.e. $\ell_{a/c} \approx -1$. Brief analysis shows that such rings are thinner compared with the overall size of the ringed disks with very small spacings. This is due to the small gap imposed on the parameter $K$. In this sense, for large values of $R$, the sequences or sub-sequences $\overbrace{\mathbf{C}}^{}_{m}$ are favoured, while for small $R$, configurations $\overbrace{\mathbf{C}}^{}_{s}$

One can rewrite Eq. (54) by saying that if there are two pairs $C^+_a < C^-_b$ where $\ell^-_b = -\ell^+_a + \epsilon_{ab}$, to add a third counterrotating ring $C_c$, the following conditions should be satisfied:

$$\overbrace{\mathbf{C}}^{}_{s} : \; C^+_c \in ]C^+_a, C^-_b[ \quad \text{then} \quad -\ell^+_c \in ]-\ell^+_a, -\ell^+(r^b_{min})[, \quad \overbrace{\mathbf{C}}^{}_{m} : \; C^-_c \in ]C^+_a, C^-_b[ \quad \text{then} \quad \ell^-_c \in ]\ell^-_b(r^a_{min}), \ell^-_b[. \tag{57}$$

As can be seen from Fig. (4), there is a region of possible common values of the specific angular momentum magnitude where the possibility to insert a couple of equal magnitude of specific angular momentum is confined to $\ell^-_c = -\ell^+_c \in [-\ell^+_a, \ell^-_b[$. On the other hand, there are forbidden specific angular momenta for one kind of ring and the other respectively, more precisely for a corotating sub-configuration with $\ell^-_c \notin ]\ell^-_b, -\ell^+(r^b_{min})[$, with high specific angular momenta possible on the contrary for the counterrotating rings, and viceversa for low momenta $-\ell^+_c \notin ]\ell^-(r_{min})^a, -\ell^+_a[$, possible instead for the corotating matter. Additional constraints can be provided by the analysis of the $K$ parameter. It is clear that in the first case, the distance between the configurations is reduced as compared to the inner range of specific angular momenta, in which the ringed disks are more spaced.

Finally in Table (2) is an overview of the results for the $\ell$counterrotating sequences.

### 4.4. On the existence and structure of the ringed configurations

In this Section we briefly discuss the ringed configurations according to the classifications **??**, $\bar{\mathfrak{C}}_{1a}$ and $\bar{\mathfrak{C}}_{1b}$ introduced in Sec. (4). The results presented here derive from the considerations outlined in Sec. (4.3.2) and we show in particular that some decompositions are possible only for limiting number of rings–see also Table (2).

**Configuration $\bar{\mathfrak{C}}_0$** Consider a couple of rings with $\Delta^{(\mathbf{i})}_{cri} \cap \Delta^{(\mathbf{o})}_{cri} = \emptyset$. Then separated configurations can *certainly* exist as it follows from the definition of minimum point, and the inner ring can be in accretion. Condition $\bar{\mathfrak{C}}_0$, clearly *excludes* $\ell$corotating matter configurations. Multiple configurations of this kind are necessarily $\ell$counterrotating, and $r^{(\mathbf{i})}_{mso} = r^-_{mso}$ and $r^{(\mathbf{o})}_{mso} = r^+_{mso}$. That is, the inner ring must be corotating with respect to the black hole, $C_- < C_+$, and the region $[r^-_{min}, r^+_{Max}] \subset \Delta^{\mp}_{mso}$–see also Sec. (4.3.2). Furthermore, from analogue considerations it follows that the maximum order of the decomposition [22] is $n_{Max}(\bar{\mathfrak{C}}_0) = 2$. However, we note that the hypothesis of $\ell$counterrotating disks is essential but not sufficient: one can always have $\ell$counterrotating disks in the Schwarzschild spacetime where $a = 0$, but $\mathbf{C}^2$ satisfying $\bar{\mathfrak{C}}_0$ are not allowed for[23] $a = 0$. As such one can say that

[22] We use the condition $\bar{\mathfrak{C}}_0 : \; \Delta^i_{cri} \cap \Delta^j_{cri} = \emptyset \; \forall i, \; j \in \{1, ..., n\}$ where in particular $\Delta^i_{cri} \cap \Delta^{i+1}_{cri} = \emptyset \; \forall i, \in \{1, ..., n\}$ combined with Eq. (12), and clearly $r_{mso} \in \Delta^{(\mathbf{i})}_{cri}$. Indeed, consider a sequences of $n = 3$ closed configurations, then explicitly: $r^{(1)}_{Max} < r^{(1)}_{mso} < r^{(1)}_{min} < r^{(2)}_{Max} < r^{(2)}_{mso} < r^{(2)}_{min} < r^{(3)}_{Max} < r^{(3)}_{mso}$ which is contradictory for any kind of rotating matter.

[23] In the static spacetime, we do not distinguish corotating or counterrotating configurations ($\ell a \lesseqgtr 0$) and *therefore* $\ell_i \ell_j \lesseqgtr 0$.

$\bar{\mathfrak{C}}_0$ configurations are features proper of the general relativistic effects induced by the rotation of the attractor, with no equivalent in the static geometry (meaning here $R^{-1} = a/r \approx 0$). Possibly the outer ring could open up for jets and this is the case of double critical sub-configurations considered in Sec. (C) and particularly in Sec. (4.3.2). The measure $\delta r^{\pm}_{mso} = \sup \bar{\lambda}_{o,i}$ increases with increasing $a/M$, from the Schwarzschild to the extreme Kerr spacetime, and the couple of rings can be more spaced with the innermost one approaching the black hole.

However we need to distinguish between the configurations orbiting **BH** attractors at $a \in ]0, a_{\aleph_1}[$ where $r^+_{mbo} < r^-_{mso}$. In these spacetimes, the outer counterrotating ring $C^+_o$ cannot open for jets. This case is possible instead for attractors with $a \in ]a_{\aleph_1}, M[$ where $r^+_{mbo} > r^-_{mso}$ and the outer ring could open in jets. In any case, the specific angular momenta must satisfy the relations $-\ell^o_+ \in ] - \ell^+_{mso}, -\ell_+(r^-_{mso})[$ and $\ell^-_i \in ]\ell^-_{mso}, \ell_-(r^+_{mso})[$. The unstable configurations for this couple are $(\mathbf{C}^{\mathbf{x}\,2}_{\odot}, \mathbf{C}^{\mathbf{2}}_{\odot}, \mathbf{C}^{\mathbf{2}}_{\mathbf{x}})$. The configurations $\mathbf{C}^{\mathbf{2}}_{\odot}$, characterized by zero spacing $\bar{\lambda}_{2,1} = 0$ at fixed specific angular momentum can exist with a proper choice of $K_{\pm}$; see also discussion in Sec. (4.3.2).

**Configurations $\bar{\mathfrak{C}}_{1a}$-$\bar{\mathfrak{C}}_{1b}$** The cases $\bar{\mathfrak{C}}_{1a}$-$\bar{\mathfrak{C}}_{1b}$ were introduced in Sec. (4) and they are is characterized by the condition $r^{i+1}_{Max} < r^i_{min}$. In order to trace some conclusions on the $\bar{\mathfrak{C}}_{1a}$-$\bar{\mathfrak{C}}_{1b}$ decompositions, we should focus on the role of the maximum points.

As a closed surface centered in the minimum always exists (for definition of critical point), one can always check for two separated $\bar{\mathfrak{C}}_{1a}$-$\bar{\mathfrak{C}}_{1b}$ surfaces. But the location of the maximum $r^{i+1}_{Max}$, when it exists, selects the kind of rotating matter, if it is corotating or counterrotating. The configurations are therefore divided in the two cases discussed below:

$\bar{\mathfrak{C}}_{1a}: \; r^{i+1}_{Max} \in \Delta^i_{crit}$

In $\bar{\mathfrak{C}}_{1a}$ case, $r^i_{Max} < r^{i+1}_{Max} < r^i_{min} < r^{i+1}_{min} \;\; \forall i \in \{1, ..., n-1\}$, and the rings have to be $\ell$counterrotating (see for example (a.)).

If $C_- < C_+ : \;\; r^-_{Max} < r^+_{Max} < r^-_{min} < r^+_{min}$. Assuming proper conditions on the specific angular momenta magnitude (see for example Fig. (6,7)), it is clear that the maximum order of the decomposition is[24] $n_{Max}(\bar{\mathfrak{C}}_{1a}) = 2$; moreover, we note that the location of $r^{\pm}_{mso}$ should be clarified and therefore the ratio of the specific angular momenta. This follows the discussion in the end of Sec. (4.3.2).

If $C_+ < C_- : \;\; r^+_{Max} < r^-_{Max} < r^-_{mso} < r^+_{mso} < r^+_{min} < r^-_{min}$ could not be possible, but around very slow attractors with $a \approx 0$, see Figs. (6,7), it would be at a fixed $\bar{r}$, $\ell_-(\bar{r}) + \ell_+(\bar{r}) \approx 0$, and one could consider the couple as $\ell$corotating and apply (a.).

$\bar{\mathfrak{C}}_{1b}: \; \Delta^i_{crit} \subset \Delta^{i+1}_{crit}$

This is the case defined in $\bar{\mathfrak{C}}_{1b}$ and as it follows from discussion in Sec. (4.3), it can be a $\ell$corotating sequence of rings with $n_{Max}(\bar{\mathfrak{C}}_{1b}) = \infty$, or an $\ell$counterrotating one. It can be either the couple $\ell_{(i+1)/i} = -1$, with the outer corotating ring, $\ell_- > -\ell_+$, or also $-\ell_+ > \ell_-$ within proper constraints on the specific angular momentum ratios. In general, as condition $\bar{\mathfrak{C}}_{1b}$ does not fix the differential rotation of the ringed disk, in principle there could be an infinite number of rings and further constraints on the order of the decomposition may come from the additional requirements provided on the macro-structure effective potential by means of the boundary conditions in terms of the sequence $\{K_i\}^n_{i=1}$.

---

Clearly, $\ell$counterrotating fluids can orbit around one **BH** attractor but from the point of orbital stability, and hence the toroidal configurations in equilibrium, it is the rotation of the attractor to give meaning to concept of $\ell$counterrotating or $\ell$cororotating. Then the rings in the Schwarzschild geometry can be considered always $\ell$corotating.

[24] It is clear that one cannot add a third (outer) ring to the $\bar{\mathfrak{C}}_{1a}$ couple $C_- < C_+$ for (a.) it should be $\ell$counterrotating with respect to the outer of the first couple, that is corotating, but if it is then for (a.) with respect to the inner ring $C_-$ it cannot satisfies the property $\bar{\mathfrak{C}}_{1a}$.

### 4.5. Limiting cases on the $K$ parameters for an $n$-order decomposition

In this Section we focus on the sequences $\{K_i\}_{i=1}^n$. Similarly to what seen for the case of constrained differential rotation of the ringed disk realized adopting specific and known relations between the elements of $\{\ell_i\}_{i=1}^n$, we here prove that, considering particular relations for the elements in the sequences $\{K^i_{crit}\}_{i=1}^n$, in some cases the decomposition order $n$ turns to be upper bounded, implying various constraints on the morphology of the entire ringed structure. The $K_i$ parameter sets the elongation of each sub-configurations univocally, and then it is able to provide a limit on the number of rings for a macro-configuration, that is intrinsically linked to the effective potential affecting the fluid and containing information on the gravitational field and the centrifugal force each ring is subjected to. Some basic considerations on the role of this parameter has been provided in Sec. (4.2). In the following, we focus on some limiting cases for the values of $K^i_{crit}$ as plotted in Fig. (5): for the couple of rings $(C_a, C_b)$ we investigate the case of $K^a_{Max} = K^b_{min}$ in Sec. (4.5.1) and $K^a_{Max} = K^b_{Max}$ or $K^a_{min} = K^b_{min}$ in Sec. (4.5.2), while in Sec. (4.5.3) we explore the four order ringed disk $\mathbf{C}^4$ characterized by a unique $K_{crit}$. This Section closes in Sec. (4.5.4) with the analysis of the couple of rings at $r^a_{min} = r^b_{Max}$. The examination of these limiting cases, characterized by a known and exact relation between $r_{crit}$ or $K_{crit}$, is interesting because it makes evident possibility to provide a strict upper bound for the decomposition order and therefore to constraint the number of rings of a ringed disk; the maximum order provided in these cases is a number of the set $n_{Max} \in \{2, 4\}$. As consequence of the continuity of the effective potential function, many of the considerations traced for these cases are valid, or can be easily extended for a slight change of the relation between the parameters–see also Sec. (4.3),. This indeed turns to be suitable for the perturbation analysis as sketched in Sec. (D)) and the investigation of more reliable situations where a fine tuning of the critical values imposed with the limiting cases is not required. An overview of the main results of this analysis is also in Table (2)).

Taking into account the considerations of the Note IV one could show that the number of rings can be largely constant, for a little change in the model parameters, having indeed to guarantee the ring separation[25].

#### *4.5.1. Rings $(C_a, C_b)$: $K^a_{Max} = K^b_{min}$*

Firstly we analyze the case of two rings $(C_a, C_b)$ with $K^a_{Max} = K^b_{min}$, therefore we consider the curves $K_{crit}$ =constant in Fig. (5). In general it is:

$$K^a_{mso} < K^a_{min} < K_a < K^a_{Max} = K^b_{min} < K_b < K^b_{Max}, \quad K^a_{Max} < 1, \tag{58}$$

meaning that the $C_a$ ring cannot be open. The maximum number of separated configurations with $K^a_{Max} = K^b_{min}$ is $n_{Max} = 4$, two of them having to be $\ell$counterrotating, $\ell_{(\mathbf{i})}\ell_{(\mathbf{o})} < 0$, and the others $\ell$corotating, $\ell_{(\mathbf{i})}\ell_{(\mathbf{o})} > 0$, where $(\mathbf{i})$ and $(\mathbf{o})$ are for inner and outer ring of the couple.

Indeed at $K_{min} = K^a_{min} > K^+_{mso}$ there can be two $\ell$counterrotating rings, say $C^-_a$ and $C^+_a$, with $K^{a_-}_{min} = K^{a_+}_{min} \equiv K^a_{min}$, and, respectively, given $K_{Max} \equiv K^b_{Max}$ with $K^a_{min} = K^b_{Max}$ or $K^a_{min} \neq K^b_{Max} > K^+_{mso}$. Thus there is a $\ell$counterrotating couple:

$$(C^-_b, C^+_b): \; K^-_{mso} < K^+_{mso} < K^{b_-}_{Max} = K^{b_+}_{Max} \equiv K^b_{Max} = K^{a_-}_{min} = K^{a_+}_{min} \equiv K^a_{min}, \quad n_{Max} = 4. \tag{59}$$

This case will be discussed in Sec. (4.5.2). Here we detail the situation for the couple $C^\pm_a$ and $C^\pm_b$ considering separately the $\ell$corotating pair and the $\ell$counterrotating ones.

**$\ell$corotating rings**

For a $\ell$corotating couple we consider the curves $K^\pm_{crit}$ shown in Fig. (5). Then Eq. (58) holds and to fix the ideas, we suppose that it is $K^a_{min} < K^b_{min}$, and

$$\ell_a\ell_b > 0, \quad \ell_a < \ell_b, \quad C_a < C_b, \quad r^b_{Max} < r^a_{Max} \leq y^a_3 < r^a_{min} < y^a_1 < y^b_3 < r^b_{min} < y^b_1; \tag{60}$$

[25] On the other hand, the accurate assessment of the "slight change" to maintain constant the configuration order can be easily assessable as one consider specific cases fixing the $a/M$ parameter.

see also Note I and Figs (6,7) where:

$$K^a_{mso} = K^b_{mso} < K^a_{min} < K_a = K^a_{Max} = K^b_{min} < K_b < K^b_{Max}, \quad K^a_{Max} < 1, \tag{61}$$

so that the outer ring $C_b$ cannot be unstable, and the inner $C_a$ cannot be in accretion. This is because of Eq. (24) implying that if $\lambda_a = \lambda^x_a$, then $y^a_1 = y^b_{min}$. In conclusion, considering that these results apply for the two $\ell$corotating sequence of the decomposition, the ringed disk $\mathbf{C^4_x}$, within condition (58) cannot accrete into the black hole and more generally cannot be unstable according to a P-W instability, while the possibility that the disk can be in $\mathbf{C}^n_\odot$ topology will be briefly discussed in Sec. (4.5.3).

**$\ell$counterrotating rings**

For two $\ell$counterrotating rings, when Eq. (58) holds, suppose to fix the ideas that it is $K^a_{Max} = K^b_{min}$ with $\ell_a \ell_b < 0$. Then we can realize one of the following two possibilities

$$(\mathbf{C^-_a}, \mathbf{C^+_b}): \; K^+_{mso} < K^-_a < K^{a_-}_{Max} = K^{b_+}_{min} < K^+_b < 1, \quad (\mathbf{C^+_a}, \mathbf{C^-_b}): \; K^+_{mso} < K^+_a < K^{a_+}_{Max} = K^{b_-}_{min} < K^-_b < 1. \tag{62}$$

and, respectively, the two rings $C^\pm_a$ can be in equilibrium or in accretion but cannot give rise to jets.

In the first case

$$(\mathbf{C^-_a}, \mathbf{C^+_b}): \quad r^{a_-}_{Max} < r^-_{mso} < r^+_{mso} < r^{b_+}_{min} \quad \text{and} \quad K^{a_-}_{min} < K^-_a < K^{a_-}_{Max} = K^{b_+}_{min} < K^+_b < K^{b_+}_{Max}, \tag{63}$$

in other words it is $K^-_a < K^+_b$ and $K^{a_-}_{min} < K^{b_+}_{min}$. For the last condition to be satisfied, it can be either

$$r^{b_+}_{Max} < r^{a_-}_{Max} < r^{a_-}_{min} < r^{b_+}_{min} \quad (\text{i.e.} \quad C^-_a < C^+_b \quad \text{and} \quad \ell^-_a < -\ell^+_b), \tag{64}$$

a stable ringed disk, i.e. non accreiting if $C_1 = C^-_a$, or

$$r_{Max} < r^{b_+}_{min} < r^{a_-}_{min} < \bar{r}_- : \; V(\ell^-_a, \bar{r}_-) = K^{b_+}_{min} \quad (\text{i.e.} \quad C^+_b < C^-_a). \tag{65}$$

The corotating configuration $\bar{C}_-$ with minimum in $\bar{r}_-$ has clearly $\ell_- > \ell^-_a$, and the couple $(C^+_b, \bar{C}_-)$ constitutes the case of $K^+_{min} = K^-_{min}$ analyzed below. To characterize the couple in the two cases $C^-_a < C^+_b$ or $C^+_b < C^-_a$, we need to discuss the location of $r^{a_-}_{min}$, and the situation is different for different spacetime classes, (see also results in i) ii) (a.) and b.)[26].

In the second case

$$(\mathbf{C^+_a}, \mathbf{C^-_b}): \quad K^-_{mso} < K^+_{mso} < K^{a_+}_{min} < K^+_a < K^{a_+}_{Max} = K^{b_-}_{min} < K^-_b < K^{b_-}_{Max}, \tag{66}$$

in particular $K^+_a < K^-_b$ and $K^{a_+}_{min} < K^{b_-}_{min}$; from this it follows that

$$r^{a_+}_{min} < r^{b_-}_{min} \quad \text{therefore} \quad C^+_a < C^-_b, \tag{67}$$

see Eqs. (30-34) and also Fig. (5). Equation (67) is not sufficient to fix the relative location of $r_{Max}$, neither the relation between the specific angular momentum, but the two cases listed in III. should be discussed. The inner ring is the counterrotating one of the couple and it cannot be

[26] However, considering Note II and the relations presented in Eqs. (30-34), we remind that in $r > r^+_{mso}$, the $\ell$counterrotating rings have both minimum points; then $K^-_{min}(\ell_-, r_{min}) < K^+_{min}(\ell_+, r_{min})$ at fixed $r_{min}$ where $\ell_- < -\ell_+$, see Figs. (6,7). If, on the other hand, $K^-_{min}(\ell_-, r_{min}) < K^-_{min}(\ell^-_1, r^1_{min})$ for some $(\ell^-_1, r^1_{min})$, then $\ell_- < \ell^-_1$ for $r_{min} < r_{min_1}$, see Fig. (6,7). Suppose that $K^-_{min} < K^+_{min}$ and $r^-_{min} = r^+_{min}$ then $\ell_- < -\ell_+$ and $r^-_{Max} < r^-_{mso} < r^+_{mso} < r^-_{min} = r^+_{min}$. It is clear that the position of maximum $r^+_{Max}$ depends on $r^+_\gamma < r^+_{mbo} < r^-_{mso} < r^+_{mso} < r^-_{Max} < r^+_{Max}$.

open, but it could be in accretion. This can happen if the ringed disk has order $n = 2$, with one only counterrotating couple. If a third or fourth rings are added within (14), then results for the $\ell$corotating sequence apply, and P-W unstable mode can be formed for the ringed disk.
However, from the consideration of Eq. (24), for the inner ring $C_a^+ \subset \mathbf{C}^2$ to be in accretion it has to be:

$$\lambda_a^+ = \lambda_x^+ \quad \text{and therefore} \quad K_a = K_{Max}^{a+} = K_{min}^{b-} \quad \text{with} \quad y_3^{a+} = y_{Max}^{a+} < r_{mso}^+ < y_1^{a+} < y_{min}^{b-}. \tag{68}$$

From the relation between the minima only, we are not able to fix uniquely the sign of $\ell_- + \ell_+$, in order to do this, we need the information on $K_{Max}$, (consider I. II. III.).
In any case, for the inner torus $C_a^+$ in accretion one finds

$$\text{if} \quad \delta r_{min,1}^{\mp} \equiv (r_{min}^{a-} - y_1^{a+}) \quad \text{then} \quad \partial_{r_{min}^{a-}} \delta r_{min,1}^{\mp} < 0, \quad \partial_{y_3^{a+}} \delta r_{min,1}^{\mp} > 0, \quad \partial_{K_a^+} \delta r_{min,1}^{\mp} < 0, \tag{69}$$

with obvious implications on the spacings and then in the density of the rings for more complicated decompositions with one couple satisfying the condition (58). The ranges of variation in (69) must be related to the existence of appropriate values for the counterrotating configurations in accretion, and the corotating in equilibrium, considered due to Eq. (58). However, as there is $y_3^{a+} \in ]r_{mbo}^+, r_{mso}^+[$, then one has to consider differently the attractors with spins

$$a < a_{\aleph_1} : \; r_{mbo}^- < r_{mbo}^+ < r_{mso}^- < r_{mso}^+, \quad \text{or} \quad a > a_{\aleph_1} : \; r_{mbo}^- < r_{mso}^- < r_{mbo}^+ < r_{mso}^+, \tag{70}$$

distinguished by the relative position of $(r_{mbo}^+, r_{mso}^-)$.

*4.5.2. Rings $(C_a, C_b)$: $K_{min} = K_{min}^a = K_{min}^b$ and $K_{Max} = K_{Max}^c = K_{Max}^d$*

The rings $(C_a, C_b)$ with $K_{min}^a = K_{min}^b$ *must* be $\ell$counterrotating or

$$\text{if } K_{min}^a = K_{min}^b \text{ then} \quad \ell_a^+ \ell_b^- < 0, \quad C_a^+ < C_b^- \quad \text{and} \quad n_{Max} = 2, \tag{71}$$

see also Sec. (4.2). Analogously. rings with equal $K_{Max}$ must be $\ell$counterrotatings and $n_{Max} = 2$. However, as mentioned in Sec. (4.5.1)- Eq. (59), if $K_{min}^a = K_{min}^b$, then it is possible to find two $\ell$counterrotating sub-configurations

$$(C_c, C_d) : \; K_{Max}^c = K_{Max}^d = K_{min}^a = K_{min}^b, \quad \text{then} \quad r_{Max}^{b-} < r_{Max}^{a+} < r_{min}^{a+} < r_{min}^{b-}, \quad n_{Max} = 4. \tag{72}$$

We would get exactly the same situation from fixing first $K_{Max}^c = K_{Max}^d$ for two $\ell$counterrotating rings, and it is $r_{Max}^{d-} < r_{Max}^{c+}$. Then we could set in this way a ringed disk by setting an unique $K_{crit}$. We note finally that the condition $K_{mso}^+ < K_{Max}^a = K_{Max}^b$ is not sufficient to locate the disks. This procedure requires discussion of the existence condition on the maximum points provided here for example in Sec. (4.3.2).

The couples at equal $K_{min}$ can exist only for

$$K \in ]K_{mso}^+, 1[ \quad \text{and} \quad r > r_{mso}^+ \quad \text{with} \quad r_{min}^{a+} < r_{min}^{b-} \tag{73}$$

see III.. There is

$$\partial_{K_{min}} \bar{\lambda}_{ab} < 0, \quad \text{and} \quad \partial_K \bar{\lambda}_{ab} < 0 \quad \text{where} \quad K = K_a = K_b, \tag{74}$$

and we will prove below that the case $K = K_a = K_b$ is always possible. The limiting unstable case $K = K_{mso}^+$, saddle point for the potential of $C_+$, corresponds to a maximum point of the pressure for the corotating disk $C_-$. The distance $(r_{min}^- - r_{mso}^+)$, determined by the condition $K_{mso}^+ = K_{min}^-$, provides the maximum distance among the "centers", this distance decreases with $R \equiv r/a$; in analogy with the curves of specific angular momenta $\ell_\pm$ =constant considered in Sec. (4.3.2) in Figs (6,7) it is

$$\partial_a \delta_{min}^{ba} > 0, \quad \partial_r \delta_{min}^{ba} < 0, \tag{75}$$

where $\delta^{ba}_{min}$ sets the separation between the centers and, for a fixed $K_{min}$, it has to be $r^{+}_{min} < r^{-}_{min}$. The difference of the magnitude of the specific angular momentum can be easily evaluated, it decreases with $R$ and, according to the results in Sec. (B), the magnitude of the specific angular momentum increases with $r$.

We focus now on the choice of $K_a$ and $K_b$: it is easy to prove that it can be $K = K_a = K_b$. We start our consideration by noting that there always exists a radius:

$$r_C \in ]r^{a_+}_{min} r^{a_-}_{min}[ : \; V_{eff}(\ell^{+}_{a}, r_C) = V_{eff}(\ell^{-}_{b}, r_C) \equiv K_C \in ]K_{min}, 1[ \tag{76}$$

and the pair $(K^{+}_{a}, K^{-}_{b})$ can be set so that $K \in ]K_{min}, K_C[$. The radius $r_C$ always exists, as can be proved by the Bolzano's theorem on the zeros of a continuous function[27]. Then each $K$ should be set according to $K \in ]K_{min}, K_C[$, and this means we can have $K_a = K_b$, see also (Pugliese&Montani 2015a). However, clearly it is $\partial_K \lambda_i > 0$ at $K = K_a = K_b$ , $\lambda_i$ being as usually the elongation of the $C_i$ ring, for $i \in \{a, b\}$ and $\partial_K \bar{\lambda}_{ba} < 0$, the maximum for the elongation $\lambda^{Max}_{i}$ is at $K_C$ but then the configuration has $K_a = K_b = K_C$, and constitute a $\mathbf{C}^2_{\odot}$.

### *4.5.3. macro-configurations* $\mathbf{C}^4$*:* $K = K_{crit}$

We focus here on the configuration $\mathbf{C}^4$ with a unique $K = K_{crit} = K_{min} = K_{Max}$. To fix the ideas we can set:

$$K^{+}_{mso} < K_{crit} = K^{a_-}_{Max} = K^{b_+}_{Max} = K^{c_+}_{min} = K^{d_-}_{min} < 1, \quad \text{then} \quad r^{a_-}_{Max} < r^{c_+}_{Max} < r^{+}_{mso} < r^{c_+}_{min} < r^{d_-}_{min}, \tag{77}$$

see III. $(C^{-}_{a}, C^{+}_{b})$ cannot be open up in jets and the rings $(C^{-}_{d}, C^{-}_{a})$ have to be in equilibrium. However the location of $(C^{-}_{a}, C^{+}_{b})$ and the critical values $(r^{b_+}_{Max}, r^{d_-}_{Max})$ remain undetermined. This task however is facilitated by noting that $C^{-}_{a}$ and $C^{+}_{b}$ cannot be open and

$$r^{i}_{Max} < r^{i}_{mbo} \quad \forall i \in \{a, b\} \quad \text{then} \quad r^{-}_{mbo} < r^{a_-}_{Max} < r^{-}_{mso} < r^{b_+}_{Max} < r^{+}_{mso} < r^{c_+}_{min} < r^{d_-}_{min} \tag{78}$$

with $r^{+}_{mbo} < r^{+}_{Max}$. We should locate $r^{+}_{Max}$ with respect to $r^{-}_{mso}$. For condition (78) to be satisfied, it has to be $\ell^{-}_{a} \in [\ell^{-}_{mso}, \ell^{-}_{mbo}]$ and $-\ell^{+}_{b} \in [-\ell^{+}_{mso}, -\ell^{+}_{mbo}]$. But it is $[\ell^{-}_{mso}, \ell^{-}_{mbo}[ < [-\ell^{+}_{mso}, -\ell^{+}_{mbo}]$ for sufficiently fast attractors or $a > a_{\aleph_2} : \; \ell^{-}_{mbo} = -\ell^{+}_{mso}$, in these spacetimes $\ell^{-}_{a} < -\ell^{+}_{b}$ and we can refer point ii).

Considering $a > a_{\aleph_2}$, the location of the minimum points $(r^{a_-}_{min}, r^{b_+}_{min})$ is also fixed by noting that, due to Eq. (78) we can always choice an appropriate $K^{a_-}_{min}$ and $K^{b_+}_{min}$ to be lower than $K_{min} = K^{c_+}_{min} = K^{d_-}_{min}$, but as

$$\ell_- < -\ell_+ \quad \text{then} \quad r^{a_-}_{min} < r^{b_+}_{min} \quad \text{and} \quad K^{a_-}_{min} < K^{b_+}_{min}. \tag{79}$$

However, if

$$K^{a_-}_{min} < K^{b_+}_{min} < K_{min} \quad \text{then} \quad r^{a_-}_{min} < r^{b_+}_{min} < r^{c_+}_{min} < r^{d_-}_{min}. \tag{80}$$

Thus in ringed disks around these attractors only mixed configurations $\overbrace{\underset{m}{\mathbf{C}}}$ (i-b) exist.

We focus now on the second class of attractors with $a \leq a_{\aleph_2}$. This class is split by the spin $a_{\aleph_0}$ : $-\ell^{+}(r^{-}_{mso}) = \ell^{-}_{mbo}$, see Eq. (40). But in the whole class, there is a region where the specific angular momentum could also be set in:

$$[-\ell^{+}_{mso}, \ell^{-}_{mbo}] = [-\ell^{+}_{mso}, -\ell^{+}_{mbo}] \cap [\ell^{-}_{mso}, \ell^{-}_{mbo}]. \tag{81}$$

[27] Indeed the function $f \equiv V^{a_+}_{eff} - V^{b_-}_{eff}$ is continuous as sum of continuous functions, and it takes opposite signs in $r^{a_+}_{min}$ and $r^{b_-}_{min}$ respectively and $r^{a_+}_{min} < r^{b_-}_{min}$, as $f(r^{a_+}_{min}) < 0$ and $f(r^{b_-}_{min}) > 0$. This is because for definition $K^{a_+}_{min} = K^{b_-}_{min}$, there exists at last a point $r_C \in ]r^{a_+}_{min}, r^{b_-}_{min}[$ such that $f(r_C) = 0$ and $V^{a_+}_{eff}(r_C) = V^{b_-}_{eff}(r_C)$.

In this common region, the relation between the specific angular momenta can be inverted with respect to Eq. (79). Considering the minima of the $\ell$counterrotating $(C_a^-, C_b^+)$ and the maxima of the couple $C_c^+ < C_d^-$, it is convenient to focus first on the two $\ell$corotating rings separately. We consider then $(C_a^-, C_d^-)$, as if

$$\ell_a^- \ell_d^- > 0 \quad K_{min}(\ell_a^-) < K_{Max}(l_a^-) = K_{min}(\ell_d^-) < K_{Max}(\ell_d^-), \quad \text{it follows} \quad C_a^- < C_d^-; \tag{82}$$

similarly for the counterrotating rings $C_b^+ < C_c^+$. Considering then these relations together we obtain

$$r_{min}^{a_-} < r_{min}^{d_-} \quad \text{and} \quad r_{min}^{b_+} < r_{min}^{c_+} \quad \text{with} \quad r_{min}^{c_+} < r_{min}^{d_-} \quad \text{implying} \quad r_{min}^{b_+} < r_{min}^{c_+} < r_{min}^{d_-}. \tag{83}$$

The location of $r_{min}^{a_-} < r_{min}^{d_-}$ remains undetermined , for this couple one can apply analogue discussion to those for Eq. (53)[28].

*4.5.4. Rings $(C_a, C_b)$: $r_{min}^a = r_{Max}^b$*

We finally consider the case $r_{min}^a = r_{Max}^b$, where it has to be:

$$n_{Max} = 2, \quad \ell_a^- \ell_b^+ < 0, \quad C_a^- < C_b^+ \quad r_{Max}^{a_-} < r_{mso}^- < r_{min}^{a_-} = r_{Max}^{b_+} < r_{mso}^+ < r_{min}^{b_+} < y_1^{b_+}, \\ \text{and} \quad \ell_{mso}^- < \ell_a^- < -\ell_{mso}^+ < -\ell_b^+. \tag{84}$$

The outer ring $C_b^+$ has to be in equilibrium, and it is always possible to find a couple $(K_a^-, K_b^+)$ for the two separated sub-configurations $[y_1^{a^-}, y_3^{b^+}] \subset [r_{mso}^-, r_{mso}^+]$; then

$$K_{mso}^- < K_{min}^{a_-} < K_{mso}^+ < K_{min}^{b_+} < K_b^+ < K_{Max}^{b_+} \quad \text{and} \quad K_{mso}^- < K_{min}^{a_-} < K_a < K_{Max}^{a_-}. \tag{85}$$

Eqs (84,85) do not set completely $K_{Max}^{a_-}$, particularly with respect to $K_{min}^{b_-}$ or $K_{Max}^{b_-}$. This is important to characterize the couple in its unstable phase, as the inner, corotating ring $C_a^-$ is accreting or, if possible, opened for jets. In the remaining part of this subsection we will prove, at least in a certain orbital region, that $K_{min}^{b_+} > K_{Max}^{a_-}$, immediately ruling out the possibility of a corotating jet for this couple.

To prove this result we shall consider Note III and Note II.

We should consider that the maximum possible value of $K_{max}^{a_-}$ is for $r_{min}^{a_-} \in \Delta r_{mso}^{\pm}$ approaching $r_{mso}^+$, also $K_{min}^{a_-}$ approaches $K_{Max}^{b_+}$, decreasing $r_{Max}^{a_-}$, while the difference of the two specific angular momenta increases correspondingly, or it is:

$$r_{Max}^{b_-} = r_{min}^{a_-} \in ]r_{mso}^-, r_{mso}^+[, \quad \partial_{r_{min}^{a_-}} K_{Max}^{b_+} < 0, \quad \partial_{r_{min}^{a_-}} K_{Max}^{a_-} > 0, \quad \partial_{r_{min}^{a_-}} (K_{Max}^{b_+} - K_{Max}^{a_-}) < 0, \tag{86}$$

see Figs. (5,6,7). Therefore the difference $(K_{Max}^{b_+} - K_{Max}^{a_-})$ reaches its minimum at the upper extreme of the radial range, i.e., at $r_{mso}^+$, where $K_{min}^{b_+} < K_{Max}^{b_+}$. Conversely, if $\partial_r (K_{Max}^{b_+} - K_{min}^{a_-}) < 0$ in the range $]r_{mso}^-, r_{mso}^+[$, then the maximum range $(K_{Max}^{b_+} - K_{min}^{a_-})$ is reached at $r = r_{mso}^-$. Then we evaluate the difference $(K_{Max}^{b_+} - K_{min}^{a_-})$ close to the extreme of the orbital boundaries that is at some $\bar{r} = r_{mso}^+ - \epsilon$ and $\bar{r} = r_{mso}^- \pm \epsilon$ for $\epsilon \gtrless 0$. Summarizing, the supremum of $K_{Max}^{a_-}$:

$$\sup K_{Max}^{a_-} : \; r_{min}^{a_-} = r_{mso}^+ - \epsilon \quad \epsilon \geqslant 0 \quad \text{gives} \quad K_{min}^{a_-} \approx K_{min}^{a_-}(r_{mso}^+) < K_{mso}^+, \tag{87}$$

more precisely

$$\sup(K_{Max}^{b_+} - K_{min}^{a_-}) > 0 : \quad r_{min}^{a_-} = r_{Max}^{b_+} = r_{mso}^- + \epsilon, \tag{88}$$

$$\inf(K_{Max}^{b_+} - K_{min}^{a_-}) > 0 : \quad r_{min}^{a_-} = r_{Max}^{b_+} = r_{mso}^+ - \epsilon. \tag{89}$$

[28] In this case however one can consider that $r_{Max}^{a_-} < r_{Max}^{b_+} < r_{mso}^+$ and then $\ell_a^- > -\ell_b^+$ or $r_{min}^{a_-} > r_{min}^{b_+}$ and analogously, if $K_{Max}(\ell_a^-) = K_{min}(\ell_c^+)$ then $K_{min}(\ell_a^-) < K_{Max}(\ell_a^-) = K_{min}(\ell_c^+) < K_{Max}(\ell_c^+)$ and $K_{min}(\ell_a^-) < K_{min}(\ell_c^+)$ and $K_{Max}(\ell_a^-) < K_{Max}(\ell_c^+)$ with $K_{Max}(\ell_b^+) < K_{Max}(\ell_c^+)$ and then $K_{min}(\ell_b^+) < K_{Max}(\ell_b^+) < K_{Max}(\ell_c^+)$.

Now consider a couple of rings which satisfies (88), having the center for the corotating ring $r^{a_-}_{min} = r^-_{mso} + \epsilon$, then with reference to Fig. (6), we have $r^{a_-}_{Max} = r^-_{mso} - \tilde{\epsilon}(\epsilon)$ where $\tilde{\epsilon}(\epsilon) \gtrapprox 0$ is a function of $\epsilon : \tilde{\epsilon}(\epsilon) < \epsilon$. It has to be $K^{a_-}_{min} < K^{a_-}_{Max} \approx K^-_{mso} \ll K^{b_+}_{Max}$, but $r^{a_-}_{min} = r^{b_+}_{Max}$, from which it follows that $r^{b_+}_{min} \gg r^{a_-}_{min}$ that implies $K^{b_+}_{min} > K^{a_-}_{min}$. On the other hand, $r^{a_-}_{Max} = r^-_{mso} - \tilde{\epsilon}$ also $K^{a_-}_{Max} = K_{mso} + \tilde{\tilde{\epsilon}} < K^{b_+}_{min}$, being $K^{b_+}_{min} > K^+_{mso}$. By considering these relations together, we finally obtain: $K^{a_-}_{min} < K^{a_-}_{Max} < K^{b_+}_{min} < K^{b_+}_{Max}$ which constitutes the proof for points $r^{b_+}_{Max} = r^{a_-}_{min}$ close to the supremum in (88). In this discussion we are clearly assuming that $r^+_\gamma < r^+_{mso}$ for the existence of the maximum for the counterrotating ring. In fact it could be that one of the elements $r_i \in \{r^+_\gamma, r^+_{mbo}\}$ be $r_i \in \{r^-_{mso}, r^+_{mso}\}$. The first case occurs, if the spin-mass ratio of the attractor $a/M > 0.61$ c.a., and $r^+_{mbo} \in \Delta r^\pm_{mso}$ if $a > a_{\aleph_1}$.

We focus now on an orbital range near the infimum in (89). The situation in this case can not be treated as in the previous case for the orbital upper boundary. In the first place, the maximum for the corotating matter can also not exist, in fact similar conditions to those in Sec. (4.3.2) should be valid. In particular it has to be $\ell_-(r^+_{mso}) < \ell^-_\gamma$ which is the case only for spacetimes sufficiently slow, say $a/M \ll 0.7$ c.a.–see Fig. (7). For attractors $a/M \in ]0.43, 0.7[$ c.a. it is $K^{a_-}_{Max} > 1 > K^{b_+}_{Max}$ and only for slower attractors, there is $K^{a_-}_{Max} < 1$. This can be easily seen by investigation of the couples orbiting attractors with center of maximum pressure near the upper boundary $r^+_{mso} - \epsilon$: for the corotating ring the specific angular momentum is $\ell_-(r^+_{mso} - \epsilon)$, function of $a/M$ and defines uniquely $r_{Max}$, if this exists. The counterrottaing ring cannot give rise to a jet while, for sufficiently fast attractors ($a/M \in ]0.43, 0.7[$ c.a.) the inner corotating one can result in its unstable phase in open funnels of jets and the reverse occurs in the vicinity of lower orbital boundary $r^-_{mso}$.

## 5. Discussion and Future Perspectives

In this work we propose a model of ringed disk made up by several toroidal perfect fluid configurations, a ringed disk, orbiting an axially symmetric attractor, namely a supermassive Kerr black hole. Such ringed disks could be created during the evolution of matter configurations around supermassive black holes. To model each ring of the disk, an hydrodynamic model based on the Boyer theory of equipressure surfaces in General Relativity is considered. We define and characterize the morphology and equilibrium of the ringed macro-configurations. The ringed disk, has been assumed to posses a well defined equatorial plane of symmetry, coincident with the equatorial planes of each ring. The (reflection) symmetry plane of the rotating attractor is also the ringed disk equatorial plane. Each ring is governed by the Euler equation for fixed values of the parameter couple $\mathbf{p} = (\ell, K)$, and coupled to the next-neighbor (consecutive) rings of the decomposition by some boundary conditions, specifical constraints on the inner and outer edges of each ring, or equivalently by the sequence of parameters $\{K_i\}^n_{i=1}$ of the decomposition, by the model set up assumed a priori. The configurations are characterized providing constraints and limits on the number of rings and their dynamics (if in equilibrium or unstable) considering both the corotating or counterrotating fluids. The unstable ringed configurations are also considered. The (structural) perturbation and unstable modes of the ringed disks, as defined in Sec. (D), are also discussed. Perturbations of the ringed accretion structure are namely perturbation *of* and *in* its decomposition into rings. The model adopted for each ring of the decomposition, determined according to the Boyer condition, is essentially governed by the geometric properties of the gravitational background and the constants of the fluid motion associated with the symmetry of the system. Essentially, we based our analysis taking advantage of these symmetries and basing our results according to various geometric considerations, emphasizing the role of the curvature effects and especially the rotation of the central attractor.

We can recognize two fundamental aspects of this investigation:

**1.** We considered mainly separated sub-configurations, as defined in Sec. (3), assuming a non-overlapping (non penetration) of matter between the rings of the decomposition. This hypothesis is indeed suitable and necessary for rings in equilibrium. Where a penetration or intersection of sub-configurations occurs, an instability arises, in closed $C$ configurations these correspond to the $\mathbf{C}^n_\odot$ topology. They are interpreted

as the initial stages of the unstable modes involving matter collisions, or feeding, or accretion, of a sub-configuration to one another. In each case these are argued to be unstable phases of the ringed disk, not immediately described by the Boyer theory. These configurations, introduced and briefly discussed here, are investigated in more details in future studies of the unstable modes of the ringed disks (Pugliese&Stuchlik 2015).

In fact, the assumption of non-overlapping can be relaxed for the decompositions with at least one unstable open point, considering therefore the possibility of a decomposition with launching points of the jets as discussed in Sec. (C).

**2.** A second remarkable aspect that reveals (surprisingly) as a result of this analysis is the distinction between $\ell$counterrotating tori, in other words the role of the relative rotation of the fluids belonging to different sub-configurations. We should note that this distinction is induced by the rotation of the central attractor and has less relevance to determine the macro-structure decomposition as the dimensionless radius $R \equiv r/a$ increases according to the analysis detailed in particular in Sec. (B). This aspect is much more surprising since, as emphasized in different points, the rings are not related by one dynamic law regulating the entire decomposition, but the considerations of the gravitational background are sufficient to deduce very stringent constraints providing the boundary conditions in the (ad hoc) definition of the effective potential of the macro-structure, provided in Sec. (A.1). Characterization of the equilibrium morphology of such objects represents a starting point for characterization of the unstable phases of the ringed disks. Especially in the unstable modes, this model could prove to be a promising approach for the analysis of the emergence of high energy phenomena as jets. In fact, a possibly interesting perspective of this work is the study of global instability inside the ringed disk induced by the gravitational instability or breaking of the geometric constraints as described in the Sec. (3.1), leading to the collapse of a ring on the Kerr accretor or on the consecutive ring, or feeding of matter between the rings. The unstable phases are essentially associated with the (super Eddington) accretion and jet emission. From the description of these states we determine the instability points (considering also the possibility of several points) associated with accretion and launching of jets from the ringed disk as well as the specific angular momentum initially characterizing the unstable phases.

The present study of the ringed disks can be seen as a starting model of more complex systems. The majority of the results traced here hold or can be simply extended to more general situations with different equation of state, for example. The extension of this analysis to different fluids, including for example the dissipative effects, or the electromagnetic contributions an a GRMHD scenario, is also possible. This study could be easily generalized to the case of non-constant angular momentum (Lei et al. 2008; Abramowicz 2008), or to the case of non-coplanar rings rotating the same attractor (see for the off-equatorial tori around compact objects (Cremaschini et al. 2013)). However we have shown in Sec. (A.1) that the ringed disk turned to be a geometrically thin model of the disk with negligible spacings. The role of the second lobe, here completely neglected except in accreting configurations, should be then deepened. The generalization to other models for the sub-configurations could involve essentially two types of difficulties: first one (perhaps less relevant), is the algebraic complication in extended frameworks, for example in the GRMHD thick disks, whose analytical treatment today is practically limited to the study of solutions with magnetic field with exclusively toroidal component(Komissarov 2006; Abramowicz&Fragile 2013; Pugliese&Montani 2013b; Zanotti&Pugliese 2014; Vincent et al. 2014; Adamek&Stuchlik 2013; Ciolfi&Rezzolla 2013; Hamersky&Karas 2013). The second significant aspect is constituted by the fact that the many disk models, such as the majority of thin disks, are essentially not geometric in the sense explained in Sec. (2). An important example of the "non-geometrical nature" of these models is the determination of the rotational law for each torus and the specific angular momentum $\ell$ here assumed a constant parameter or otherwise known function of $r$ and other variables. It is clear that, to carry out the analysis given here, we should provide an appropriate set of parameters to determine and characterize the decomposition. Finally, we focused on the analysis of the critical configurations, here considered in the two modes of $C_x$ or $O_x$. As proved in Sec. (C), these configurations are generally the inner ones and must be interpreted by saying that the Boyer theory is only able to describe the dynamical situations at $t$ fixed. The discussion of these cases is expected to be carried

out in a future work.

We also stressed the possibility that, during its unstable phases, an interaction with the attractor can occur with the consequent change of the geometrical characteristics of the spacetime. The mutation of the attractor properties will determine in turn a change of the dynamical properties of the orbiting structure resulting in an iterative process to be analyzed, which could lead also to a form of runaway instability(Abramowicz et al. 1983, 1998; Font&Daigne 2002a; Korobkin et al. 2013; Hamersky&Karas 2013; Pugliese&Quevedo 2015b).

As a first attempt to characterize these structures, a part of this article was necessarily descriptive: a number of definitions has been introduced, and the formalism has been extensively explained.

## 6. Summary and Conclusions

The main steps of this analysis are as follows:

**I-Part: Introduction of the model** This part was developed in Secs. (2) and (3). We provided a precise definition of ringed accretion disks by clarifying the fundamental concepts of ring, decomposition of the internal structure and sub-sequences. We emphasized the role of the$\ell$counterrotating sub-sequences. We have shown that the decomposition can be mixed or isolated according to definition of Sec. (2). We characterized the unstable configurations showing that there are essentially two types of unstable systems or a combination of these. Depending on whether the instability is due to a P-W mechanism for one or more elements of the ring decomposition or to some phenomena of collisions between material belonging to consecutive rings. We provided the definition of some morphological properties. Having naturally identified the inner (outer) edge of the ringed disk as that of the first ring of its ordered decomposition, we defined the elongation and the spacing and, discussing the minimum number of quantities to be specified to characterize the entire decomposition, we showed that in general the macro-structure can be a geometrically thin disk.

**II part: characterization of the ringed disk decomposition** The second part of the article, developed in Sec. (4), was dedicated to the analysis of the macro-structure and its characterization. In general, we focused on the macro-structures in equilibrium. We then characterized the decomposition showing that there are only two types of configurations, and accretion disks can exist in one or in a combination of these. The role of the model parameters has been extensively characterized. Rings are not possible with equal specific angular momentum, with the exclusion of the $\ell$corotating couple $(C, O_x)$, where condition in (15) could be relaxed. We show that the configurations determined by special relationships between $K$ parameters, have a maximum number of rings (order of decomposition) equal to 2 or 4. An important point of this work was the definition of the effective potential of the whole macro-structure addressed in Sec. (A.1). The discussion of this aspect has naturally emphasized the nature and value of the boundary conditions. We introduced the definition of differential rotation of the disk and different notions of the specific angular momentum in Sec. (4.3). We found a number of results related to the configurations with instability points, especially for the $\ell$counterrotating case. The elongation of the equilibrium disk is smaller than the elongation of its accretion closed configuration and increases with the magnitude of the specific angular momentum. The marginally stable orbit is included in the accretion disk. Some key considerations have driven this analysis. The specific angular momentum of each $\ell$corotating sub-sequence increases in magnitude with the configuration index. Given a ringed disk of the order $n$, each $\ell$corotating sub-sequence allows *only* one $C_x$ configuration, that is only the inner ring of the disk can accrete onto the Kerr attractor and the inner one has the lower specific angular momentum in magnitude. Thus the outer configuration must be in $C$ topology and the rank $\mathfrak{r}_{\mathfrak{r}\,Max} = 1$. It follows then that the rings of the $\ell$corotating sub-sequences satisfy, whether or not consecutive, the property $\bar{\mathfrak{C}}_{1b}$ as in $(\bar{\mathfrak{C}}_{1b})$. Increasing the spacing between the rings centers, or by adding a ring to a $\ell$corotating ringed configuration, it is necessary to supply additional specific angular momentum to the outer ring such that $\ell_{i/i+1}| \in ]0, 1[$, or the distance between the two minima $(r^a_{min}, r^b_{min})$ increases with increasing difference between the two specific angular momenta in magnitude. The derivative $\partial_r(\mp\ell^{\pm})$

has a maximum point at $r^{\pm}_{\mathcal{M}}$, respectively, different for each attractor, as we detailed in Sec. (B). Increasing of the specific angular momentum with the radial distance from the attractor magnitude is not constant but it rises up to a limiting radius, different for the $\ell$counterrotating sequences and for any spacetime, being the $r^{\pm}_{\mathcal{M}}$ function of the attractor spin-mass ratio. This is a relativistic effect that disappears in the Newtonian limit when the orbital distance is large enough with respect to $r^{\pm}_{\mathcal{M}}$, these effects are mainly due to the presence of the intrinsic spin of the attractor.

The special behavior of the specific angular momenta in the Kerr black hole spacetimes distinguishes the two $\ell$corotating sub-sequences of corotanting and counterrotating rings respectively of a generic decomposition. The Kerr **BH** spin has a stabilizing effect for the corotating matter and destabilizing for the counterrotating one. As $\partial_{|a|} r^{\mp}_{\mathcal{M}} \lessgtr 0$, the region where less additional specific angular momentum is due increases with the spin-mass ratio of the spacetime in one case, and decreases in the other, in Sec. (B).Many morphological characteristics of a toroidal accretion disks show a symmetry under the transformation $\ell \rightarrow -\ell$, then we expect a similar symmetry to be conserved in the macro-structure $\mathbf{C}^n$, and so find analogies between the $\ell$corotating and $\ell$counterrotating sub-sequences. We therefore characterized the configurations with critical points from the point of view of the differential rotation and for the presence of points of accretion and jets.

Table (2) gives an overview of the most relevant results. This work is mostly focused on the equilibrium configurations leaving, for a following analysis, (Pugliese&Stuchlik 2015), a more careful treatment of the topologies associated with the unstable phases of the macro-structure. However, through the study of internal structure of the ringed disk as the collection of many parts, the rings, we pointed out two types of processes emerging possibly with evidences in various astrophysical phenomena. Firstly, the existence of any configuration composed by several orbiting rings, in which the single ring may reasonably undergo the model introduced in Sec. (2) (which is well-known in the literature and widely used, especially in the analysis of geometrically thick disks) should be finally adjusted in the analysis presented here, and subjected to the constraints related to the orbital locations and specific angular momentum here provided in details. It is clear that the morphological characterization of the equilibrium is a first step in the study also for the gravitational environments where the traces of these objects would be expected, and whose effects should be evident. In fact, one of the objectives of this work is to propose precisely the existence of such formations, characterize them and open the way for further analysis. Secondly, it is evident from the thoughtful discussions in this paper, that the ringed disk is subjected to a very peculiar internal dynamics, in which rings have also their own independent evolution that, at some stage, may be unstable: rings could move, collide and even grown one into one another, giving rise to accretion phenomena with a sort of feeding–dry processes between two rings(Pugliese&Stuchlik 2015). Effects, usually related to the "direct" interaction of unstable matter in accretion with the attractor, may possibly be associated to this type of internal dynamics, including jets,

| | | | |
|---|---|---|---|
| $\bar{\mathfrak{C}}_0$-$\ell$counterrotating; | $n_{Max}(\bar{\mathfrak{C}}_0) = 2$ | $C_- < C_+$ | $(a \in [a_{\aleph}, M] - C_+ \rightarrow O^+_x)$ |
| $\bar{\mathfrak{C}}_{1a}$-$\ell$counterrotating; | $n_{Max}(\bar{\mathfrak{C}}_{1a}) = 2$ | $C_- < C_+$-$(C_+ < C_- \text{–} a \gtrapprox 0)$ | |
| $\bar{\mathfrak{C}}_{1b}$-$\ell$counterrotating-$\ell$corotating; | $n_{Max}(\bar{\mathfrak{C}}_{1b}) = \infty$ | | ($\ell$corotating -$\mathfrak{r}_{\mathfrak{x}_{Max}} = 1$; $C^1_x$) |
| $\ell$counterrotating-$\ell_{i/j} = -1$ $\bar{\mathfrak{C}}_{1b}$; | $n_{Max} = 2$ | $C_+ < C_-$ | $\exists\, r^-_{Max}\ a < a_{\aleph}$ :-$\check{C}_I :\ a \in [0, a_{\aleph_1}[\ \check{C}_{II} :\ a \in [a_{\aleph_1}, a_{\aleph}[$ |
| | | $C_- \rightarrow O^-_x\ (a < a_{\aleph})$, $C_- \rightarrow C^-_x\ (a < a_{\aleph_2})$; | $C_+ \rightarrow (C^+_x, O^+_x)\ a > a_{\aleph_0}\ (\check{C}_\alpha - \check{C}_\beta)$ |
| $K^c_{Max} = K^d_{Max} = K^a_{min} = K^b_{min}$ | $n_{Max} = 4$ | | |
| $K^a_{Max} = K^b_{min}$ | $n_{Max} = 4$ | n=2- $\ell$counterrotating;$C_b > C_a$ | n=2-$\ell$corotating-$C^-_a \lessgtr C^+_b$ $\quad C^+_a < C^-_b$ $(a \in ]a, a_{\aleph_1}[-]a_{\aleph_1}, M])$ |
| $K^a_{min} = K^b_{min}$ | $n_{Max} = 2$ | $\ell$counterrotating | $C^+_a < C^-_b$ |

Table 2: Overview of some restrictions on the decomposition order $n$ of the macro-structure $\mathbf{C}^n$. It follows the analysis of Sections (4.3.2,4.4,4.5). The existence of the minimum of the hydrostatic pressure (maximum of the effective potential) $r_{Max}$ is assumed; therefore there is $\ell \in ]\ell_{mso}, \ell_\gamma[$, both for the corotating and counterrotating configurations. The sequentiality, according to the location of the maximum points of the hydrostatic pressure is also briefly summarized. Some considerations on the existence of cusped topologies, associated with the unstable configurations according to the Paczyński-Wiita mechanism, are provided ($\rightarrow$). $\bar{\mathfrak{C}}_0, \bar{\mathfrak{C}}_{1a}, \bar{\mathfrak{C}}_{1b}$ are the principal classes of decompositions.

as it will be shown in more details in (Pugliese&Stuchlik 2015). A further, interesting, possibility would be that some phenomena should lead traces of this ringed,"discrete", structure of the initial equilibrium state. The perturbative analysis, only hinted here in Sec. (D), tries to enter into the argumentation of this issue. Thirdly, the ringed disk can be considered actually one orbiting body: one of the challenges of this work was the construction and interpretation of this aspect of the ringed disk model. We realized this through what we have been defined as constraints on the decomposition, for example in the definition of the effective potential of the ringed disk. Therefore, those phases and phenomena usually attributable to an accretion disk in interaction with the attractor and with its environment could be also analyzed in view of an internal dynamics of a ringed disk model. The dynamics of a ringed disk, as a single body in interaction should be affected by, as shown here, the internal phases and particularly by the distribution of angular momentum, especially when formed by the $\ell$counterrotating fluids. We can therefore conclude that the analysis of the ringed disks around supermassive black hole could give a new insight into the accretion processes in active galactic nuclei and quasars, and could be helpful especially in relation to the instability of the ringed disks.

The authors acknowledge the institutional support of the Research Center of Theoretical Physics and Astrophysics at the Faculty of Philosophy and Science of the Silesian University of Opava. Z.S. acknowledges the Albert Einstein Center for Gravitation and Astrophysics supported by the Czech Science Foundation grant No. 14-37086G. D. P. also acknowledges useful discussions with Prof. J. Miller, Prof. M. A. Abramowicz, Prof. V. Karas and Prof. W. Kluzniak, in the early stages of this work.

## A. Notes of the ringed disk morphology and the effective potential of the ringed disk

We introduce the definition of ringed disk *height* and thickness, following the discussion of Sec. (3.2).

We define the $\mathbf{C}^n$ disk *height* $h_{\mathbf{C}^n}$ as:

$$h_{\mathbf{C}^n} \equiv \max\{h_i\}_{i=1} = h_h, \tag{A1}$$

where $h_i$ is the height associated to the sub-configuration $C_i$, or the maximum point $x^i_{Max}$ (*not* $2x^i_{Max}$) corresponding to the point $y^i_{Max} \in \Lambda_i$ of the surface $\partial C_i$ in Fig. (2)[29]. More generally, in the set $H^n = \{h_i\}^n_{i=1}$, associated to the elements of the ordered decomposition $\{C_i\}^n_{i=1}$, the toroidal surface $\partial\mathbf{C}^n$ can show up with several local maxima and relative minima. More precisely let us define $h_i$ to be a *local maximum* of the set $H^n$ if $h_{i-1} < h_i > h_{i+1}$, and we define *local minimum*, if $h_{i-1} > h_i < h_{i+1}$. The set $H^n$ has one and only one maximum if $h_1 < ... < h_{i-1} < h_i > h_{i+1} > ... > h_n$. Definition (A1) assumes implicitly $h_{Max}$ will be an absolute maximum correspondent to one and only one sub-configuration $C_h$, however this can be not the case. The case of several configurations with $h_{Max} \equiv \sup h_i$, can occur up to $n$-sub-configuration with $h_i = h_h \ \forall i \in \{1, ..., n\}$ for a $\mathbf{C}^n$ macrostructure.

We can define the *thickness* $R_{\mathbf{C}^n}$ and $R_{\mathbf{C}^n_\odot}$ of a $\mathbf{C}^n$ ringed disk and of a saturated $\mathbf{C}^n_\odot$ ringed disk, respectively, as

$$R_{\mathbf{C}^n} \equiv \frac{2h_{\mathbf{C}^n}}{\lambda_{\mathbf{C}^n}} = \frac{2h_{Max}}{\sum^n_i \lambda_i + \bar{\lambda}_{\mathbf{C}^n}} = \frac{R_h}{1 + \sum^{n\neq h}_{i=1} \lambda_i + \bar{\lambda}_{\mathbf{C}^n}\lambda_h^{-1}} \tag{A2}$$

$$R_{\mathbf{C}^n_\odot} \equiv \frac{R_h}{1 + \sum^{n\neq h}_{i=1} \lambda_i} \quad \text{for} \quad \mathfrak{r} = \mathfrak{r}_{Max}, \tag{A3}$$

where $R_i \equiv 2h_i/\lambda_i \cong 1$ is the thickness of a single torus. However from (A2) it follows that the macroconfiguration $\mathbf{C}^n$, made by thick rings, can be considered properly to be a geometrically thin disk as

[29] We note that generally $r^i_{min} \neq y^i_{Max}$, when both exist.

$R_{\mathbf{C}^n} < 1$ or even $R_{\mathbf{C}^n} \ll 1$. In the definition (A2) we considered Eq. (10) where $h_{Max}$ is associated to one and only one ring of the decomposition and $R_{\mathbf{C}}$ is related to the only $R_h$. We can generalize Eq. (A2) to the case where there are $m < n$ rings with equal, maximum height $h_{Max}$. In this case the ringed disk thickness, defined in (A2), can be written as $R_h \equiv \max\{R_j\}_{j=1}^m$, in other words in the evaluation of $R_h$, we use the elongation $\lambda_h \equiv \min\{\lambda_j\}_{j=1}^m$.

### A.1. The effective potential of the $\mathbf{C}^n$ macro-structure

In this Section we provide a definition for an effective potential of the macro-structure $\mathbf{C}^n$. We will use the fact that the decomposition $\{C_i\}_{i=1}^n$, introduced in Sec. (3), is uniquely determined by considering a fixed $\mathbf{p}_{\mathbf{C}^n}$ in the appropriate range of values determined by the existence conditions for $\mathbf{C}^n$. The rings of the decomposition $\{C_i\}_{i=1}^n$ are not dynamically tied, as ruled by $n$ different Euler equations, but they are related only by being rings of $\mathbf{C}^n$. The sub-configurations are bound by the boundary conditions given on each scalar function of the effective potential $V_{eff}^i$ regulating its own stability, morphology and the location in the ordered decomposition. One can ask whether it is possible to associate the macro-configuration $\mathbf{C}^n$ to a single scalar, say an effective potential or $V_{eff}^{\mathbf{C}^n} = V_{eff}^{\mathbf{C}^n}(\mathbf{p}, r, a)$, depending on the sequences $\{\ell_i\}_{i=1}^n$ and $\{K_i\}_{i=1}^n$ and regulating the macro-structure and its decomposition, just as $V_{eff}^i$ is associated for each ring $C_i$. Clearly, each $V_{eff}^i$ is determined by a dynamical equation for the pressure of the $C_i$ ring and by the constraint of the ring separations, i.e., Eq. (15). As we have no such an equation for the entire ringed disk $\mathbf{C}^n$, any attempt to elaborate an effective potential approach for the $\mathbf{C}^n$ macro-configuration reduces in this scheme to build up an ad hoc scalar, from the set $\{V_{eff}^i\}_{i=1}^n$ and the model parameters. However, the potential of the macro-structure should be able to regulate the dynamics of each ring, as not isolated extended bodies but as being parts of one decomposition to describe the situation in the spacing regions of the ringed disk.

In general, if $V_{eff}^i$ is the effective potential regulating the $C_i$ ring of a macro-structure $\mathbf{C}^n$, at fixed $\{\ell_i\}_{i=1}^n$, or at fixed order $n$ and $\{K_i\}_{i=1}^n$, we can introduce the following two definitions regulating the ringed disk:

**The effective potential $V_{eff}^{\mathbf{C}^n}\Big|_{K_i}$ of the *decomposed* $\mathbf{C}^n$ macro-structure** defined as

$$V_{eff}^{\mathbf{C}^n}\Big|_{K_i} \equiv \bigcup_{i=1}^{n} V_{eff}^i \Theta(-K_i), \tag{A4}$$

where $\Theta(-K_i)$ is the Heaviside (step) function such that $\Theta(-K_i) = 1$ for $V_{eff}^i < K_i$ and $\Theta(-K_i) = 0$ for $V_{eff}^i > K_i$, so that the curve $V_{eff}^{\mathbf{C}}(r)$ is the union of each curve $V_{eff}^i(r) < K_i$ of its decomposition. This is a piecewise smooth curve[30]

[30] In fact, each potential $V_{eff}^i$ and, therefore, in particular $V_{eff}^i\Theta(-K_i)$ is clearly a smooth function of $r$ in $\Lambda_i$ (certainly $\ell_i$ is a fixed parameter), with a minimum point $r_{min}^i \in \Lambda_i$ as there is $K_i \geq K_{min}^i$. Therefore it is certainly possible to evaluate the minimum points $\{r_{min}^i\}_{i=1}^n$ of the overall potential $V_{eff}^{\mathbf{C}^n}\Big|_{K_i}$ by differentiating the single potential $V_{eff}^i$. As stated in the text, the curve $V_{eff}^{\mathbf{C}^n}\Big|_{K_i}$ shall be in general discontinuous at the edges $(y_1^i, y_3^i)$–see for example Fig. (4) where the $\{K_i\}_{i=1}^n$ are explicitly shown. Finally, we note that the "cut" provided by the Heaviside (step) function $\Theta(-K_i)$ makes sure that there is in fact no "overlap" of curves, in the spacings $\bar{\Lambda}_{i,i+1}$, for the effective potential $V_{eff}^{\mathbf{C}^n}\Big|_{K_i}$ of the *decomposed* macro-structure (a part the case of double points when there is $\bar{\Lambda}_{i,i+1} = 0$ and also $K_i = K_{i+1}$). Thus, except some cases of $\mathbf{C}_\odot$ configurations, in any ranges $\Lambda_k$ the potential $V_{eff}^{\mathbf{C}^n}\Big|_{K_i} = V_{eff}^k$ is well defined, with no overlapping with the potential $(V_{eff}^{k-1}, V_{eff}^{k+1})$ of the consecutive rings, and with $V_{eff}^{\mathbf{C}^n}\Big|_{K_i} = 0$ in any range $\bar{\Lambda}_{i,i+1} \neq 0$. Finally, we stress that in Eq. (A4), as in the entire work, we are neglecting to consider the innermost surface (associated with the $y_2^i$ solutions) for any topology but not the $C_x$ one for an accretion torus.

The curve $V_{eff}^{\mathbf{C}^n}\Big|_{K_i}$ has $n$ minimum points, defining the order of the decomposition and the centers of each rings, a maximum number $n-1$ of ranges $\bar{\Lambda}_{i+11}$ (spacing), reduces to zero for saturated $\mathbf{C}^n_{\odot}$, bounded for the $\Lambda_{\mathbf{C}^n} = [y_3^1, y_1^n]$ with $2n-2$ points of discontinuity, and eventually up to $n$-maximum points for a saturated $\mathbf{C}^n_x$ macro-structure. Thus, for fixed couple $(C_i, K_i)$, the problem to find and characterize the decomposition of $\mathbf{C}^n$ is reduced to the problem to fix the sequence $\{\ell_i\}_{i=1}^n$. The usefulness of this definition is that at fixed ordered sequence $\{K_i\}_{i=1}^n$, it remains to determine the elongations ranges $\Lambda_i$ and the specific angular momentum to determine the decomposition [31]. In Fig. (3) an example of decompositions at fixed $\{\ell_i\}_{i=1}^n$, being induced by different choices of eligible $\{K_i\}_{i=1}^n$, is shown, where each decomposition corresponds to a different $V_{eff}^{\mathbf{C}^n}\Big|_{K_i}$ potential.

**The effective potential $V_{eff}^{\mathbf{C}^n}$ of the configuration** More generally one can define the effective potential of the configuration $\mathbf{C}^n$ of order $n$ as

$$V_{eff}^{\mathbf{C}^n} \equiv \bigcup_{i=1}^{n} V_{eff}^i(\ell_i)\Theta(r_{min}^{i+1} - r)\Theta(r - r_{min}^{i-1}), \quad r_{min}^0 \equiv r_+, \quad r_{min}^{n+1} \equiv +\infty \tag{A5}$$

The potential $V_{eff}^{\mathbf{C}^n}$ certainly is not a function but has the advantage to describe the situation in the spacing regions among the rings and the orbital ranges $]r_+, r_{min}^1[$ and $r > r_{min}^n$. For each choice of eligible $\{K_i\}_{i=1}^n$, different decompositions will be identified, as shown in Fig. (3) where, at fixed $\{\ell_i\}_{i=1}^n$, the potential $V_{eff}^{\mathbf{C}^n}$ of the ringed disk is uniquely determined for each decomposition. The potential given by the definition (A4) regulates the set of rings in the configuration $\mathbf{C}^n$ at fixed $\{K_i\}_{i=1}^n$, but it is not able to characterize completely the matter with proper specific angular momentum $\ell_i$ in any of the spacings of consecutive rings $C_i$. In other words, the ranges $\bar{\lambda}_{i\pm k_\pm, i\pm k_\pm - 1}$ for $k_+ \geq 2$ and $\forall k_- \geq 1$, the cut is imposed by the double, right and left, Heaviside function in (A4). Indeed, the spacings $(\bar{\lambda}_{i+1,i}, \bar{\lambda}_{i,i-1})$ are obviously governed only by the potential of the consecutive sub-configurations with respect to $C_i$, that is the rings $C_{i\pm1}$. This is because the possibility of forming separate tori is governed only by the potential of the next closest rings and, therefore, the cuts provided by $(K_i, K_{i\pm1})$ in definition (A4). The parameters $(K_i, K_{i\pm1})$ in fact determine the location of the inner and outer edges of the sub-configurations and $(\Lambda_i, \Lambda_{i\pm1})$, respectively. It is clear then that Eq. (A5) *is* the potential associated with each separate ring *and* the spacings, and therefore it is not the simple collection of potentials associated with each individual ring, seen as independent and isolated, but rather the actual effective potential of the entire structure, formed by the rings, as components of a single macro-configuration, and related through conditions at their boundaries and the spacings. Thus, potential (A5) fully describes the macro-configuration $\mathbf{C}^n$: by setting the ordered sequence $\{\ell_i\}_{i=1}^n$, and then the *ordered sequence of potentials* $\{V_{eff}^i\}_{i=1}^n$, where the definition of ordered sequence of potentials is inferred straightforwardly from the order of the sequence of minima.Then we say $V_{eff}^{\mathbf{C}^n}$ is the potential of the $\mathbf{C}^n$ configuration and the set $\{V_{eff}^i(\ell_i)\Theta(r_{min}^{i+1} - r)\Theta(r - r_{min}^{i-1})\}_{i=1}^n$, its *decomposition*. The determination of decomposition of the disk potential is then essential for the determination of the decomposition of the disk itself.

We conclude this Section with some notes on potentials introduced in Eq. (A4) and Eq. (A5). Firstly potential $V_{eff}^{\mathbf{C}^n}$ in Eq. (A5) has been defined explicitly having into account $r_{min}^i$ of each rings, as parameters, in contrast with the potential of the individual rings. In fact, despite the fact that the effective potential in Eq. (A5) fails to be a well defined function because of the discontinuity points due to the "cuts" imposed

[31] Definition (A4) stands not as the simple collection of the single, independent, effective potential of the rings, but rather it includes the collection of the constraints (as they are the $\{K_i\}_{i=1}^n$) that each single ring has to comply with as a part of the overall structure of the ringed disk. This will be in fact more clear dealing with the perturbation approach as in Sec. (D). Therefore definition (A4) captures a key aspect of the coupling of the potentials of each toroidal ring, by the "boundary conditions" provided by each sub-configuration determining the macro-configuration.

by the Heaviside functions $\Theta(r^{i+1}_{min}-r)\Theta(r-r^{i-1}_{min})$, and for the consequent "overlapping" of the curves $(V^i_{eff}, V^{i+1}_{eff})$ pertaining to the potentials of the consecutive rings, we can still associate to the potential $V^{\mathbf{C}^n}_{eff}$ the collection of critical points $\{r^i_{min}\}^n_{i=1}$ (and possibly $\{r^i_{Max}\}^n_{i=1}$) as, for simplicity, the "minimum (maximum) points" of the potential $V^{\mathbf{C}^n}_{eff}$. Potential $V^{\mathbf{C}^n}_{eff}$ has, as $V^{\mathbf{C}^n}_{eff}\Big|_{K_i}$ in Eq. (A4), $n$ minimum-points, but we can have also $m \leq n$ maximum points, then we are neglecting the possible maximum $r^{i+1}_{Max} < r^i_{min}$. The unstable phase of $C_{i+1}$ would violate the principle of non-penetration of matter. Perhaps a more interesting situation would be when $K^{i+1}_{Max} > 0$, that is an outer $O^{i+1}_x$ sub-configuration occurs. In this case, the assumptions of not-overlapping of matter could be relaxed. This case, related to the matter jet production will be also addressed for completeness in the next Sections and particularly in Sec. (C). We note that the constraint imposed by the step functions in Eq. (A5) do not exclude the $\mathbf{C}^{n\,x}_{\odot}$ configurations. Moreover, the curve $V^{\mathbf{C}^n}_{eff}$ can be interwoven and, as $V^{\mathbf{C}^n}_{eff}\Big|_{K_i}$ has $2n-2$ discontinuity points, apart from the interweaving points, it is not properly a function, but a multivalued function or, in the strict sense a multi-valued map in the spacing ranges $\bar{\Lambda}_{i+1,i}$ with double points (as it should be considered as only consecutive potentials or potentials of consecutive rings). The spacings are not necessarily equidistant. As we will see in Sec. (D) and Sec. (B) their location and the precise arrangement is relevant in the treatment of perturbations of the macro-structure as a perturbation *of* and *inside* its decomposition. Finally we can discuss the relation between the potential $V^{\mathbf{C}^n}_{eff}\Big|_{K_i}$ of the decomposed $\mathbf{C}^n$ macro-structure in (A4) and the definition $V^{\mathbf{C}^n}_{eff}$ in (A5). Clearly, the last one is more general and includes any possible potentials $V^{\mathbf{C}^n}_{eff}\Big|_{K_i}$ (at $\{\ell_i\}^n_{i=1}$ fixed). Therefore by fixing $\{K_i\}^n_{i=1}$ in Eq. (A5), we obtain

$$V^{\mathbf{C}^n}_{eff}\Big|_{K_i} = \bigcup_{i=1}^{n} V^i_{eff}(\ell_i)\Theta(y^{i+1}_3 - y)\Theta(y - y^{i-1}_1) = \bigcup_{i=1}^{n} V^i_{eff}(\ell_i)\left[\Theta(y-y^{i-1}_1) - \Theta(y-y^{i+1}_3)\right]. \tag{A6}$$

However, we stress that if $V^{\mathbf{C}^n}_{eff}$ is known, one can use it to establish its decomposition and therefore the ringed disk decomposition together with other basic features, as the envelope surface mentioned in Sec. (3.2). It can be used to set up the perturbation analysis according to the discussion of Sec. (D). In fact, by means of the definitions (A4) and especially definition (A5), each ring turns to be regulated by an effective potential defined by taking into account the constraints imposed due to the fact that the rings actually form part of a whole macro-structure and, as such, they must comply to specific constraints, captured here by the presence of the Heaviside functions $\Theta(r^{i+1}_{min}-r)\Theta(r-r^{i-1}_{min})$ in Eq. (A5) and $\Theta(-K_i)$ in Eq. (A4).

## B. Maximum points of the function $\ell' \equiv \mp\partial_r \ell^{\pm}$

In this Section we discuss in detail the properties of the ring specific angular momentum as function of $r$, and we will prove some of the results mentioned in Section (4) and particularly in (A.1) and (4.3). The results are however of general relevance related to the properties of rings governed by the Boyer model and then a generic macro-structure of the order $n$. This analysis leads in a natural way to the characterization of two special macro-configurations $\mathbf{C}^n$, defined by constraining the $\ell$corotating sub-sequences of its decomposition $\{C_i\}^n_{i=1}$: in particular we assume some conditions on the set of centers $\{r^i_{min}\}^n_{i=1}$, or the parameters $\{\ell_i\}^n_{i=1}$. The first disk made by rings with equally spaced centers, or otherwise spaced with a known general relation, the second disk with equally spaced specific angular momenta, or related by a known law. In other words, the elements of each sequence $\{r^i_{min}\}^n_{i=1}$ (for example this is the case in Fig. (3)) or $\{\ell_i\}^n_{i=1}$ respectively, are not independent but related by a fixed relation. The presence of this maximum point has an immediate consequence on the formation and dynamics of the ringed disks through the characterization of the orbital location and specific angular momentum distribution of its decomposition in particular, in relation to the density of rings and the differential rotation of the ringed disk. Clear distinction can be seen in the presence of the $\ell$counterrotating subsequences. In fact, study of the two particular cases helps to better enlighten

this distinction: firstly, the maximum points also correspond to points of maximum density of the rings, located in different orbits depending on the rotation with respect to the attractor. Secondly, there are six different orbital areas, respectively, three for the two $\ell$counterrotating subsequences, for which a change of the angular momenta in magnitude has very different effects on the location of the disk, not changing the ring topology and therefore the stability of the disk: specifically, the inner orbital area of the maximum points, a neighborhood of the maximum and the outside area. In (Pugliese&Stuchlik 2015) this analysis will be extended also to the unstable topologies. The simplest case is when the difference between the elements is independent from the index $i$ of the sub-configuration and are constants, for example $\epsilon_{i\ i+1} = \epsilon_{j\ j+1} : \forall\ (i,j)$, where $\epsilon_{ij}$ are the displacement matrices introduced in Eq. (21). Given the constraint on $\{r^i_{min}\}^n_{i=1}$ in the first case, and separately $\{\ell_i\}^n_{i=1}$ in the second case, we want to characterize the decomposition $\{C_i\}^n_{i=1}$ (i.e. the two $\ell$corotating sequences) finding how it is changed the sequence $\{\ell_i\}^n_{i=1}$ in the first case, $\{r^i_{min}\}^n_{i=1}$ in the second one. We have noted in different points in this work that each $\ell_i$, in the model we are considering, set uniquely $r^i_{min}$ and, viceversa, if one considers the $\ell$corotating sequences only. However in this Section we intend to consider a variable configuration index as already done in Sec. (4.3.1) and for example in Sec. (E). These results are intended to be considered in the perturbative approaches with the perturbation of $\mathbf{C}^n$ as a perturbation *in* and *of* its decomposition $\{C_i\}^n_{i=1}$, introduced in Sec. (D). In this Appendix we will focus primarily on the $\ell$corotating sub-sequences of the decomposition, some of these results can be extended considering more general situations in mixed decompositions (i-b).

### B.1. Analysis of the decomposition and the differential rotation of the disk

The specific angular momentum of the $\ell$corotating sub-configurations in equilibrium, corresponding to the $C$ topology, grows in magnitude with the distance from the source, which means that $|\ell_{i+j}| > |\ell_i|\ \forall (i,j)$ and $\ell_{i+j}\ell_i > 0$. However, this increasing is not constant with the radial distance: the curves $\ell' \equiv \mp\partial_r \ell^{\pm}$, have a maximum point, as function of $r/M$, in $r^{\pm}_{\mathcal{M}}(a) > r^{\pm}_{mso}$ respectively[32], see Figs. (8,9). From now on, to avoid encumbering the notation and discussion, where there will create no confusion, we shall always understand an increase or decrease in magnitude of the specific angular momenta and accordingly we will avoid to report the notation $|\ |$.

This means that, moving the center of the $\ell$corotating rings (no matter whether consecutive or not) outwards, it is necessary to increase the magnitude of the ring specific angular momentum, in a way not proportional to the displacement of the ring centers, i.e.,

$$\delta\ell_{i+j,i} \equiv |\ell_{i+j} - \ell_i| \neq \alpha(r^{i+j}_{cent} - r^i_{cent}) \equiv \alpha\delta r^{i+j,i}_{cent}, \quad \alpha = \text{constant}, \forall j > 0, \quad \ell_i\ell_j > 0, \tag{B1}$$

$\ell_i$, is as usual the specific angular momentum of the $C_i$ ring. For the adopted model of thick accretion tori, there is $\ell_i \equiv \ell^{\pm}(r^i_{cent})$ if the fluid is counterrotating or corotating. Or in other words, to move the center of the $C_i$ ring far from the attractor, for the shift $\mathfrak{S}_{i,i+j} : C_i \to C_{i+j}$ preserving the stability of the $C_{i+j}$ ring, $\delta\ell_{i+j,i}$ should be increasingly large as $i$ increases, at fixed $j$ (which means physically equidistant center rings), i.e. $\partial_r\delta\ell_{i+j,i} > 0$, at equal $\delta r^{i+j,i}_{cent}$ up to the maximum $r_{\mathcal{M}}(a)$ after which $\partial_r\delta\ell_{i+j,i} < 0$, see also considerations in Note III. We are considering a macro-configuration $\mathbf{C}^n$ consisting of sequences of $\ell$corotating equidistant rings see–Figs. (3), along the entire disk $\mathbf{C}^n$ with respect to their center, or $\partial_i \delta r^{i+j,i}_{cent}\Big|_j = 0$, and we are investigating how the ordered sequence of the specific angular momentum $\{\ell\}^n_{i=1}$ should be fixed. In the model we are considering here, the index $i$ corresponds to one and only one center (and therefore to a single $\ell_i$) then $\partial_r$ also becomes $\partial_i$ at fixed (shift) $j$ and the former relations can then also be written in terms of the variation on the configuration index $i$: i.e. $\partial_i|\ell_i| > 0\ \forall i$ but $\partial^2_i|\ell_i| > 0$ up to a $i_{\mathcal{M}}$ correspondent to the

[32]The maximum point $r_{\mathcal{M}}$ is a root of the polynomial: $-9a^6 - 8a^4 r + 6a^2\left(-14 + 23a^2\right) r^2 + 3\left(48 - 124a^2 + 75a^4\right) r^3 + \left(288 - 389a^2\right) r^4 - 30\left(-4 + a^2\right) r^5 - 24r^6 + r^7$. For convenience here we consider a dimensionless $a$ and $r$.

ring with the center in $r_{\mathcal{M}}$ where[33] $\partial_i^2|\ell_i| = 0$. Then $\partial_i^2|\ell_i| < 0$ for higher indexes $i > i_{\mathcal{M}}$ or also:

$$\partial_i\ \delta\ell_{i+j,i}\big|_j \gtreqless 0 \quad \text{for} \quad i \lesseqgtr i_{\mathcal{M}} \quad \text{and} \quad i \in ]i_{mso}, +\infty[, \tag{B2}$$

where $i_{mso}$ corresponds to the ring with the *cusp*[34] in $r_{mso}$. Clearly the commuted relation with respect to the couple $(i, j)$: $\partial_j\ \Delta\ell_{i+j,j}|_i > 0\ \forall\ j > 0\ i > i_{mso}$ always holds, see also Sec. (4.3.1).

The surplus of specific angular momentum $\delta\ell_{i+j,i}$ that should be provided increases more and more slowly in far away regions ($r(i) \gg r_{\mathcal{M}}(a)(i_{\mathcal{M}})$), where the Newtonian limit could be considered and, as asymptotically it is $\lim_{r\to\infty} \ell' = 0$, with[35] $\lim_{r\to\infty} \ell^{\pm} = \pm\infty$, then $\delta\ell_{i+j,i}$ remains constant.

Equivalently, increasing regularly the specific angular momentum $\ell_i$ (in magnitude) of a $C_i$ sub-configuration of a sequence of $\ell$corotating rings for a certain constant amount $\bar{\delta}_\ell$, i.e. $\epsilon_{ii+1} = \bar{\delta}_\ell\ \forall i$, the disk center $r^i_{cent}$ moves outwards, but the distance $\delta r^{i,i+\epsilon}_{cent}$ between the centers of the configurations decreases until $r = r_{\mathcal{M}}$. Indeed, $\delta r^{i,i+\epsilon}_{cent} = \delta\ell_{i,i+\epsilon}/|\ell'| = \bar{\delta}_\ell/|\ell'|$ as $\epsilon \gtrapprox 0$. Approaching $r_{\mathcal{M}}$, the distance $\delta r^{i,i+\epsilon}_{cent}$ decreases (as $\epsilon \approx 0$):

$$\partial_\epsilon r^{i+\epsilon}_{cent}\big|_i > 0 \quad \text{and} \quad \partial_i r^{i+\epsilon}_{cent}\big|_\epsilon > 0, \quad \partial_{|\ell|} r^i_{cent}(\ell) > 0 \quad \forall i > i_{mso} \quad \epsilon > 0, \quad \partial_i \delta r^{i,i+\epsilon}_{cent} \lesseqgtr 0, \quad i \lesseqgtr i_{\mathcal{M}} \tag{B3}$$

for $i \in ]i_{mso}, +\infty[$. Note that in this case, unlike the similar case for the specific angular momentum (where the shift parameter $j$ was kept constant), the shift parameter $\epsilon$ must vary as $\delta\ell_{i,i+\epsilon} = \bar{\delta}_\ell$ is kept constant. Then the analysis of the variation of $\delta r^{i,i+\epsilon}_{cent}$ actually corresponds to the analysis of the variation of the shift (which is always spatial) $\epsilon$ required to keep the shift in the specific angular momentum constant.

In the region $r > r_{\mathcal{M}}$, with constant, $\bar{\delta}_\ell$, i.e. equal difference between the specific angular moments of the rings, the disk decomposition becomes more and more extended, the separation between the centers of the sub-configurations more and more spaced, so that spacings among the rings from the maximum point increase while they are closer in the region $r \in ]r_{mso}, r_{\mathcal{M}}]$. In terms of the rings density, Note IV, one could say that

$$\partial_r\ n(r)|_{\bar{\delta}_\ell} \gtrless 0 \quad \text{for} \quad r \lessgtr r_{\mathcal{M}}, \tag{B4}$$

for any $\ell$counterrotating sub-sequence. The ring edges are still to be defined. To do this we need to combine the given analysis with some evaluations of the choice of the $K$ parameter, investigating consequences of the assumed conditions on $\{r^i_{cent}\}_{i=1}^n$ or $\{\ell_i\}_{i=1}^n$ in the sequence $\{K_i\}_{i=1}^n$. In any cases, these considerations are relevant to determine the differential rotation of the disk $\mathbf{C}^n$ as discussed in Sec. (4.3.1), the specific angular momentum of the configuration according to the definitions (19) and discussed in Sec. (4.3.1), and finally to define the effective potential for the ringed disk according to Eq. (A4) and Eq. (A5) as discussed in Sec. (A.1). We can consider these results with respect to a mixed or isolated decomposition of a generic ringed disk $\mathbf{C}^n$. Given the two $\ell$corotating sub-sequences $\{C_i\}_{i=1}^{n_\mp}$ of $\mathbf{C}^n$ with $n = n_- + n_+$, there are two relative maxima of the magnitude of the specific angular momentum $\ell_{Max} \equiv \{\ell_{n_-}, \ell_{n_+}\}$, clearly related to the outer edge of the disk (still undetermined) of $\mathbf{C}^n$. Thus $\ell_{n_\pm}$ are respectively the specific angular momentum of the outer or inner ring of the two sequences, but do not determine $\ell_n$ as we can have $C_n = C_{n_-}$ or $C_n = C_{n_+}$, neither the inner edge, as we can have $C_1 = C_{1_-}$ or $C_n = C_{1_+}$, where $\ell_{1_\pm} = \min\{|\ell|_{i_\pm}\}_{i_\pm=1}^{n_\pm}$. Moreover, to identify the specific angular momenta $(\bar{\ell}^n_{\mathbf{C}}, \bar{\bar{\ell}}^n_{\mathbf{C}})$ or $(\bar{l}_{\mathbf{C}^n}, \ell_h)$ as defined in Sec. (4.3.1) Eqs (19,20), we have to present some further considerations on the morphological features of the rings $C_i$, as the height $h_i$ and the area $\mathcal{A}_i$:

[33] In fact, the physical meaning of the point of maximum $r_{\mathcal{M}}$ in terms of the gap in the specific angular momentum is immediate and it trivially follows the definition of relative maximum of a smooth real function: $\forall j \approx 0$ there exists a couple of sub-configurations, $C_{i_{\mathcal{M}}\pm j}$ such that $\delta\ell_{i_{\mathcal{M}},i_{\mathcal{M}}+j} - \delta\ell_{i_{\mathcal{M}},i_{\mathcal{M}}-j} = 0$ respectively.

[34] So far we have considered the configuration index as attached to the ring center, that is at $r_{min} > r_{mso}$. This is because the critical points, for each $\ell$corotating sequence at $r > r_{mso}$ are only minimum points of the effective potential. At $r = r_{mso}$, there is not a minimum of the effective potential.

[35] Actually, the limit under consideration is related to the dimensionless ratio $r/M \to \infty$, equivalently, one can see a similar asymptotic behavior with respect to the dimensionless quantity $R \equiv r/a \to \infty$. The asymptotic limit with respect to $r/M$ goes to zero as $r^{-1/2}$.

it is then $y_3^{n_\pm}\ell_{n_\pm} = \sup\{y_3^i \ell^{n^i}\}_{i=1_\pm}^{n_\pm}$ *whatever* $K$ is. The greater is $K$, the greater is the elongation $\lambda_i$, in other words $\partial_K \lambda_i > 0 \; \forall K \in ]K_{mso}, 1[$.

Concerning the two $\ell$counterrotating sub-sequences, it is worth noting that

$$r^+_{\mathcal{M}} > r^-_{\mathcal{M}}, \quad -\ell^+_{\mathcal{M}} > \ell^-_{\mathcal{M}}, \quad \mp\ell^\pm_{\mathcal{M}} \in ] \mp \ell^\pm_{mbo}, \mp\ell^\pm_\gamma [, \quad r^\pm_{\mathcal{M}} > r^\pm_{mso}, \tag{B5}$$

while $a > 0.93M$ it is $\ell^-_{\mathcal{M}} > \ell^-_\gamma$, when the corotating rings have to be in equilibrium (Pugliese&Stuchlik 2015), see also Sec. (4.3.2)[36]. Therefore, $r^\pm_{\mathcal{M}}$ can be always a center for a counterrotating or corotating disk but, as it turns from the analysis of the specific angular momenta, the only instability possible for such a ringed disk is in its open configuration. It cannot be in accretion, but only jets are possible because of the high specific angular momenta. The launching point of the jet would be at $]r^\pm_\gamma, r^\pm_{mo}[$ respectively. Moreover, as mentioned in Sec. (4.3),

$$\partial_{a_*} r^\pm_{\mathcal{M}} \gtrless 0, \quad \partial_{a_*} K^\pm_{\mathcal{M}} \gtrless 0, \quad \mp\partial_{a_*} \ell^\pm_{\mathcal{M}} \gtrless 0 \quad a_* \equiv a/M, \tag{B6}$$

see Figs (8,9)). We could say that for high attractor spins the Newtonian limit for the corotating sub-configuration is reached, in regions close to the source, and with lower specific angular momenta magnitude with respect to the counterrotating one. This is in agreement with the discussion in Sec. (4.3). The spin of spacetime clearly distinguishes the two types of configurations and the relativistic effects are essentially determined by the rotation of the attractor. Indeed, considering the two mixed sequences and Figs (8,9)), we note that for increasing spin:

$$r^-_{\mathcal{M}}(a_{\mathcal{M}_1}) = r^+_{mso}(a_{\mathcal{M}_1}), \quad r^-_{\mathcal{M}}(a_{\mathcal{M}_1}) = r^+_{mbo}(a_{\mathcal{M}_2}), \quad r^-_{\mathcal{M}}(a_{\mathcal{M}_3}) = r^+_\gamma(a_{\mathcal{M}_3}), \quad a_{\mathcal{M}_1} < a_{\mathcal{M}_2} < a_{\mathcal{M}_3}. \tag{B7}$$

Then we see a clear difference for sources with $a > a_{\mathcal{M}_1}$ and particularly with $a > a_{\mathcal{M}_3}$ where the Newtonian limit for the corotating rings approaches the source. In terms of the ring density, in $]r^-_{\mathcal{M}}, r^+_{\mathcal{M}}[$, the $\ell$counterrotating sub-configurations can have points of maximum pressure (thus particularly for $a > a_{\mathcal{M}_1}$ at $]r^+_{mso}, r^+_{\mathcal{M}}[$). Having in mind the relation (B4), we find the relation $\partial_r \; n^\pm(r)|_{\bar{\delta}_\ell} \gtrless 0$.

### B.2. Characterization of the two macro-structures

In Sec. (B.1) we considered two different ringed disks: the first, say $\mathbf{C}^n_r$ disk made by equally spaced rings (according to the location of their centers), and we have characterized the differential rotation of the ($\ell$corotating) rings. In the second case, say $\mathbf{C}^n_\ell$ disk, we considered a constant specific angular momenta gap between the $\ell$corotating sub-configurations and we determined the ring location in each sub-sequence $\mathbf{C}^{n_+}$ or $\mathbf{C}^{n_-}$ respectively. We have found that the ring density defined as the density of the centers in a closed orbital region, i.e. $n = n_{min}/\delta r$ where $n_{min}$ is the number of centers located in the orbital range $\delta r$, is greater close to the maximum $r \leq r_{\mathcal{M}}$. Then the maximum variation of the orbital specific angular momentum corresponds to the maximum of the density of ring number (not necessarily of the maximum disk mass, as it depends also on $K_i$, and on the distance $r_{min}$ from the center) at constant gap of specific

[36] The function $\ell' = |\ell_{i+\epsilon} - \ell_i|/\delta^{i,i+\epsilon}_{cent}$, obtained for composition of the specific angular momenta of two corotating consecutive disks (for $\epsilon \approx 0$ the rings $C_{i+\epsilon}$, the outer, and $C_i$, the inner, are very close) increases with $r/M$, as the rings are sufficiently close to the source or $r \in ]r^\pm_{mso}, r_{\mathcal{M}}]$, at greater distances ($r > r_{\mathcal{M}}$) this rise reduces increasingly to become zero. These results apply in any Kerr spacetime, but depending on the attractor spin, the maximum $r_{\mathcal{M}}$, being a function of $a$, occurs in a different orbital regions. As shown in Figs (8,9)) for the rings counterrotating with respect to the black hole, the position $r^+_{\mathcal{M}}$ increases with the **BH** spin, then the greater the **BH** spin, the greater is the specific angular momentum of the $\ell$corotating rings made up by counterrotating matter with respect to the attractor. Inversely, for the case of corotating rings, the region of increasing gap of specific angular momentum decreases with the spin, that is, the increasing of the **BH** spin corresponds to a decrease for the additional specific angular momentum to be supplied to locate the ring centers in an exterior region. Thus, one could say in general that if the $\ell$corotating disks are corotating with respect to the black hole we need less additional specific angular momentum to locate outwardly ($\ell$corotating and corotating) rings with respect to the other case. In this sense, one could say also that the corotation with respect to the **BH** rotation has a stabilizing effect for the orbital properties of ringed disks in equilibrium.

angular momentum (whatever the value is of specific angular momentum) for every $\ell$corotating sequence belonging to the generic decomposition $\{C_i\}_{i=1}^n$, see Eq. (B4).

There are two density peaks corresponding to the two $\ell$counterrotating sequences. Obviously, to ensure the separation between the rings, the sequences should be fixed accordingly, so that each value $K_i$ is small enough to guarantee the separation. Then it follows that higher number density corresponds to a lower spacing of the disk in the range of fixed $r$ and smaller rings in its decomposition. We expect that increasing the number of rings in a neighborhood of the $r_{\mathcal{M}}$, the disk height will be lower with lower spacing $\bar{\lambda}$ and the rings would be considered constituting a geometrically thin disk. These considerations have some relevance in the analysis of the perturbations of $\mathbf{C}^n$ rings and precisely in the sequence $\{\ell_i\}_{i=1}^n$ or $\ell$-modes. Indeed, more generally one can use a general functional relation in the differential rotation. For example, this is certainly the case in the perturbation theory, where the displacement matrices $\epsilon_{ij}$ could also be not constant, see Sec. (4.3.1) and Sec. (D).

Suppose that in the $\mathbf{C}_r^n$ disk the distance $\delta r_{min}^{i+j,i}$ among the centers is not constant, and for the $\mathbf{C}_\ell^n$ disk model the gap between the specific angular momenta is not constant but there is a (known) relationship such that $(\clubsuit)_r : \ \delta r_{min}^{i+j,i} = \delta r_{min}^{i+j,i}(r)$ or, using the ring indices $j = j(i)$ for the first disk and, in the same way for the second model $(\diamondsuit)_\ell : \ \delta\ell_{i+\epsilon,i} = \delta\ell_{i+\epsilon,i}(\ell)$. We aim to find a characterization of a ringed disk subjected to generic conditions $(\clubsuit)_r$ and $(\diamondsuit)_\ell$ respectively. First, one needs to clarify the choice of the functional dependence in the conditions $(\clubsuit)_r, \quad (\diamondsuit)_\ell$. Regarding $(\clubsuit)_r$, the condition on the indices $j = j(i)$ is immediate: we mean that the distance between the centers, defined by the shift $j$, depends on the disk $C_i$, and thus on its position as $r_{min}^i$, which is moved by the translation $\mathfrak{S}_{i,i+j} : \ C_i \to C_{i+j}$ that changes with $i$. Since this is a one-dimensional problem, the shift is uniquely determined by $j$, if $j = j(i)$ then in terms of $r$ it is $\delta r_{min}^{i+j,i}(r_{min}^i)$.

A different consideration must be made for the conditions of $(\diamondsuit)_\ell$; in terms of configuration index it should be $(\diamondsuit) : \ \epsilon = \epsilon(i)$. For the definition of $\ell_i$ the parameter $\epsilon$ follows the movement associated with the centers of the configuration, and this obviously depends on the distance between the specific angular momenta fixed a priori. Even if not constant, the specific angular momentum $\ell_{i+\epsilon}$ then will be a function of the momentum $\ell_i$. (The indexes of $\ell$ are always intended to be related to the ring position, but $\epsilon$ in the definition of $(\diamondsuit)_\ell$ is not constant). These considerations can be generalized to any mixed decompositions having in mind the conditions and constraints for the separation of matter, discussed in Sec. (D) on the perturbative $\ell$-modes and $K$-modes.

## C. Some notes on the open configurations

Following the discussion in Sec. (4.3.2), In this Section we investigate some aspects of the decompositions with one or more critical P-W points and in particular the decompositions with $O_x$ sub-configurations, as shown in Fig. (10). We avoid to constraint the $O_x$ surfaces with the principle of non-overlapping (non-penetration) of matter considering therefore the possibility of a decomposition with more than one launching point of the jet. For the critical configuration, it is useful to introduce, together with the notation $<$ and $>$ for the ordered sequence of maximum points of the pressure (or $r_{min}$, minimum of the effective potential and the disk centers for the closed sub-configurations), also the symbols $\succ$ and $\prec$ intended to refer to sequentiality ordered location of the minimum points of the pressure (or $r_{Max}$ of the effective potential, or the instability points of accretion or launching of jets), while the terms "internal" (equivalently inner) or "external" (equivalently outer), in relation to a couple of rings, will always refer, unless otherwise specified, to the usual ordinate sequence according to the location of the centers.

### Critical points in a $\ell$corotating sequence

We consider first the case of $\ell$corotating sequences, focusing first on a ring couple.

In the case of an *outer jet* it can be: $O_x^i < O_x^o$, $C_x^i < O_x^o$ or $C_i < O_x^o$ where, for definition, it is always $r_{min}^i < r_{min}^o$, and $r_{Max}^i > r_{Max}^o$ (according to the existence conditions) and then if $()^i < ()^o$, where $\ell_i\ell_o > 0$,

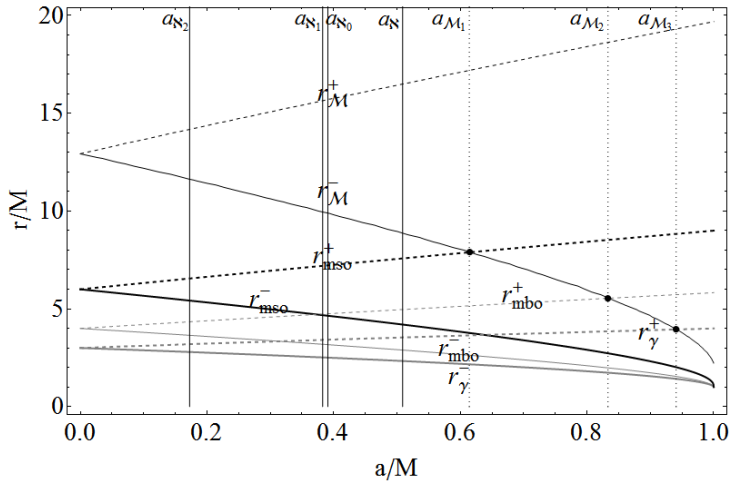



Fig. 8.— The marginally stable circular orbits $r^{\pm}_{mso}$, marginally circular orbits $r^{\pm}_{\gamma}$, last bounded orbits $r^{\pm}_{b}$ functions of the spin-mass ratio of the attractor $a/M$. $r^{\pm}_{\mathcal{M}}$ are the orbits of maximum growing of the specific angular momentum magnitude, for corotating $(\ell_-, K_-)$ and counterrotating $(\ell_+ < 0, K_+)$ fluids.

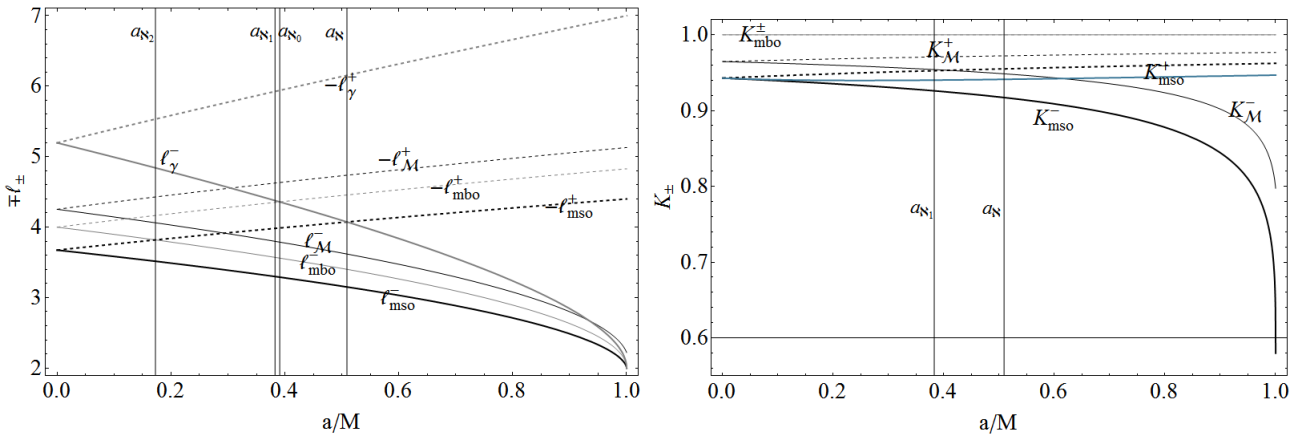



Fig. 9.— Angular momenta (left) and parameter $K$ (right), for corotating $(\ell_-, K_-)$ and counterrotating $(\ell_+ < 0, K_+)$ fluids on the marginally stable circular orbits $r^{\pm}_{mso}$, last circular orbits $r^{\pm}_{\gamma}$, last bounded orbits $r^{\pm}_{b}$ functions of the spin-mass ratio of the attractor $a/M$.

then $()^i \succ ()^o$.

In the case

$$O^i_x < O^o_x \quad \text{it is} \quad O^i_x \succ O^o_x \quad , |\ell_i| < |\ell_o| \in ]|\ell_\gamma|, |\ell_b|[: \tag{C1}$$

there are two $\ell$corotating jets starting from the points $(r^o_{Max}, r^i_{Max})$.

In the second case:

$$C^i_x < O^o_x \quad \text{it is} \quad C^i_x \succ O^o_x \quad |\ell_i| < |\ell_o| \in ]|\ell_\gamma|, |\ell_b|[ \quad \text{where} \quad |\ell_i| \in ]|\ell_{mso}|, |\ell_b|[; \tag{C2}$$

the launching point of the jet is internal with respect to the accretion point. An interesting situation occurs

when the two instability points (location of minimum of the pressure) are very close or coincide; the last case is possible only for $\ell$counterrotating couple.

In the third case, there is only one instability point and it has to be

$$C_i < O^o_x \quad \ell_i < \ell_o \quad r^i_{min} < r^o_{min} \quad K_i < 1. \tag{C3}$$

We now consider the case of an *inner jet*: $O^i_x < C^o_x$ or $O^i_x < C_o$. Regarding the case, $O^i_x < C^o_x$, it is has to be $O^i_x \succ C^o_x$, but this is not a possible configuration for $\ell$corotating couple–in fact it should be $|\ell_i| < |\ell_o| \in ]|\ell_{mso}|, |\ell_b|[$ and on the other hand it has to be $|\ell_i| \in ]|\ell_b|, |\ell_\gamma|[$ that is contradictory. In a $\ell$corotating couple with an accretion point and a jet, the launching point must be *internal*, with respect to the accretion point. The case $O^i_x < C_o$ and $O^i_x \succ C_o$, similarly to the case $O^i_x < C^o_x$, leads to a contradiction.

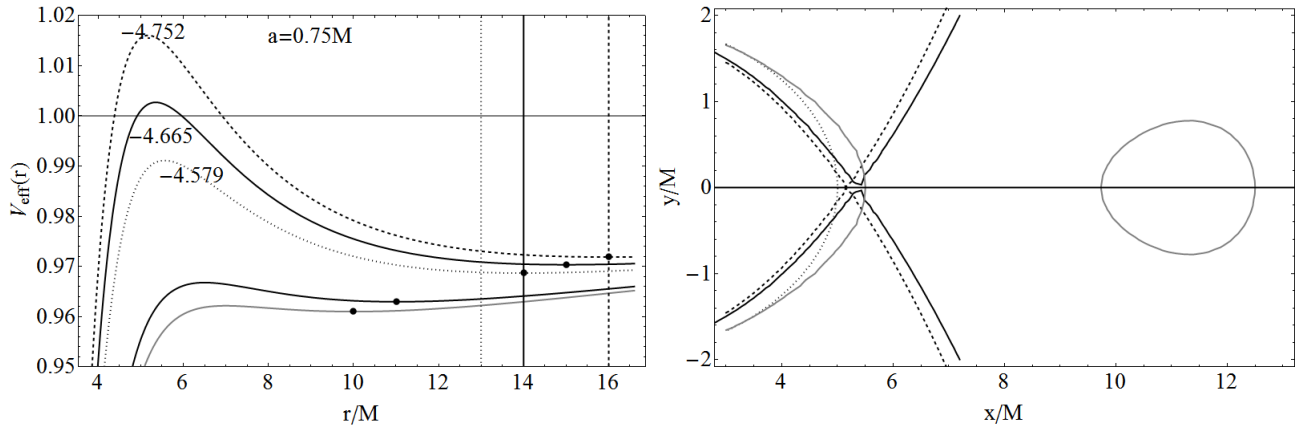



Fig. 10.— Spacetime spin $a = 0.75M$, $\ell$corotating sequences, $\ell_i\ell_j > 0$, of counterrotating disks $\ell_i a < 0$ $\forall ij$. Decompositions including open-cusped sub-configurations $O_x$. The outer horizon is at $r_+ = 1.66144M$.

**Double critical points in a $\ell$counterrotating sequence**

This note follows the discussion in Sec. (4.3.2), a part of the results shown here are discussed in the section on the $\ell$counterrotating sequences from Eq. (48). First, we consider the case of $C^+_x \succ O^-_x$, meaning an outer accretion point with counterrotating matter followed by an inner instability point where matter, initially corotating with the black hole opens in jets, and

$$\Delta^-_J \cap \Delta^+_x = \emptyset \quad \text{it is} \quad C^+_x \succ O^-_x \quad \text{and} \quad C^+_x \not\prec O^-_x \quad \text{since} \quad \Delta^-_J < \Delta^+_x \tag{C4}$$

see also Figs. (8).

Consider now a couple of $\ell$corotanting jet configurations. Then

$$O^+_x \succ O^-_x \quad \text{for} \quad a \gtrsim 0.35M; \quad O^+_x \succ O^-_x \quad \text{or} \quad O^+_x \prec O^-_x \quad \text{for} \quad a \lesssim 0.35M, \tag{C5}$$

see Fig. (8), i.e. at smaller attractor spin-mass ratio, where $r^-_{mbo} > r^+_\gamma$, it can be also: $O^+_x \prec O^-_x$. But as Eq. (C5) stands, for large values of spin the inner jet must be corotating.

On the other hand, the couple $C^-_x \succ O^+_x$, with an inner counterrotating jet and an outer accretion point from a corotating ring are possible for small enough spin, i.e. $a \lesssim 0.6$, where $r^-_{mso} > r^+_\gamma$, while for larger spin, $C^-_x \prec O^+_x$, or the accretion point of corotating material follows the launch of a counterrotating jet.

For the double disk in accretion, it has to be $C_x^- \prec C_x^+$ for every spin. We note that for large spin, $a > a_{\aleph_1}$, this relation could not be inverted to $C_x^+ \prec C_x^-$, as clear from Fig. (8)[37] . For the couple $C_x^- \prec C_x^+$ a penetration of matter occurs from the material of the outer accreting ring to the inner one. However the case of two disks in accretion clearly results in a penetration of matter that affects the more internal lobe of the outer configuration and the outer lobe of the internal one.

Finally, we note that a critical decomposition $\mathbf{C}^x_\odot$ could be formed by a couple of critical sub-configurations when $y_1^i = y_3^{i+1} = r_{Max}^{i+1}$. The condition in Eq. (14) still holds formally as here we are not considering the inner lobe of the ring in accretion, however, within this setup, no more then two accreting points in a ringed disk can exist and they must be $\ell$counterrotating (indeed, $r^\pm_{mso} \in C_x^\pm$ respectively). The spacings $\bar{\lambda}_{i+1,i}$ are in general increasing with the attractor spin and decreasing with the magnitude of their specific angular momentum (corresponding to a decrease of their elongation) see Eqs (29,43). As can be seen also from Fig. (8), this case can be always possible, and clearly the outer ring of the $\ell$counterrotating couple has to be counterrotating independently of the equilibrium state of the inner one, with $y_1^- = y_3^+ = r^+_{Max} \in \Delta^\pm_{mso}$. To simplify the discussion, we consider here an unstable inner corotating ring implying $\lambda < \lambda_x$, according to Eq. (24) and we can refer to Fig. (8). The inner ring is then in accretion but it could be $C_x^- \prec C_x^+$ or $C_x^- \prec O_x^+$, and the considerations made before apply, distinguishing slow and fast attractor according to the former analysis–see also (Pugliese&Stuchlik 2015).

### D. General considerations on the perturbations of the ringed disks and their equilibrium

In this section we consider possible perturbative approaches to the study of the equilibrium and the unstable phases of $\mathbf{C}^n$ as defined in Sec. (3). The perturbations arising in the ringed disk structure are meant to be perturbations of its decomposition $\{C_i\}_{i=1}^n$, generated by perturbing the decomposition effective potential in Eq. (A4) or Eq. (A5), or perturbations of the sequences of parameters $\mathbf{p}_{\mathbf{C}^n} = \{\mathbf{p}_i\}_{i=1}^n$.

We introduced in Sec. (A.1) the effective potential $V_{eff}^{\mathbf{C}^n}$ of Eq. (A5), governing the equilibrium structure of the $\mathbf{C}^n$ macro-configuration. By coupling the potentials of each toroidal ring, we have defined the boundary conditions for each sub-configuration determining the structural "rigidity" of the macro-configuration. In this work we will not perturb the macro-configuration $\mathbf{C}^n$, but we limit here to set up the problem clarifying some aspects of the configuration such as the relationship between the elongation and the spacings as discussed in Sec. (3.2) and Sec. (A.1). We can indeed perturb the structure by a perturbation of its effective potential, as defined in Eq. (A4) or A5. The ringed disk $\mathbf{C}^n$ is determined by the multidimensional ordered parameter $\mathbf{p}_{\mathbf{C}^n} = \{\mathbf{p}_i = (K_i, \ell_i)\}_{i=1}^n$. The perturbations of the decompositions can be constructed by perturbing one or both sequences of the $\mathbf{p}_{\mathbf{C}^n}$ parameter: $\{K_i\}_{i=1}^n$, and therefore the boundary conditions, see for example definition (A4), or $\{\ell_i\}_{i=1}^n$. Keeping the other parameters fixed, we could then speak of *$K$-mode* or *$\ell$-mode* of the perturbation respectively. The ringed disk can be perturbed in one of these modes or in a combination of these, and each mode can have some sub-modes defined by the restrictions on the perturbation, bounded by specific relationships on the spacings and elongations. From the analysis of the decomposition in Sec. (4.1) it follows that the associated order parameters of the perturbation, the sequences $\epsilon_K = \{\epsilon_{K_i}\}_{i=1}^n$ and $\epsilon_\ell = \{\epsilon_{\ell_i}\}$ respectively, are not independent.

The system is unstable, if it endures one of the unstable topologies introduced in Sec. (3.1) that is $\mathbf{C}^n_x$ or $\mathbf{C}^n_\odot$ or a combination of these. The maximum rank of $\mathbf{C}^n_x$ is $\mathfrak{r} = 2$ (for $\ell$counterrotating disks of the order $n \geq 2$) and the cusps are located in the inner tori of the two ordered sequences of corotating and counterrotating rings of the decomposition. No feeding between the $\ell$-corotating disks is possible, but an exchange of matter can occur as driven by the cusp. However, the instability of the ringed disk occurs due, for this case, to the combined effect of the violation of the hydrostatic equilibrium by means of the P-W

[37] A pointed out in Sec. (4.3), it follows from the relation $r^\pm_{mso} \in C_x^\pm$, respectively, and the considerations of Eq. (24): in the case $C_x^+ \prec C_x^-$ : $r^+_{mbo} < r^+_{Max} < r^-_{Max} < r^-_{mso} < r^+_{mso}$ and it has to be in accordance to the Eq. (24): $r^+_{Max} < r^-_{Max} < r^-_{mso} < r^+_{mso} < y_1^+$ and $y_1^- > r^-_{mso}$, should lead to a penetration of material between the first lobe of the two configurations, thus this case is always forbidden.

mechanism at the cusps of one or more sub-configurations, and the collision or penetration of matter from one ring to the other. An interesting situation occurs for the perturbation of a decomposition of $\mathbf{C}^n$ that preserves the stability of each sub-configuration, i.e., for variation of the parameters $\mathbf{p}_{\mathbf{C}^n}$ far from the values for a P-W instability for each of its rings. The breakdown of the equilibrium of the entire macro-configuration causes the emergence of the $\mathbf{C}^n_\odot$ topology, up to a saturated configuration where the total spacing is reduced to $\bar{\Lambda} = 0$. In this case, as mentioned in Sec. (4.3) for the deformations introduced by the displacement matrix $\epsilon_{ij}$, the perturbation is strongly constrained on the initial decomposition. In fact, as mentioned before, the order parameters $\epsilon_{\mathbf{p}} \equiv (\epsilon_\ell, \epsilon_K)$ are related each other being constrained by conditions on the spacings $\bar{\lambda}_{i+1,i}$ and the distances between the minima (or equivalently the elongations). In the following discussion we always consider sequences of ordered parameters and maintaining a constant $K_i$ or $\ell_i$ means to consider a constant $K$ or $\ell$ for the $i$-ring that maintains its identity as fixed in the initial decomposition[38]

**The $K$-modes** Keeping the sequence of parameters $\{\ell_i\}_{i=1}^n$ fixed, the perturbations will be only on the (variable of ) Heaviside functions in the effective potential (A4). Then we are dealing with a one dimensional problem in each $K_i \in [K^i_{min}, K^i_{Max}]$, the boundary of each range being fixed by $\ell_i$. It should be noted that a perturbation of $K_i$ is equivalent to a (rigid) perturbation of the inner and outer edges of each ring (or also the elongations $\lambda_i$ at fixed $r^i_{min}$), shift-parameters of the Heaviside in (A6); the perturbation of an edge is transmitted rigidly in the second ring margin, being bounded by the $K_i$ value only. For this to set a perturbation in terms of (A4) would be more convenient, keeping constant the centers $r^i_c$, and resulting finally in an expansion or contraction of the sub-configurations, i.e. causing a change in the morphological properties of the rings. In any case the maximum pressure points (but not the minimum pressure points) are fixed as initial data. Thus one can study the sub-$K$-mode considering whether the spacings between consecutive rings are fixed or not. If so, in the *$K_{\bar{\lambda}}$-modes*, then the sequence $\{\bar{\lambda}_i\}$ is fixed, and the perturbation is bound to preserve the initial internal topology of the ringed disk. It cannot reach the $\mathbf{C}_\odot$, but it could still be unstable for the P-W mechanics with a $C^i_x$ in its decomposition or allowing even a $O_x$. Then, $\bar{\lambda}_{i,i-1} =$ constant would connect rigidly the two consecutive parameters $(K_i, K_{i-1})$. In other words, the perturbation of one of the couple will propagate, through this constraint, rigidly to the other parameters $(K_{i+1}, K_{i-1})$. Proceeding iteratively, fixing one starting point of the perturbation, say a $K_*$, attached to any of the rings of the decomposition, will set the perturbation of the entire decomposition in the $K_{\bar{\ell}}$ modes. This subcase however clearly preserves the initial condition of stability of the decomposition, as long as $K_*$ obeys precise constraints. Then we should repeat similar arguments to the Eqs. (28) or Eq. (41) for the determination of ring spacings. In the procedure introduced in Sec. (4.3.2), it was not necessary that the starting point of the iterative process was the inner edge of the first configuration (or $K_1$), but it can be as well any of the margins associated with any elements of the decomposition $\{C_i\}_{i=1}^n$. The outlined procedure is a good example to test the effects of the rigidity of this structure on the choice of the parameters. The reasons for the choice of the $K_1$ as initial data was motivated by the convenience, as the inner edge of $C_1$, that is also the inner edge of the $\mathbf{C}^n$ configuration, is bounded below by the marginally stable orbit as the outer edge of $C_n$, and $\mathbf{C}^n$ can extend outward to infinity. It is sufficient to have only a single initial data on a ring of the decomposition to constrain the range of variation for the parameter of the entire initial decomposition. Having in mind also Eqs (29,43 ,49) we obtain for generic indices of the decomposition the relations

$$\partial_{K_j}\lambda_j > 0, \quad \partial_{K_s}\lambda_j \lesseqgtr 0 \quad \text{if} \quad j \gtrless s. \tag{D1}$$

[38] If $\breve{\mathbf{Q}}$ are the perturbed quantities $\mathbf{Q}$, and $\mathbf{Q}_0$ the initial ones, keeping $\mathbf{Q}_i$ constant does not mean assuming $\exists j \neq i : \breve{\mathbf{Q}}^i = \mathbf{Q}^j_0$ but instead $\breve{\mathbf{Q}}^i = \mathbf{Q}^i_0$. The perturbations are not intended to produce a shift in the ordered sequence of the background even if this could be possible (these are somehow formalized as Eulerian and not Lagrangian perturbations). The configuration index has been assigned to ring center or equivalently to its specific angular momentum $\ell_i$, as such in the $\ell$mode perturbation which induces a change of the $i$ index. We follow the trajectory of the single center which undergoes a translation along the equatorial axis. Then in the $\ell$mode perturbation it is $\breve{\mathbf{Q}}^i = \mathbf{Q}^{\check{i}}$, we say that the $C_i$ ring is now in the position $r^{\hat{i}}_{min}$, with specific angular momentum $\ell_{\hat{i}}$.

It is worth noting that the procedure is antisymmetric with respect to the difference $(j-s)$, i.e. for increasing configuration index moving towards the outer rings, or decreasing indices, going inwardly towards the attractor. Applying a chain rule, there is

$$K_{j-1} = K_{j-1}(K_s), \quad \partial_{K_s} K_j < 0, \quad \partial_{K_{j-1}} K_j < 0. \tag{D2}$$

We finally note that fixing the distances $(\lambda_i, \bar{\lambda}^{i,j})$ (or equivalently functions of these distances) does not fix the position of margins that could translate on the radial axis $r$. The spacings $\bar{\lambda}_{i+1i}$ in this scheme must be bound as: $\bar{\lambda}_{i+1,i} = \delta^{i+1,i}_{min} - (\delta^i_{min_1} + \delta^{i+1}_{min_3})$, where we introduced the part of elongation $\delta^i_{min_3} = r^i_{min} - y^1_3$ in general different from $\delta^i_{min_1} = y^1_1 - r^i_{min}$ : $\lambda_i = \delta^i_{min_3} + \delta^i_{min_1}$. Noting that $\delta^{i+1,i}_{min}$ does not depend on $K$, then

$$\partial_K \delta_{min} = 0, \quad \partial_{K_i} \bar{\lambda}_{i+1,i} = -\partial_{K_i}(\delta^i_{min_1} + \delta^{i+1}_{min_3}), \tag{D3}$$

the first term in the brackets is always greater then zero and the second one is negative; the sum can be positive, negative or zero considering the constraint $\delta^{i+1}_{min_3} \leq \delta^i_{min_1}$. The choice of $K_1$ is restricted to the values $K^i \in [K^i_{min}, V_{eff}(\ell_i, r^{i+1}_{min})]$, in particular this is true for $i = 1$ that is the starting point of the procedure in Eq. (28) or Eq. (41). But the constraint can be further restricted for any $K^i$ (general condition on the elements of the sequence $\{K_i\}^n_{i=1}$) by $K^i \in [K^{i-1}_{min}, K^{i+1}_\bullet]$ being true in particular for $K^i = K_*$, where:

$$K^i_\bullet = \inf\{V_{eff}(\ell_i, y^{i-1}_1), V_{eff}(\ell_i, y^{i+1}_{min})\} \quad \text{for} \quad i \neq 1 \; i \neq n \tag{D4}$$

$$\text{with} \quad K^1_\bullet = V_{eff}(\ell_1, y^2_{min}), \quad K^n_\bullet = V_{eff}(\ell_n, y^{n-1}_{min}). \tag{D5}$$

These can set the boundary conditions for the perturbation of our model depending on the initial data. Thus we can write now:

$$\partial_{K_i} \bar{\lambda}_{i+1,i} = -\partial_{K_i}(\delta^i_{min_1} + \delta^{i+1}_{min_3}). \tag{D6}$$

Assuming the spacing set a priori, not necessarily zero, not necessarily constant with respect to the configuration index, the spacing is rigid but the elongation varies, and in this case we obtain

$$\partial^1_K \delta^i_{min_1} = -\partial^1_K \delta^{i+1}_{min_3}. \tag{D7}$$

We finally note that fixing the spacing means ensuring the hypothesis of rigidity on the ringed disk for the spacing would be independent of the perturbations.

**The $\ell$-modes** An increase in the specific angular momentum magnitude means a perturbation outwards, leading to a radial movement outside. On the other hand, varying $\ell_i$ at fixed $K_i$, the Boyer surfaces are not rigidly translated (a shift in $r^i_{min}$) on the radial direction, but the ring morphology changes and in particular its thickness. This affects the morphological characteristics of the ringed structure as the thickness and elongation, but not the total spacing $\bar{\Lambda}_{\mathbf{C^n}}$ if the spacings are kept fixed, as it is in the $\ell_{\bar{\lambda}}$-*modes*. We note that considering fixed the $\{K_i\}^n_{i=1}$ sequence in the effective potential of the decomposed structure means keeping fixed the Heaviside functions in Eq. (A4 but not in Eq. (A6) or in Eq. (A5). Indeed, at $K_i$ fixed, varying $\ell_i$ does not imply neither fixed, ring edges neither fixed elongation $\lambda_i$, but one should impose a priori this further restrictions, considering the combined variation in Eqs (29,43,49) and Note II. This is again a one dimensional problem in the radial direction, where different submodes are possible: if we keep constant $\lambda_i$ during the perturbation, we could have $\ell_\lambda$-*modes*, and these segments can move forward or backward in the radial direction (increasing and decreasing respectively the specific angular momentum in magnitude, having in mind that one can possibly avoid to consider a "turning point" at $\ell = 0$), oscillating along $r$, undergoing only radial translations by translation of $r^i_{min}$ preserving the length (but clearly not the verticality of each ring $h_i$).

However, we have to point out that formally the $\ell_{\lambda_i}$-modes do not allow the condition $K_i$ =constant (it could be perhaps possible for a $\ell$couuterrotating couple, but the case $\breve{\ell}_i \ell_0^i < 0$ is excluded here), so that we still consider $\ell$ the perturbation variable, having $\lambda_i$ =constant for the perturbation and therefore let the $K_i$ parameter changing accordingly.

A further submode is due to the double restriction of $\lambda_i$ =constant *and* $\bar{\lambda}_{i,i+1}$ =constant, or $\ell_{\bar{\lambda}\lambda}$-*mode*, for each pair of consecutive indices of the decomposition. In this case, however, the perturbation leads to a change of the verticality of each ring ($h_i$) and the shift (oscillation of) the entire elongation of the ringed disk $\lambda_{\mathbf{C}_n}$, without a fixed point. Optionally, one can relax these conditions assuming a known generic relation between these displacements; for a more general discussion see also Sec. (B).

In the $\ell_{\bar{\lambda}}$-mode, as in the $\ell_{\bar{\lambda}\lambda}$-mode, and for the $K_{\bar{\lambda}}$-mode, the initial internal topology of $\mathbf{C}_n$ is preserved, making possible a P-W instability for a ring of the decomposition. Each ring finally changes the thickness. A perturbation of $\ell$ (then a change in velocity in the toroidal direction), at $K$ fixed, leads in general to a radial perturbation with consequent displacement of the constraint $\lambda_i$. The perturbations under consideration here induce a radial oscillation of the ringed disk with general non-periodic or quasi-periodic character depending on the spacing. The frequencies of each one, attached to each spacing is then linked to an equation representing a chain of coupled oscillators. The change of specific angular momentum creates an overall variation of the associated chain of oscillators which may be used for example in models based on observed QPOs (Kluzniak&Abramowicz 2001, 2002; Abramowicz et al. 2007; Torok et al. 2011, 2005; Blaes et al. 2006) and also (Rubio-Herrera&Lee 2005a,b; Rezzolla et al. 2003; Wagoner 2012; Mondal 2010; Nagar et al. 2007). The oscillator is then centered in the center of each sub-configuration $C_i$. Each oscillator is associated with a section of the torus in the equatorial plane. The oscillators are connected by the spacings within the constraint that the spacing can be at most zero but not negative (no penetration of matter, this "rigidity" of the surfaces should not be broken).

This kind of perturbations preserves the equatorial symmetry of the toroidal structure for which the only degree of freedom is the radial direction. In other words, it represents a one-dimensional problem. But the shift of the center of each ring in the radial direction, varying the specific angular momentum, or of its elongation in the case of $K$-modes (note that there cannot be a $K_\lambda$-mode) the perturbation generally leads also to a change in the vertical direction with a change of the height $h_i$ in each sub-configuration. We stress that the constraints on the spacings or the elongations, for example in the $()_\lambda$ or $()_{\bar{\lambda}}$ modes, address also the problem of how many different decompositions are possible in fixed sequence $\{\lambda_i\}_{i=1}^n$ or $\{\bar{\lambda}_{ii+1}\}_{i=1}^n$ respectively. The perturbation of a sequence of parameters of the decomposition, holding the other constant $\ell$-mode or $K$-mode respectively[39], is then one of two possible ways to deform the ringed structure. The $K$-modes do not allow a translation of the centers of the rings, but only a deformation (a kind of breathing, expansion or contraction of the rings).

In the $\ell$-modes the center of pressure moves *together* with the ring leaving the elongation in the $\ell_\lambda$-modes, and the spacings in the $\ell_{\bar{\lambda}}$-modes, fixed, but with vertical deformation of the sub-configuration. In other words, one cannot keep the elongation $\lambda_i$ =constant and the shift parameters in the Heaviside potential Eq. (A5) fixed, and let $r^i_{min}$, i.e. the point of maximum pressure in the ring $C_i$, to move inside the ring, with the corresponding change in $h_i$. Such a case would require a combined variation of $\ell_i$ and $K_i$, to compensate the effects of the variation of $K$, therefore a combination of $\ell$- and $K$-modes (however, this case albeit possible may require, at least for some range of variation for the parameters, orders of $\epsilon_K$ and $\epsilon_\ell$ significantly different, therefore in some situations one cannot deal with "small" perturbations of the sequences of initial parameters anymore). A similar situation was mentioned in Sec. (4.3.1), where a compensatory effect between combined perturbations of the same decomposition through perturbation of its differential rotation was considered .

In the case of $\ell_\lambda$-modes being (as mentioned with the $K$-modes analysis), $\delta^i_{min_1}$ and $\delta^i_{min_3}$, generally nor

[39] We note that the $K_i$ parameters are related to the specific enthalpy and temperature of each ring, see for example (Pugliese&Montani 2015a).

equal or constant for perturbations at $K$ or $\ell$ (and therefore $r_{min}$) fixed, one could set $\lambda_i$ =constant, but the ring translates (not in rigid way) along $r$ and in general $\breve{\delta}^i_{min_1}$ and $\breve{\delta}^i_{min_3}$ are such that $r_{min}$ is moved in the range $\Lambda_i$, and also relatively to the inner and outer edge on the ring. In other words, combining a translational motion of the structure $C_i$, to a translational motion within the structure, we are considering the variations of the measures $\delta^i_{min_3}$ and $\breve{\delta}^i_{min_1}$ with respect to a shift of $r_{min}$. In this way, the perturbation induces a variation of the pressure gradient in the radial direction, and therefore a change in its vertical dimension, even if it is not leading to an instability of the ringed disk. On the other hand, the $\ell$-modes induce in general changes of the pressure gradient inside the ringed disk, even if they are not leading necessary to an unstable point.

We conclude this Section with the following general considerations on the ringed model and its perturbations: each sub-configuration of $\mathbf{C}^n$ is an equilibrium configuration at $\ell$ =constant, and dynamically not related with the other rings of the decompositions when this is far from its instability phase or not in contact.

By requiring that the barotropic surfaces uniquely define the ring surfaces, we can provide a solution characterized by the parameter $p_i$, but there is *no* physical law in this scheme that relates $p_i \neq p_j$ for two different rings, but a relation must be established in advance by an ad hoc considerations, considering properly the boundary conditions. We have addressed this aspect in many points in this work and especially in Sec. (A.1) where we have provided an effective potential for the ringed disk $\mathbf{C}_n$, using the effective potential of each ring and the boundary conditions trough the Heaviside functions. When one perturbs $p_i$, it is $p_i \neq p_j = p_i + \epsilon_i \breve{p}_i$ where $\epsilon_i$ sets the perturbation order of the $p_i$ model parameter. For example, we can refer to Eq. (21) where the displacement matrices $\epsilon_{ij} = \epsilon_i \breve{p}_i$ were introduced in this perturbative scheme.

Any perturbation on the potential (A4) or (A6), or also (A5), introduces implicitly a dynamical relationship between the rings through the perturbation of the boundary data, in each case by the cuts imposed by means of the Heaviside functions. As in the case of any evolutionary model built up with the time-independent Boyer model, discusses in (Pugliese&Montani 2015a), any dynamic relation among the various evolutionary phases of the ringed disk, has to be explained considering the time variable in the model, but also the interaction with the surrounding matter with which the configuration may be in interaction. Analogue arguments can be done for the perturbations that could be possibly associated to some real physical process, being not just a study of the structure stability for changes in initial conditions, testing various eligible decompositions for the appropriate model setup.

### E. Some Notes

**For $\ell$corotating sequences a.** For $|\ell_{\mathbf{a}}| > |\ell_{\mathbf{b}}|$ the relations $r^a_{Max} < r^b_{Max} < r_{mso} < r^b_{min} < r^a_{min}$, $K^b_{Max} < K^a_{Max}$ and $K^b_{min} < K^a_{min}$ hold necessarily. Note that this is not fixing the relation between the couples $(K^b_{Max}, K^a_{min})$ and $(K^a_{Max}, K^b_{min})$, because for $|\ell_a| - |\ell_b|$ sufficiently large, one can also have $K^a_{min} > K^b_{Max}$ and viceversa.

**b.** For $\mathbf{r^b_{min} < r^a_{min}}$ we should have $|\ell_a| > |\ell_b|$, $K^b_{min} < K^a_{min}$ and $r^a_{Max} < r^b_{Max}$; therefore, also $K^b_{Max} < K^a_{Max}$. One of the four inequalities is *enough*, within the condition $\ell_a \ell_b > 0$, to ensure the remaining three hold, see also Note III.

**For $\ell$counterrotating sequences** It follows from the discussion in Sec. (4.3.2) that

**i)** If $\ell_- > -\ell_+ > \ell^+_{\mathbf{mso}}$, then always $r^-_{Max} < r^+_{Max} < r^+_{mso} < r^+_{min} < r^-_{min}$.

**ii)** If $\ell_- < -\ell_+$ neither the maximum or the minima are fixed, and it can be either $C_- < C_+$ or $C_+ < C_-$, and $r^-_{Max} < r^+_{Max}$ or $r^+_{Max} < r^-_{Max}$.

From the analysis in Sec. (4.3.2) it follows that:

**I.** If $\mathbf{r^-_{min}} < \mathbf{r^+_{min}}$, then $\ell_- < -\ell_+$, but the relation between the maximum points has still to be established, see ii)

**II.** But if $\ell_- \in ]\ell^-_{\mathbf{mso}}, -\ell_+[$, then either $r^-_{min} < r^+_{min}$, *or* $r^-_{min} \in ]r^+_{min}, \bar{r}_-[$ where $\bar{r}_- :\ \ell_-(\bar{r}_-) = -\ell_+$, see ii).

**III.** Therefore, if $\mathbf{r^-_{min}} > \mathbf{r^+_{min}}$, then either $\ell_- > -\ell_+$ if $r^-_{min} > \bar{r}_-$ see (i)), *or* $\ell_- < -\ell_+$ if $r^-_{min} < \bar{r}_-$.

*E.0.1. Some notes on* $(K_{crit}, r_{crit}, \ell)$

Below are some general considerations useful to determine the relationship between $K_{crit}$, $r_{crit}$ and $\ell$ of two or more sub-configurations of a generic decomposition.

**Note I** : In the $\ell$corotating case, $\ell_a \ell_b > 0$, at fixed $r$, the effective potential increases with the magnitude of the specific angular momentum, i.e.,

$$V_{eff}(\ell_b) > V_{eff}(\ell_a) \quad \text{as} \quad |\ell_b| > |\ell_a| \quad \text{or} \quad \partial_{|\ell|} V_{eff}\big|_r > 0, \tag{E1}$$

and therefore:

$$r^b_{Max} < r^a_{Max} < r_{mso} < r^a_{min} < r^b_{min}, \quad K^b_{Max} < K^a_{Max} < K^a_{min} < K^b_{min}, \tag{E2}$$

see Fig. (5).

**Note II** : There is $\partial_r V_{eff}(\ell) > 0$ where $\partial_r |\ell| > 0$ and viceversa. At fixed $r = \bar{r}$, $V_{eff}(-\ell)|_{\bar{r}} > V_{eff}(\ell)|_{\bar{r}}$, then $V_{eff}(\ell)$ is increasing with $|l|$ increasing and $(V_{eff}(\ell_+), V_{eff}(\ell_-))$ and $(\ell_-, |\ell_+|)$ are mutually decreasing with $r \in ]r^-_\gamma, r^-_{mso}]$ or increasing for $r > r^+_{mso}$, and viceversa, they are decreasing with respect to the other in $r \in ]r^-_{mso}, r^+_{mso}[$ where it can be $r^-_{min} = r^+_{Max}$.

**Note III** : Referring to Figs (5,6) together, one can say

$$\begin{aligned} &\partial_{r_{min}} r_{Max}\big|_{\mathbf{q}} < 0 \quad \mathbf{q} \in \{\ell, K_{crit}\}, \quad \partial_{r_{min}} |\ell| > 0, \quad \partial_{|\ell|} K_{crit} > 0, \\ &\partial_{r_{min}} K_{min} > 0, \quad \partial_{r_{Max}} K_{min} < 0, \quad \partial_{r_{Max}} K_{Max} < 0; \end{aligned} \tag{E3}$$

with $\partial_{\mathbf{B}} \mathbf{Q} > 0$, we intend that the quantity $\mathbf{Q}$ increases where the quantity $\mathbf{B}$ increases and viceversa. Then the first inequality of Eq. (E3) means that smaller value of $r_{min}$ etc. corresponds to larger values of the maximum $r_{Max}$ of a given sub-configuration if $\mathbf{q} = \ell$, or $\mathbf{q} = K_{crit} = K_{min} = K_{Max}$ at two different configurations, respectively,

**Note IV: On the ring number $n$ and the ring density**

We consider the range of specific angular momenta $\Delta\ell$ (difference of magnitudes), or the range $\Delta K$ for values of $K \in ]K_{min}, K_{Max}[$. Define $\Delta r_{min}$ as the orbital range whose boundaries are the minimum points for the inner and outer rings of a given sub-sequence of the decomposition. We could consider the order $n$ as function of the quantities $\{\Delta\ell, \Delta K, \Delta r_{min}\}$; one can say that for $\Delta\ell \approx 0$ there is $K_i \approx K^i_{min}$ and $\Delta K_i - \Delta K_j \approx 0$. This is trivial for the $\ell$corotating configurations, but for the $\ell$counterrotating ones, we need to consider separately the isolated $\overbrace{\mathbf{C}}^{}_{s}$, see (i-a), or mixed $\overbrace{\mathbf{C}}^{}_{m}$ decompositions, see (i-b). In any case, as can be seen in Fig. (6), $\Delta\ell \approx 0$ means $\Delta r_{min} \approx 0$ and this happens for $r_{min}$ sufficiently large. In principle, the number $n$ of the rings in the range $\Delta r_{min}$, for given $K$ as the sub-configuration

parameter and $\delta K$ as the maximum difference of the ring parameters (or the outer and inner ring parameters–see discussion in Secs. (4.2, A.1), it has to be:

$$\partial_{\delta K} n|_{\delta r_{min}} < 0, \quad \partial_{\delta|\ell_{\pm\pm}|} n > 0, \quad \partial_{\delta|\ell_{+-}|} n > 0, \quad \text{and} \quad \delta|\ell_{+-}| = 0 \quad \text{with} \quad n = 2, \tag{E4}$$

where $\ell_{+-}$ is the difference between the *magnitude* of the specific angular momenta of the outer and inner ring $\ell$counterrotating and as $\ell_{\pm\pm}$ for $\ell$corotating ones. The first inequality, depending on the choice of the ring parameters at fixed $K_{crit}$, has to be intended following the discussion in Sec. (4.3.2), especially with references to the relations in Eqs. (28,41).

## REFERENCES


Ziolkowski J. 2005 Mon. Not. Roy. Astron. Soc. , 358, 851

Remillard R. A., & McClintock J. E. 2006, Ann. Rev. Astron. Astrophys., 44, 49

Bardeen J. M. 1970, Nature, 226,64 -65

Bardeen J. M., Press W. H.,& Teukolsky S. A. 1972 Astrophys. J., 178, 347

Stuchlik Z. 1980, Bull. Astron. Inst. Czechosl.,31, 129-144

Stuchlik Z., Hledik S., Truparova K. 2011, Class. Quantum Grav., 28, 155017

Abramowicz M. A. & Fragile P. C. 2013, Living Rev. Relativity, 16, 1,

Shakura N. I. 1973, Sov. Astronomy, 16, 756

Shakura N.I.& Sunyaev R. A. 1073, Astron. Astrophys., 24, 337

Novikov I. D. & Thorne K. S. 1973, Black holes (Les astres occlus), p. 343 - 450

Page Don N. & Thorne Kip S. 1974, ApJ, 191, 499-506

Abramowicz M. A. & Straub O. 2014, Accretion discs, Scholarpedia ,9(8):2408

Narayan R., Mahadevan R.& Quataert E. 1998 arXiv:astro-ph/9803141

Kozłowski M., Jaroszyński M., Abramowicz M. A. 1998 Astron. Astrophys., 63, 209

Abramowicz M. A.,Jaroszyński M.,Sikora M. 1978 Astron. Astrophys, 63, 221

Jaroszynski M., Abramowicz M. A., Paczynski B 1980, Acta Astronm., 30, 1

Stuchlík Z.,Slaný P.,Hledík S. 2000 Astron. Astrophys., 363, 425

Stuchlik Z. &Slany P. 2004 Phys. Rev. D , 69, 064001

Rezzolla L., Zanotti O., Font J. A. 2003 Astron. Astrophys., 412, 603

Slaný P. & Stuchlík Z. 2005 Class. Quantum Gravity, 22, 3623

Stuchlik Z. 2005, Mod. Phys. Lett.,A, 20, 561

Pugliese D., Montani g. & Bernardini M. G. 2013, Mon. Not. R. Astron. Soc., 428 (2), 952

Pugliese D. & Montani G. 2013, Europhys. Lett., 101, 19001

Rees M. J., Phinney E. S., Begelman M. C., R. D. Bl&ford 1982Nature, 295, 17

Hawley J. F., Smarr L. L., Wilson J. R. 1984, Astrophys. J., 277, 296

Hawley J. F. 1987 Mon. Not. R. Astron. Soc., 225, 677

Hawley J. F. 1991, Astrophys. J., 381, 496

De Villiers J-P.& Hawley J. F. 2002, Astrophys. J., 577, 866

Stuchlík Z., Slaný P., Kovar J. 2009, Class. Quantum Gravity, 26, 215013

Komissarov S. S. 2006, Mon. Not. R. Astron. Soc., 368, 993-1000

Adamek K. & Stuchlik Z. 2013, Class. Quant. Grav. 30, 205007

Hamersky J. & Karas V. 2013, Astron. Astrophys., 32, 555

Larsen A. L. 1994, Class. Quant. Grav., 11, 1201

Kolo M. & Stuchlk Z. 2013, Phys. Rev. D, 88, 065004

Stuchlik Z. & Kolos M. 2012, JCAP, 1210, 008

Stuchlk Z. &Kolo M. 2014, Phys. Rev. D, 89, 6, 065007

Cremaschini C. & Stuchlik Z. 2013, Phys. Rev. E, 87, 043113

Kovar J, Slany P., Stuchlik Z., Karas V., Cremaschini C., Miller J.C. 2011, Phys. Rev.,D ,84, 8, 084002

Slany P., Kovar J. , Stuchlik Z. & Karas V. 2013, Astrophys. J. Suppl. 205, 3

Kovr J., Slan P., Cremaschini C., Stuchlk Z. , Karas V. & Trova A. 2014, Phys. Rev. D, 90, 4, 044029

Cremaschini C., Kovr J., Slan P, Stuchlk Z. & Karas V. 2013, Astrophys. J. Suppl., 209, 15

Paczyński B. & Wiita P. 1980, Astron. Astrophys., 88, 23

Paczyński B. 1980, Acta Astron., 30, 4

Abramowicz M. A., Calvani M., Nobili L. 1980, Astrophys. J., 242, 772

Stuchlík Z., Kovář J. 2008, Int. J. Mod Phys D, 17

Pugliese D. &Montani G. 2015, Phys. Rev. D., 91, 083011

Volonteri M., Haardt F. & Madau P. 2003, Astrophys. J., 582 559

Volonteri M., Madau P. & Haardt F. 2003, Astrophys. J., 593, 661

Meier D. L. 2012, *Black Hole Astrophysics The Engine Paradigm*, (Springer-Verlag, Berlin Heidelberg, 2012).

Boyer R. H. 1965, Proc. Camb. Phil. Soc., 61, 527

Torok G., Abramowicz M. A., Kluzniak W., & Stuchlik Z. 2005,Astron. Astrophys., 436, 18

Stuchlik Z., Kotrlova A. & Torok G. 2013, Astron. Astrophys., 552, A10

Abramowicz M. A. , M. Calvani, L. Nobili, Nature,,302, 597

Abramowicz M. A., Karas V., Lanza A. 1998, Astron. Astrophys., 331, 1143

Font J. A. & Daigne F. 2002, Mon. Not. Roy. Astron. Soc., 334, 383

Korobkin O., Abdikamalov E., Stergioulas N., Schnetter E., Zink B., Rosswog S., Ott C. D. 2013, Mon. Not. Roy. Astron. Soc., 431, 1, 354

Pugliese D. & Quevedo H. 2015 Eur. Phys. J. C, 75, 5, 234

A. Font J. A., Daigne F. 2002, Astrophys. J., 581, L23-L26

Abramowicz M. A. 2004, In: Growing black holes: accretion in a cosmological context. Proceedings of the MPA/ESO/MPE/USM Joint Astronomy Conference held at Garching, Germany, 21-25 June 2004. A. Merloni, S. Nayakshin, R. A. Sunyaev (Eds.). ESO astrophysics symposia. Berlin: Springer, ISBN 3-540-25275-4, ISBN 978-3-540-25275-7, 2005, p. 257 - 273.

Igumenshchev I. V., Abramowicz M. A. 2000, Astrophys. J. Suppl.,130, 463

Hawley J. F 1990, Astrophys. J., 356, 580

Fragile P. C., Blaes O. M., Anninois P. , Salmonson J. D. 2007, Astrophys. J., 668, 417-429

Font J. A. 2003, Living Rev. Relat., 6, 4

Abramowicz M. A. 1971, Acta. Astron., 21, 81

ChakrabartiS. K. 1990, Mon. Not. R. Astron. Soc., 245, 747

Chakrabarti S. K. 1991, Mon. Not. R. Astron. Soc., 250, 7

Zanotti O. & Pugliese D. 2015, Gen. Rel. Grav., 47, 4, 44

Lei Q., Abramowicz M. A., Fragile P. C., Horak J.,Machida M.,Straub O. 2008, Astron. Astrophys., 498, 471

Shafee R., McKinney J. C, Narayan R., Tchekhovosky A., Gammie C. F., McClintock J. E. 2008, Astrophys. J., 687, L25

Abramowicz M.A., Lanza A., Percival M.J. 1996, Astrophys. J., 479, 179

Fishbone L. G., Moncrief V. 1976, Astrophys. J., 207, 962

Frank J., King A., Raine D. 2002, *Accretion Power in Astrophysics*, (Cambridge University Press, Cambridge 2002)

Kucakova H., P. Slany, Stuchlik Z. 2011, JCAP, 01, 033

Stuchlik Z. & Schee J. 2012, Class. Quant. Grav., 29, 065002

Stuchlík Z., P. Slaný P. 2006, AIP Conf. Proc., 861, 770

Stuchlk Z., Pugliese D., Schee J. & Kuckov H. 2014, arXiv:1412.4149

Abramowicz M. A. 2008, arXiv:astro-ph/0812.3924

Misner C. W.,Thorne K. S., Wheeler J. A. 1973, *Gravitation*, (Freeman, San Francisco, 1973).

Pugliese D. & Kroon J. A. V. 2012, Gen. Rel. Grav., 44, 2785

Pugliese D., Quevedo H. & Ruffini R. 2013, Phys. Rev. D, 88, 2, 024042

Pugliese D., Quevedo H. & Ruffini R. 2011, Phys. Rev. D, 84, 044030

Chandrasekhar S., *The mathematical theory of Black Holes*, (International Series of Monographs on Physics, Hardcover, 1983).

Pugliese D. & Stuchlík Z., *in preparation.*

Kern, W. F., Bland J. R. 1948, "Theorem of Pappus", in Solid Mensuration with Proofs, 2nd ed. New York: Wiley

Vincent F. H., Yan W., Straub O., Zdziarski A. A., Abramowicz M. A. 2014, arXiv:1406.0353

Ciolfi R. &Rezzolla L. 2013, Mon. Not. R. Astron. Soc. Let., 435, 1

Kluzniak W. & Abramowicz M. A. 2001, preprint (arXiv:astro-ph/0105057)

Kluzniak W. & Abramowicz M. A. 2002,arXiv:0203314

Abramowicz M., Kluzniak W., Bursa M., Hork J., Rebusco P.,Török G 2007 Revista Mexicana de Astronoma y Astrofsica (Serie de Conferencias), 27, 8-17

Torok G., Kotrlova A., Sramkova E., & Stuchlik Z. 2011 Astron. Astrophys.,531, A59, 7

Rubio-Herrera E. & W. H. Lee W. H. 2005, Mon. Not. R. Astron. Soc., 362, 789798

Rubio-Herrera E. & Lee W. H. 2005, Mon. Not. R. Astron. Soc., 357, L31L34

Rezzolla L., Yoshida S.,Maccarone T. J. &Zanotti O. 2003, Mon. Not. R. Astron. Soc., 344, 37-L41

Blaes O. M., Arras P., & Fragile P. C. 2006 Mon. Not. R. Astron. Soc., 369, 12351252

Wagoner R. V. 2012, Astrophys. J., 752, L18

Mondal S. 2010, Astrophys. J., 708, 1442

Nagar A. , Zanotti O. , Font J. A. & Rezzolla L. 2007, Phys. Rev. D, 75, 044016

This 2-column preprint was prepared with the AAS LaTeX macros v5.2.